The Thesis Committee for Almas Aitkulov
Certifies that this is the approved version of the following thesis:

Two-dimensional ASP Flood for a Viscous Oil

APPROVED BY
SUPERVISING COMMITEE:

Kishore K. Mohanty, Supervisor

Kamy Sepehrnoori

Two-dimensional ASP Flood for a Viscous Oil

by

Almas Aitkulov, B.S.P.E.

Thesis

Presented to the Faculty of the Graduate School of

The University of Texas at Austin

In Partial Fulfilment

of the Requirements

for the Degree of

Master of Science in Engineering

The University of Texas at Austin

December 2014

Dedication

Dedicated to my grandmothers Azhar and Kalykoz, my parents Saule and Sabitkhan, and my wonderful little sister Zaure for their love and support throughout my life.

Осы жылы менің апам Ажар апа кайтыс болды. Мен апамды соңғы рет көре алмадым, айналайын апам жаткан жерін жайлы болсын! Келе алмағаныма қатты өкіндім! Осы жұмысымды саған арнаймын!

Acknowledgements

I would like to express my sincere thanks to my supervisor, Dr. Kishore K. Mohanty for his tremendous support and constant encouragement throughout my studies at the University of Texas at Austin. He has been my professor, supervisor and mentor for 4 years, and supported me like no other. I sincerely thank him for believing in me and my abilities.

I would like to extend my thanks to Dr. Kamy Sepehrnoori whose wealth of experience and knowledge have been invaluable to me. I enjoyed discussing not only research topics, but also history and culture related themes.

My special thanks to Dr. Eric Dao for helping me throughout my research work and always being ready to answer my questions and concerns. I also want to give special thanks to Barbara Messmore for her help with logistics of the research process. I wish to thank my colleagues and friends from Dr. Mohanty's research group for their help and cooperation.

I would also like to thank Dr. Gary Pope and his research group for their help and valuable advice on this project. I thank Glen Baum and Gary Miscoe for helping me to install the experimental equipment. I want to thank Frankie Hart and Mary Pettengil for all their help in finding information needed for my overall progress. Finally I would like to thank my parents and all my friends for providing me the strength and moral support I always needed for getting me through a very special phase of my life.

Abstract

Two-dimensional ASP Flood for a Viscous Oil

Almas Aitkulov, M.S.E.
The University of Texas at Austin, 2014

Supervisor: Kishore Mohanty

There is a vast deposit of viscous and heavy oil, especially in Canada and Venezuela. Typically thermal methods are used to recover heavy oil. However, thermal methods are inefficient when the depth of the reservoir is high and pay thickness is low. Non-thermal methods need to be developed for viscous and heavy oils. Alkaline-surfactant-polymer (ASP) floods can be used for improving the displacement efficiency, but its effect on sweep efficiency in viscous oil recovery has not been studied. The objective of this research was to investigate 2D ASP floods in a quarter five-spot pattern. Through careful phase behavior screening, the surfactant formulation was developed that produced ultra-low interfacial tension with reservoir viscous oil (100 cp). After verifying that the design of surfactant formulation was robust and can recover more than 90% of oil in a 1D ASP sandpack flood, it was tested in a 2D geometry.

Both stable and unstable tertiary ASP floods were performed in a 2D quarter five-spot sandpack using the surfactant formulation developed in 1D ASP sandpack flood. In a stable ASP quarter five-spot sandpack flood, the oil recovery was excellent (~97% of

ROIP). Oil recovery in the stable 2D ASP flood behaved similar to oil recovery in the 1D stable ASP flood. However, pressure drop obtained was high which would be unsustainable in field applications. Interestingly, unstable 2D flood performed well even with an adverse mobility ratio between oil/water bank and ASP slug with a recovery of 80% ROIP. Decreasing the viscosity of ASP slug 6 times decreased the maximum pressure drop 5 times; thus, the maximum pressure drop was almost proportional to the ASP slug viscosity in a 2D pattern. This research showed that unstable ASP flood in a 2D geometry can recover significant amount of oil with a practical pressure gradient.

Table of Contents

List of Tables

List of Figures

CHAPTER 1: INTRODUCTION

1.1 Motivation

The current worldwide oil consumption is roughly 90 million barrels per day, or around 33 billion barrels per year. Most of the recoverable oil is currently concentrated in giant fields (>1 billion barrels of recoverable oil), however, at current pace of oil consumption per year the world needs to discover at least three super giant fields (>10 billion barrels of oil of recoverable oil) per year in order to replenish current oil reserves. In the last decade, only 4 super giant fields were discovered, nevertheless, none of them have started production, and most of them have harsh reservoir conditions making oil extraction more expensive. Therefore, there is a need to enhance recovery efficiency in current producing oil reservoirs.

A conventional waterflooding technique leaves about half of the oil behind in the reservoirs. In the known oil reservoirs more than a trillion barrel of light oil has been left behind. There is also a vast deposit of viscous and heavy oil, especially in Canada and Venezuela. Typically thermal methods are used to recover heavy oil. However, thermal methods are inefficient when the depth of the reservoir is high and pay thickness is low. Non-thermal methods needs to be developed for viscous and heavy oils.

In viscous oil fields (~100 cp viscosity), waterflooding is inefficient due to viscous fingering. Chemical enhanced oil recovery (CEOR) methods can improve the oil recovery. Polymer floods can improve sweep efficiency. Alkaline-surfactant-polymer (ASP) flooding can improve the oil recovery by increasing capillary number and decreasing mobility ratio at the same time. Oil recovery is a function of surfactant, co-solvent, alkali amount and properties, ASP and polymer slug viscosities and slug sizes. This research investigates factors affecting recovery efficiency of viscous oils.

The first objective of this work was to identify effective surfactant formulations for viscous oils. Phase behavior experiments were conducted to identify surfactant formulations and sandpack flood experiments were conducted to evaluate their effectiveness. The second objective of this research was to study the effectiveness of alkaline-surfactant-polymer formulations in multidimensional floods. ASP floods were conducted in a quarter of a 5-spot.

1.2 Description of Chapters

Chapter 2 describes the background information that is relevant for this research. Chapter 3 describes the experimental methodology which includes materials, equipment, procedures and calculations used for conducting the phase behavior and sandpack flooding experiments. Chapter 4 discusses the results of the phase behavior tests, 1D ASP sandpack floods, and 2D quarter five-spot ASP sandpack floods. Chapter 5 summarizes the results of this research work and discusses the conclusions.

CHAPTER 2: LITERATURE REVIEW AND BACKGROUND

Chapter 2 discusses the background literature relevant to alkaline-surfactant-polymer flooding and other related topics such as surfactant-oil-brine phase behavior, microemulsions, and description of chemicals used in this research.

2.1 Main Recovery Mechanisms in ASP flooding

One of the main mechanisms of surfactant floods in chemically enhanced oil recovery (CEOR) is lowering the interfacial tension (IFT) between oil and water. Lowering of the IFT leads to reduction of residual oil saturation.

In general, residual oil saturation is controlled by the dimensionless number capillary number (Nc). It was first introduced by Moore and Slobod (1955) as the ratio of viscous forces to capillary forces and is equal to

$$Nc = \frac{Fv}{Fc} = \frac{v\mu}{\sigma \cos\theta}. \tag{2.1}$$

Here, Fv stands for viscous forces and Fc stands for capillary forces, v is the interstitial velocity of displacing fluid, μ is viscosity of displacing fluid, θ is contact angle measured in displacing fluid, and σ is interfacial tension between displacing and displaced fluids. Furthermore, several other modifications of capillary number were derived in other studies. For instance, Foster (1973) omitted $\cos\theta$ term and changed interstitial velocity to superficial velocity, and thus, introduced porosity into the capillary number definition as follows

$$Nc = \frac{u\mu}{\phi\sigma}. \tag{2.2}$$

In addition, it is often convenient to include the pressure drop term in the capillary number definition. Dombrowsky and Brownell (1954) version of capillary number is written in terms of the potential gradient of displacing fluid

$$Nc = \frac{k\left|\bar{\nabla}\Phi_p\right|}{\sigma\cos\theta}. \tag{2.3}$$

Here $\bar{\nabla}\Phi_p$ is potential gradient of displacing fluid, k is permeability, μ is viscosity of displacing fluid, θ is contact angle measured in displacing fluid, and σ is interfacial tension between displacing and displaced fluids.

During typical waterflooding, capillary number is estimated to be about 10^{-7} and in order to recover more oil capillary number needs to be increased further. Stegmeier (1976) presented the relationship between capillary number and residual saturation; later Lake (1989) named the relationship as the capillary desaturation curve (CDC). Figure 2.1 shows CDC published for several rocks (Stegemeier, 1976).

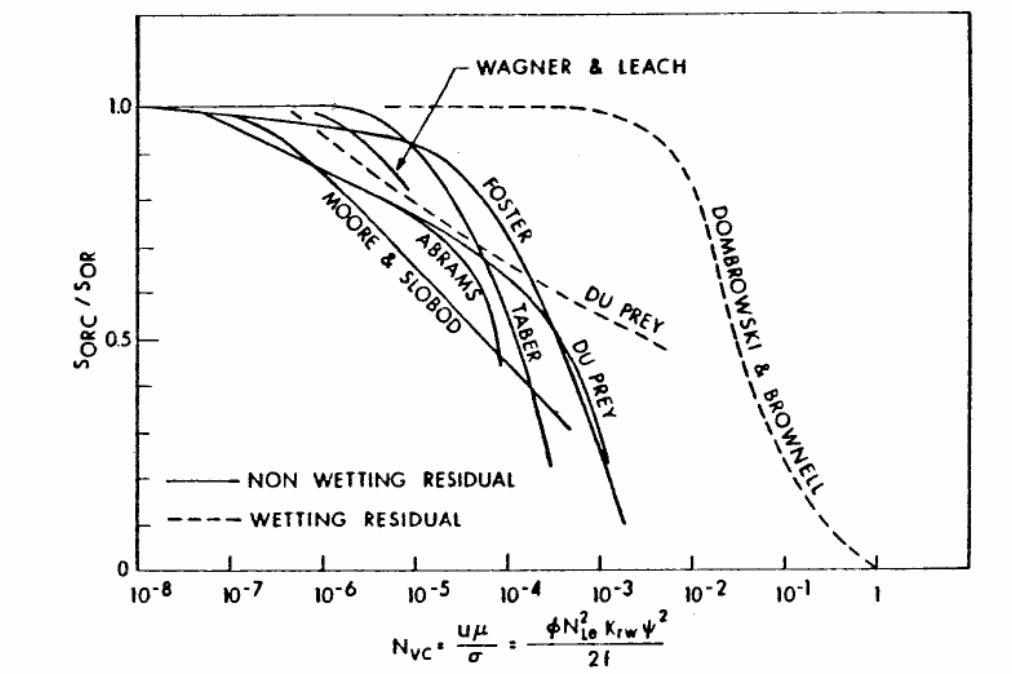

Figure 2.1: Capillary Desaturation Curve (Stegemeier, 1976)

It was determined from several experiments that critical capillary number that would produce additional oil after waterflooding is around 10^{-5} (Mohanty and Salter, 1983; Delshad et al., 1986;

Gupta, 1984). To reduce the residual saturation to zero, it is required to increase capillary number at least 1000 times to about 10^{-2}. The way to increase capillary number from typical waterflood values of 10^{-7} to values higher than 10^{-5} is to either increase pressure drop or decrease IFT. Pressure can be increased by increasing injection flow rate or viscosity; however, it is not feasible to increases pressure drop several orders of magnitude due to limited availability of pressure drop in field conditions. The only way to increase capillary number several folds of magnitude is to decrease IFT from about 30 dynes/cm in typical waterflooding to ultra-low values ($<10^{-3}$ dynes/cm) between fluids which is possible to achieve using well designed surfactant formulations (Green and Willhite, 1998).

In order to reach ultra-low values, interaction energy across the interface must be large which can be achieved only if nature of material on both sides of interface is very similar. Since oil and water are very dissimilar in nature, in order to have similar nature at the interface, there must be a third phase that would have similar concentration of surfactant, oil, and water (Rosen, 1989). Furthermore, ultra-low interfacial tension can be achieved in the three-phase region (Puig, 1979). The presence of surfactant leads to micelle formation. When surfactant concentration in the interface region reaches certain critical concentration called critical micelle concentration (CMC), the surfactants start aggregating into micelles. The solutions where micelles have solubilized phase that is immiscible with solvent are called microemulsions (Green and Willhite, 1988). Formation of a separate microemulsion phase which solubilizes both oil and water creates three phase region of microemulsion, oil and water. The three phase region is very important in surfactant EOR since microemulsion has ultra-low IFT against both water and oil (Green and Willhite, 1998).

2.2 Microemulsions

Definition

Bourrel and Schechter (1988) defined microemulsion as thermodynamically stable transparent or translucent blends of oil, water, surfactants, and other additives. Furthermore, aside from being thermodynamically more stable than ordinary emulsions (macroemuslions), microemulsions also have an order of magnitude smaller drop size compared to macroemulsions. Lastly, microemulsions unlike macroemulsions are independent of mixing and can return to its original state after mechanical disturbance and perturbations in temperature.

2.2.1 Microemulsion Phase Behavior and Transition Parameters

In general, surfactant solution phase behavior is mainly affected by salinity. Increasing the salinity of a surfactant solution decreases the solubility of surfactants in the aqueous phase. Further salinity increase drives anionic surfactants out of the aqueous phase while also solubilizing some water inside reverse micelles. Thus, at high salinities the phase behavior is represented by two phases: oil-external microemulsion and excess water. At low salinity, behavior is reversed and oil is essentially free of surfactant and some oil is solubilized inside micelles dispersed in the water phase. Therefore, at low salinities, phase behavior is represented by two phases: excess oil phase and water-external microemulsion. At intermediate salinities, three phases could exist: excess oil, middle phase microemulsion, and excess water. Winsor (1954) classified oil-external, middle phase microemulsion (also called bicontinuous), water-external microemulsion as Winsor Type I, II, III respectively. Reed and Healy (1976) stated that microemulsion phase transitions may occur due to changes in salinity, temperature, surfactant and co-solvent (alcohol) molecular structure, composition of oil and dissolved solids in the

aqueous phase. For example, increasing surfactant hydrophobicity by increasing hydrophobe chain length causes shift from Type I microemulsion to Type II microemulsion; the trend is reversed when surfactant hydrophilicity is increased. It can be achieved by addition of alkoxy groups such as ethylene oxide into surfactant structure. An increase in pressure typically shifts Type II microemulsion to Type I microemulsion behavior (Skauge and Fotland, 1986). An increase in temperature typically causes shift from Type II to Type I behavior for anionic surfactants (Walker, 2011). Oil composition can be characterized by the equivalent alkane carbon number (EACN). An increase in EACN commonly causes optimum salinity to increase; thus microemulsion behavior shifts from Type II to Type I (Solairaj, 2011). Furthermore, Reed and Healy (1976) found that higher molecular weight alcohols tend to shift microemulsion behavior from Type I to Type II. Lastly, Hsieh and Shah (1976) stated that branched co-solvents tend to be more hydrophilic compared to linearized co-solvents, and thus, optimum salinity is shifted to a higher value which means microemulsion phase behavior is shifted from Type II to Type I behavior.

2.2.2 MICROEMULSION PHASE BEHAVIOR AND INTERFACIAL TENSION

As salinity is increased, IFT between water and microemulsion is increased and IFT between oil and microemulsion is decreased. The point where both IFT's are equal to each other is termed optimum salinity and the solubilization ratio at this salinity is called the optimum solubilization ratio (Reed and Healy, 1976). The middle phase microemulsion has the most favorable condition for oil recovery because both oil-microemulsion and water-microemulsion IFT's are ultra-low. Furthermore, IFT is closely related to solubilization ratio. Solubilization ratio is defined as ratio of solubilized oil (water) volume to surfactant amount in the

microemulsion. When solubilization of oil is equal to that of water, IFT reaches minimum. Huh (1979) derived a relationship between oil / water solubilizations and IFT

$$\gamma = \frac{C}{\sigma^2} \tag{2.4}$$

where σ is a solubilization ratio, C is a constant with value equal to 0.3 dynes/cm, and γ is an interfacial tension.

2.2.3 VISCOSITY OF MICROEMULSION

Microemulsion viscosity is one of the most significant parameters affecting surfactant formulation design. In general, surfactants are very prone to forming viscous microemulsions, gels, complexes and liquid crystals under different conditions (Sheng, 2011). Depending on the structure of microemulsion, its viscosity can increase an order of magnitude compared to the oil viscosity. In general, viscosity increases to a maximum value at a composition where water and oil contents are equal (Green and Willhite, 1998). Injecting highly viscous microemulsion can lead to high surfactant retention, very high pressure gradients and reduced sweep efficiency. Thus, overall oil recovery suffers significantly due to surfactant performance and mobility control design (Walker, 2011). Viscosity of microemulsion can be decreased by the following methods such as adding branched surfactants, mixture of surfactant blends (Levitt et al., 2006), co-solvents, and increasing temperature.

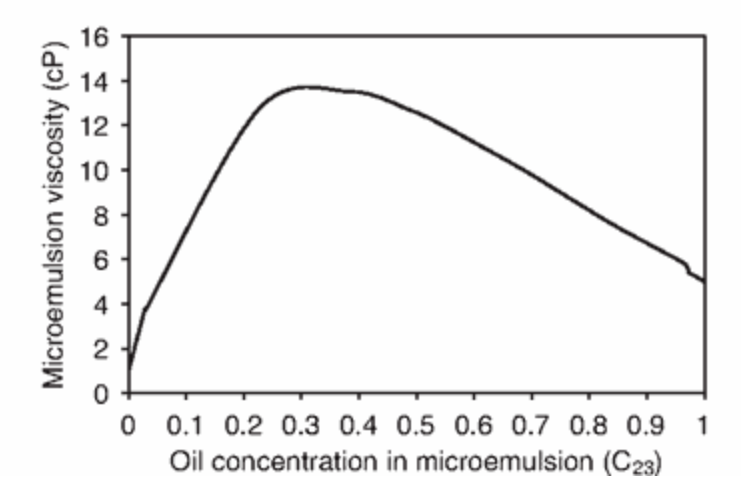

Figure 2.2: Microemulsion viscosity as a function of oil concentration (Sheng, 2011)

2.3 Importance of Mobility Control in CEOR

The main objective of mobility control is to improve sweep efficiency during displacement processes. Bansal and Shah (1977) defined mobility control for the microemulsion processes as changing the properties of the injected fluids such that stable movement of the separate banks is achieved with minimum of mixing and dispersion. In surfactant related CEOR processes main chemicals in ASP slug are very expensive; thus, only small portion of main chemical slug (about 5% to 40% of pore volume) can be injected in economically feasible manner (Green and Willhite, 1998). Typically, main surfactant slug is displaced by less expensive polymer bank, which in turn is displaced by water. It is important to have good mobility control in all three slugs. In main chemical slug, good mobility control is required so that the main slug does not finger through the oil/water bank. Adverse mobility control would cause main slug to finger through the oil/water bank and have early breakthrough. Furthermore, significant amount of chemicals would be trapped and retained, if mobility control is not properly designed. Dissipation is minimized if there is favorable mobility control between main

chemical slug and polymer bank. Lastly, mobility control prevents water drive from fingering through polymer bank into the chemical slug. Therefore, it is very important to have good mobility control during CEOR processes. Mobility control is usually characterized by mobility ratio,

$$M = (k_{rD}/\mu_D)_{S_D} / (k_{rd}/\mu_d)_{S_d} \tag{2.5}$$

where, k_{rD} is the relative permeability of displacing phase, k_{rd} is the relative permeability of displaced phase, μ_D is the displacing phase viscosity, μ_d is the displaced phase viscosity, S_D is the average displacing phase saturation in the region behind displacing front , S_d is the average displacing phase saturation in the region ahead displacing front. Volumetric sweep efficiency generally increases as M is decreased, and M less than one is considered favorable mobility ratio and displacement is stable.

Another important parameter in mobility control design for chemical flooding processes is an estimation of total relative mobility in the stabilized oil bank:

$$\lambda_{rw} + \lambda_{ro} = (\frac{k_{rw}}{\mu_w} + \frac{k_{ro}}{\mu_o})_b \tag{2.6}$$

where, $\lambda_{rw} = \frac{k_{rw}}{\mu_w}$ is the relative mobility of water, $\lambda_{ro} = \frac{k_{ro}}{\mu_o}$ is the relative mobility of oil, k_{rw} is the relative permeability of water, k_{ro} is the relative permeability of oil, μ_w is the water viscosity, μ_o is the oil viscosity.

Gogarty et al. (1970) obtained the total relative mobility as a function of water saturation as shown in Figure 2.3.

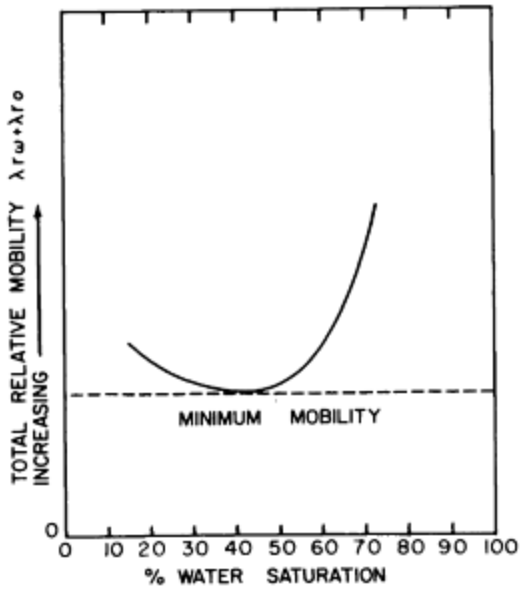

Figure 2.3: Total relative mobility of oil and water versus water saturation (Gogarty et al., 1970)

Gogarty et al. (1970) stated that the relative mobility for the microemulsion bank must be equal or less than minimum total relative mobility of the oil/water bank. Furthermore, the reciprocal of the relative mobility gives the maximum apparent viscosity for oil/water bank (Green and Willhite, 1998). To conclude, in order to have stable displacements, viscosities of both the chemical slug and mobility buffer (polymer drive) must be equal to or higher than the maximum apparent viscosity of the oil/water bank.

2.4 Importance of Salinity Gradient in CEOR

During the ASP flood, there typically exist at least three distinct fluid zones which are the residual oil after waterflooding, followed by ASP slug, and finishing with polymer drive slug. Each of these zones can have different salinities. It is very important to take into account the effect of salinities of each zone on the displacement efficiency. Nelson (1984) first presented work on the relationship between salinities of each fluid zone and the performance of the chemical flood. Furthermore, he also introduced the term called salinity gradient and illustrated

its effect on the oil recovery as well as surfactant retention. He conducted several experiments where he changed only the salinity of each slug. This work showed that keeping salinity of the polymer drive slug lower in Type I region while having the leading waterflood salinity and/or the microemulsion salinity at Type II or Type III regions increases chances of passing through the Type III region where ultralow IFT can be achieved. The experimental results showed that the salinity gradient design led to very low residual oil saturation after chemical flood and also significantly lower surfactant retention compared to the constant salinity design flood. The ideal case would be having salinity of all fluid zones in Type III region; however, it is very risky to do that due to factors such as dilution and cation exchange with the formation rock which can easily affect in situ salinity of the fluid. The salinity gradient offers a more robust chemical flood design and decreases risk of missing the Type III salinity window.

2.5 Chemicals Used in ASP

In alkaline-surfactant-polymer flooding alkaline, surfactant and polymer are injected to improve oil recovery. In addition, ASP formulations include co-surfactants, co-solvents and electrolytes.

2.5.1 Primary Surfactant and Co-Surfactant

Surface-active agents, or surfactants, are chemicals that at low concentrations have ability to adsorb onto water-oil interfaces (Rosen, 1978). Furthermore, they can significantly decrease interfacial tension (IFT) between fluids. They are usually organic in nature, and consist of a nonpolar hydrocarbon chain called hydrophobic tail and polar, ionic portion called hydrophilic head (Bourrel & Schechter, 1988). Based on the ionic nature of the head group, surfactants are divided into anionic, cationic, nonionic, and zwitterionic (Lake, 1989). Anionic surfactants are

the most common type of surfactants currently used in CEOR. The reasons are low interfacial tension, low adsorption on reservoir rocks, thermal stability and low cost (Green and Willhite,1998). Nonionic surfactants are used mainly as co-surfactants to improve overall phase behavior of the solution. They have high salinity tolerance, but cannot reduce IFT as good as anionic surfactants (Lake, 1989). Due to strong adsorption on sandstone rocks, cationic surfactants are not used with sandstones; they are used to change wettability of carbonate rocks from oil-wet to water-wet. Zwitteronic surfactants have both positive and negative charges, but they are rarely used due to high cost (Lake, 1989). Over several decades, surfactant formulations were improved continuously to exhibit better qualities such as low cost of manufacturing, improved compatibility with polymers and alkali. Few of the recent developments are discussed next.

From recent developments, branched alcohol propoxy sulfates, internal olefin sulfonates, and branched alpha olefin sulfonates have been identified as high performance surfactants. They exhibit high oil recovery both in sandstone and dolomite, and low surfactant retention (Levitt et al., 2008).

Furthermore, a novel class of surfactants such as Guerbet alkoxy sulfates exhibits substantial improvement in performance. Carboxylation of large Guerbet alkoxylates produces high performance surfactants that can withstand harsh reservoir conditions of high temperature, high salinity, and high hardness (Adkins et al., 2012). Furthermore, addition of alkoxy groups such as propylene oxide and ethylene oxide as extenders to the Guerbet alcohol can be used as a tailoring technique to achieve specific surfactant qualities (Adkins et al., 2010). The addition of EO groups, for instance, enhances hydrophilicity of the surfactant, and thus, increases the

optimal salinity. The addition of PO groups has opposite effect of increasing hydrophobicity of the surfactant (Maerker & Gale, 1992).

Wang et al. (2010) used zwitteronic surfactants "Betaine Amphotoreic Surfactants" that can achieve ultra-low IFT without alkali, salts, co-surfactants and co-solvents. In addition, these surfactants can tolerate very high salinity (229,000 ppm), high divalent ion concentrations (21,000 ppm) and high reservoir temperature (up to 98 ^{o}C).

Gao and Sharma (2013) developed novel series of anionic Gemini surfactants that have very high NaCl tolerance (up to 20 wt%) and high CaCl2 tolerance (up to 5 wt%). Furthermore, they found that anionic Gemini surfactants have approximately two or three orders of magnitude lower CMC values and much lower adsorption values compared to other conventional surfactants. This new class of surfactants can also be used as co-surfactant because they can significantly improve aqueous stability and interfacial activity in the mixture with other conventional surfactants.

Lastly, a lot of work was done on finding different blends of two or more surfactants that can work together and achieve synergistic effect on IFT and microemulsion viscosity. Li et al (2014) tested several mixtures of anionic and cationic surfactants. It was found that mixtures of anionic-cationic surfactants produce ultra-low CMC as well as ultra-low IFT and high solubilization ratio. Puerto et al (2014) identified optimal blends of alcohol propoxy sulfates with an internal olefin sulfonate that can have high solubilization suitable for CEOR in the absence of co-solvent.

2.5.2. ALKALI

In general, alkali is used to reduce the surfactant adsorption and to create soap by reacting with crude oil (Nelson, 1984). Addition of alkali increases pH because of its dissociation in the

aqueous phase (Green and Willhite, 1998). High pH increases the amount of negatively charged surfaces on the surface of formation rock, which is generally negatively charged for sandstones and positively charged for carbonates at a neutral pH. An increase in the amount of negative charges on the rock surface reduces surfactant adsorption because negatively charged anionic surfactants are repelled by negatively charged surface of the rock.

In addition, soap is generated when alkali reacts with naphthenic acids in crude oil. Crude oil must have acids in order to produce in situ soap when reacting with alkali. The acid number measurement of crude oil is one way to assess crude oil's ability to form soap. Acid number of crude oil is defined as the amount of potassium hydroxide (KOH) in milligrams needed to neutralize 1 gram of petroleum acid in crude oil (Green and Willhite, 1998). However, an acid number measurement is not an accurate method of quantification of soap in crude oil. The reason is that it measures only free carboxylic groups in crude oil at low temperatures (Yang, 2010). Another similar and more reliable method used to assess crude oil's ability to generate soap is saponification number, which is determined by adding potassium hydroxide (KOH) in crude oil sample and titrating it with hydrochloric acid at an elevated temperature.

Generally, in situ soap produced by reaction of alkali and reactive crude oil is quite hydrophobic; thus, a robust ASP design counters the hydrophobicity of the generated soap by more hydrophilic surfactant addition. Lastly, with good chemical design one might entirely discard use of surfactant in ASP flood and just proceed with alkali-co-solvent-polymer (ACP) flood by employing soap and compatible co-solvent to achieve optimum phase behavior (Fortenberry, 2013).

Most common alkaline agents used in CEOR are sodium carbonate, sodium hydroxide, sodium orthosilicate (Green and Willhite, 1998). Out of these three, sodium carbonate is usually

most commonly used due to its ability to propagate further into formation, relatively low cost of manufacturing, and moderate pH. However, sodium carbonates cannot be used in in formations with high gypsum or anhydrite concentrations. Sodium carbonate will precipitate in the presence of gypsum which will cause permeability damage and loss of majority of alkali. Sharma et al. (2014) have tested sodium metaborate (NaBO2) and ammonium hydroxide (NH4OH) as alternatives for sodium carbonate for application in gypsum containing formations. Through a series of ASP core floods they determined that both of alkalis can propagate through core without loss of alkalinity with pH of 10 and without permeability damage to the formation. Furthermore, he was able to achieve high oil recovery and low surfactant retention. However, sodium metaborate is more expensive compared to sodium carbonate and ammonium hydroxide has some safety concerns related to handling and transportation to surface facilities.

2.5.3 POLYMER

In ASP design, polymers are responsible for mobility control and sweep efficiency. Lower mobility enhances both vertical and horizontal sweep efficiency (Lake, 1989). Polymers are water soluble and increase the viscosity of water. Most commonly used polymers are synthetic partially hydrolyzed polyacrylamide (HPAM) and biopolymer xantan gum. Currently, HPAM and its modifications are widely employed around the world. Not only HPAM increases viscosity of the solution, but it also has suitable rheological behavior. The aqueous solution behaves as a Newtonian fluid at low shear rates; at moderate shear rates it behaves as a shear thinning fluid and at high shear rates it plateaus again into Newtonian behavior. Thus, when injecting at near wellbore region in the field one would expect low viscosity of HPAM since shear rates around the wellbore are very high which in turn increases the injectivity of polymer

solution into the formation. As a polymer slug is propagated into the formation, lower shear rates trigger increase in viscosity of the polymer solution thus improving mobility control and sweep efficiency. Without adequate polymer concentration in ASP slug, the oil recovery suffers due to adverse mobility ratio. In order to have a stable flood, mobility ratio of the chemical slug to oil bank must be equal to or less than one (Gogarty et al., 1967). Mobility ratio is defined as the mobility of displacing fluid over the mobility of displaced fluid. Furthermore, polymers are used as mobility buffer that is injected after the main ASP slug. Injection of polymer drive after the ASP slug will prevent final water drive breakthrough into ASP solution and/or oil bank. However, due to field equipment constraints such as available pressure drop between injector and producer it is much harder to use ASP in viscous oils with favorable mobility ratio. Thus, polymer concentration might be lowered, so that chemical slugs can be injected into the formation at required rate (Gogarty, 1970).

2.5.4 CO-SOLVENT

Co-solvents are alcohols that are added to improve the surfactant formulation by making the primary surfactant sufficiently soluble in the brine. Iso-butanol (IBA), triethylene glycol monobutyl ether (TEGBE), sec-butanol (SBA), isopropanol (IPA) and diethylene glycol monobutylether (DGBE) are representative co-solvents that are used in surfactant formulation development (Sahni, 2010). Co-solvents have several benefits that enhances overall formulation; however, they have also significant drawbacks.

Co-solvents can minimize development of gels, liquid crystals, emulsions, inhibit separation of polymer-rich phase from surfactants, improve formulation equilibration time, and reduce microemulsion viscosity (Bourrel and Schechter, 1988). Furthermore, co-solvents can

also shift optimal salinities. Higher molecular weight co-solvent decreases optimal salinity and lower molecular weight co-solvent increases optimum salinity (Wade et al., 1977). Hsieh and Shah (1976) found that branched alcohols are more hydrophilic compared to straight-chain alcohols, and thus have higher optimum salinity. Reduction of microemulsion viscosity is one of the most important effects of adding co-solvent because microemulsion viscosities often exceed viscosity of the oil by an order of magnitude at low shear rates (Walker, 2011). Co-solvents also improve aqueous stability of ASP solution in the presence of polymer which is one of the most important parameter in ASP food design. Lastly, formulation equilibration time is significantly reduced when co-solvent is added. The microemulsion coalescence time is shortened when alcohol is added that in turn decrease equilibration time (Flaaten, 2007).

Co-solvents also have detrimental effects on surfactant formulations. Mainly they can increase IFT at optimum salinity. Salter et al. (1977) determined that IFT increases at optimum salinity as the concentration of low molecular alcohols such as isopropanol increases. Furthermore, co-solvents add extra cost to the final formulation. Sanz and Pope (1995) and others have demonstrated that alcohol free surfactant blends of ethoxylated sulfonate and internal olefin sulfonate can perform as well as formulations with alcohol.

CHAPTER 3: EXPERIMENTAL SETUP AND METHODOLOGY

Chapter 3 describes the experimental materials, chemicals, equipment used in the experiments. Furthermore, detailed methodology of conducting the experiments and involved calculations used for data analysis are presented.

3.1 Materials

3.1.1 FORMATION AND INJECTION BRINE

The formation brine and injection brine had the same salinity for all experiments. Synthetic brine was developed from a chemical analysis supplied by a company. Furthermore, all divalent ions such as calcium and magnesium were replaced by sodium ions in order to create a softened reservoir brine (SRB) formulation with salinity of 3,164 ppm. The salts were provided by Fisher Chemicals^{TM}. Table 3.1 shows softened reservoir brine composition.

Table 3.1: Softened reservoir brine (SRB) composition

Composition		Softened Reservoir Brine (SRB)
Cations		(mg/l)
1	Potassium	9
2	Sodium	1214
Anions		(mg/l)
1	Bicarbonate	147
2	Chloride	1792
3	Sulphate	2
TDS (mg/l)		3164.6
Total Divalent Cation		0
Total Monovalent Cation		1223

3.1.2 ALKALI

The main role of alkali is to reduce surfactant adsorption and create in situ soap by reacting with naphthenic acids in a crude oil. Sodium carbonate ($Na_2 CO_3$) was used as an alkali for the formulation development. Since solubility of sodium carbonate is around 22 gm/100ml in water at room temperature, only 10 wt% -20 wt% ranged stock solutions were used for the experiment. Lastly, for every new experiment different stock solutions were prepared because after some time sodium carbonate precipitates around the bottleneck area of the glass jar, and thus, altering the concentration of the stock solution.

3.1.3 SURFACTANT AND CO-SURFACTANT

Different surfactants were tried in the phase behavior formulation development out of which Alfoterra™ anionic surfactant provided by Sasol was selected as the main surfactant. Enordet™ internal olefin sulfonate (IOS) was used as a co-surfactant; it decreased equilibration time. The main surfactant's activity was equal to 79.2% and for the co-surfactant activity was equal to 30%.

3.1.4 POLYMER

A high molecular weight (MW=18 million Daltons) hydrolyzed polyacrylamides (HPAM) Flopaam™ 3630S polymer provided by SNF™ was used for the experiments. Making polymer stock solutions correctly is very important since polymer might not be well mixed, and thus, detrimental polymeric gels might be formed. Furthermore, polymer might relatively quickly degrade as the effect of oxygen exposure. Next paragraph describes the standard procedure for the preparation of polymer stock solutions.

In a wide plastic jar of volume 750 ml, 500 ml of DI water was poured and the required electrolytes was added and stirred by using a stir bar. It is very important to have stir bar that is around 3/4 of the diameter of the jar. Then solution was mixed at ~300 rpm so that the created vortex would be barely touching the stirring bar. In order to scavenge oxygen from the solution, it was bubbled with Argon for a couple minutes. After bubbling Argon, the required amount of polymer was slowly added into the solution. It is very important to add dry polymer particles exactly to the sides of the vortex in order to ensure proper mixing. After adding polymer, the stock solution was allowed to mix at a high rate until no separate polymer particles were observed. Afterwards, the mixing rate was decreased to around 100 rpm and allowed to mix for

3-4 days. After mixing was finished, the polymer solution was tested for filtration ratio (F.R.) defined by

$$F.R. = \frac{time_{80ml} - time_{60ml}}{time_{200ml} - time_{180ml}} \tag{3.1}$$

where $time_{200ml}$, $time_{180ml}$, $time_{80ml}$, and $time_{60ml}$ are times elapsed to collect 200, 180, 80, and 60 ml of filtered polymer solution, respectively. In order to ensure that the final polymer solution is homogenous the filtration ratio must be equal to or less than 1.2.

3.1.5 CRUDE OIL

Oil was received from a company and viscosities for oil were measured. Viscosity was about 250 cp. After filtering, reservoir oil was diluted with toluene in order to decrease viscosity to 100 cp by using a quarter power mixing rule,

$$\frac{1}{\mu_{A+B}^{1/4}} = \frac{V_A / Vtot}{\mu_A^{1/4}} + \frac{V_B / Vtot}{\mu_B^{1/4}} \tag{3.2}$$

where μ_{A+B} is viscosity of the final mixture, μ_A is viscosity of oil A, μ_B is viscosity of oil B, and $V_A, V_B, Vtot$ are the volumes of oil A, oil B and the total mixture respectively. The mixed oil mimicked the live oil viscosity of the field oil.

3.1.6 RESERVOIR SAND

Reservoir sand was obtained from a reservoir. It was used for all sandpack experiments. Figure 3.1 shows sand size distribution. Most of the sand size lies between 60 and 400 micron, and the median size is about 200 micron.

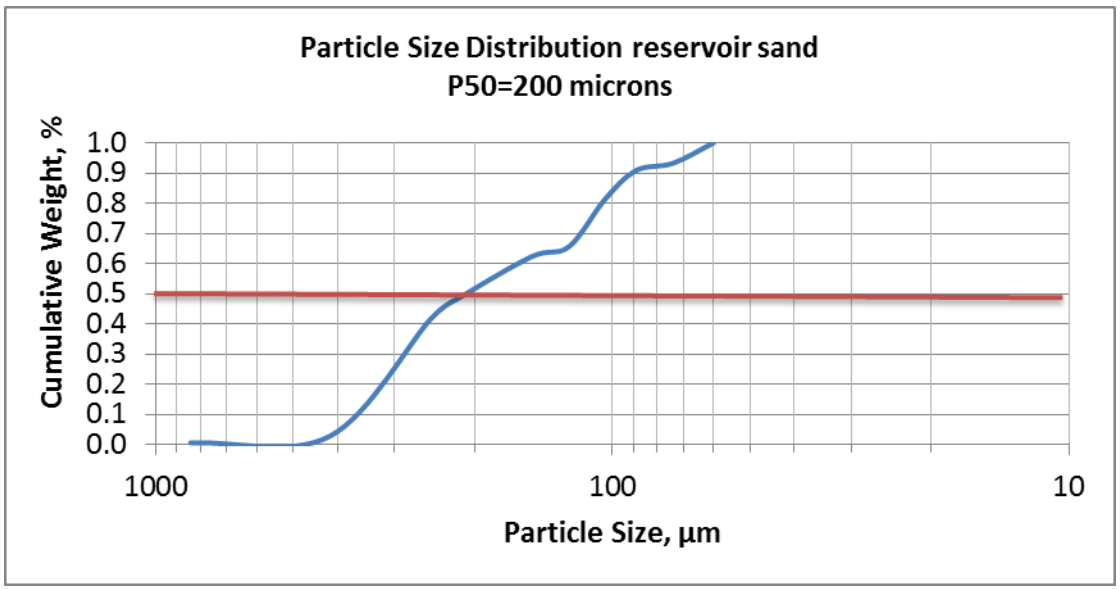

Figure 3.1: Reservoir sand size distribution

3.2 Phase Behavior Equipment and Methodology

3.2.1 Phase Behavior Equipment

Spinning Drop Interfacial Tensiometer

Interfacial tension (IFT) between ASP solution and crude oil was measured with a spinning drop interfacial tensiometer provided by TEMCO. It can measure ultra-low interfacial tension values. Interfacial tension value obtained from the solubilization ratio by using Huh's correlation (1979) at optimum salinity was confirmed by directly measuring IFT between the crude oil and ASP solution.

Fisherbrand™ Borosilicate Pipettes

Borosilicate pipettes provided by Fisher Scientific™ were used to perform phase behavior analysis. The pipettes have 5 ml of total volume and 0.1 ml graduations. After adding oil, ASP solution was blanketed with argon and sealed by using a propane torch. Worthington

propane torch was used to seal the borosilicate pipettes. A high-intensity flame with temperature in air that reaches 3,600 ^{o}F was created through Bernz-O-Matic^{TM} flame nozzle.

Pipette Repeater

Pipette repeater provided by Eppendorf^{TM} was used to dispense accurately oil and ASP solution into the borosilicate pipettes. It can dispense different values ranging from 25 microliters to 1000 microliters.

3.2.2 PHASE BEHAVIOR METHODOLOGY

Aqueous Stability

Injection of homogenous ASP solution that does not exhibit any phase separations, cloudiness, and precipitation is very important because otherwise it leads to nonuniform delivery of chemicals and significant phase trapping in the formation. A surfactant solution must be clear or single-phase up to or higher than the injection salinity. This is called the aqueous stability test. In general, aqueous stability test is done by mixing a surfactant formulation which includes the main surfactant, co-surfactant and co-solvent with polymer over wide range of salinities at the target temperature. There are two methods to change salinity. One way is to fix salinity concentration and change alkali concentration and the other one is to fix alkali concentration and change salt concentration. If the surfactant formulation does not pass aqueous stability test, the contents of the formulation are changed until the formulation is stable over the required range of salinities.

Phase Behavior Screening

After a surfactant formulation (a unique blend of surfactant, co-surfactant, and co-solvent) passed the aqueous stability test, the phase behavior experiments were performed on the

surfactant formulation with oil. Initially, no polymer was added into the formulation because polymer has been shown to have little effect on the phase behavior. Pope et al. (1982) stated that the phase behavior sequence was the same with and without polymer over the range of salinities tested except for a limited range of salinities where three-phase region shifts left by a small salinity.

The surfactant formulation was pipetted into borosilicate pipettes and gently tapped on the table so that no trapped air was in the bottom of the pipette. After the aqueous levels recorded, oil was added on top of the surfactant formulation. The amount of oil and the surfactant formulation depends on the chosen water oil ratio (WOR). Generally, initial phase behavior experiments are performed on WOR's equal to one. Next, argon was blanketed on top of the samples, and the pipette sealed with a flame torch. For the first couple of hours, samples were put into an oven at 59 ^{o}C, and the tubes were mixed every 30 minutes. Since temperature of the reservoir of interest was equal to the ambient room temperature, the samples were taken out of the oven and were mixed every 3-4 hours over the next few days until no change in the interface reading was observed.

Microemulsion Viscosity Measurements

The microemulsion viscosity is very important for successful flooding is measured in a rheometer. The rheometer requires at least 0.6 ml of the sample to measure viscosity in a 2^{o} cone and plate geometry. Therefore, after getting successful microemulsion phase behavior in the 5ml borosilicate pipettes, bigger (in volume) samples of the final surfactant formulation along with oil were created. All components' volumes were increased such that ratio of all components stays the same as in the small pipettes and the expected Type III phase volume was at least 1ml in volume. The samples were made in the same salinity range as the pipette samples.

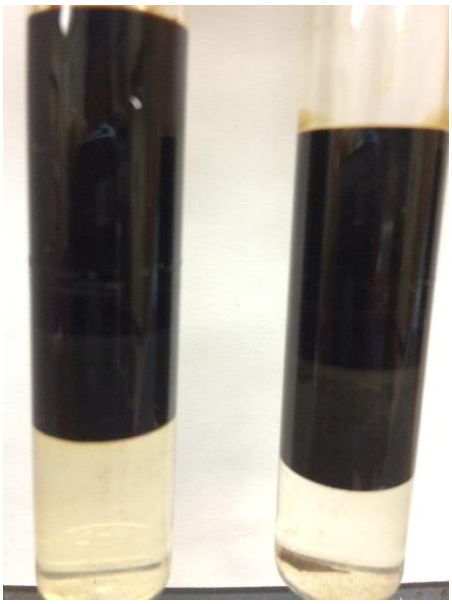

Figure 3.2:Two equilibrated Type III microemulsions

3.2.3 PHASE BEHAVIOR CALCULATIONS

Solubilization Plots

The oil or water solubilization ratio is defined as the ratio of volume of oil or water in the microemulsion phase over the volume of surfactant in the microemulsion phase, and expressed by Equation 3.3 for oil and Equation 3.4 for water, i.e.,

$$\sigma_o = \frac{V_o}{V_s} \tag{3.3}$$

$$\sigma_w = \frac{V_w}{V_s} \tag{3.4}$$

where, σ_o is the oil solubilization ratio , V_o is the volume of oil in the microemulsion phase , σ_w is the water solubilization ratio , V_w is the volume of water in the microemulsion phase, and V_s is the volume of surfactant in microemulsion phase.

The oil and water solubilization ratios are calculated over the range of salinities and plotted on solubilization plot shown in Figure 3.3.

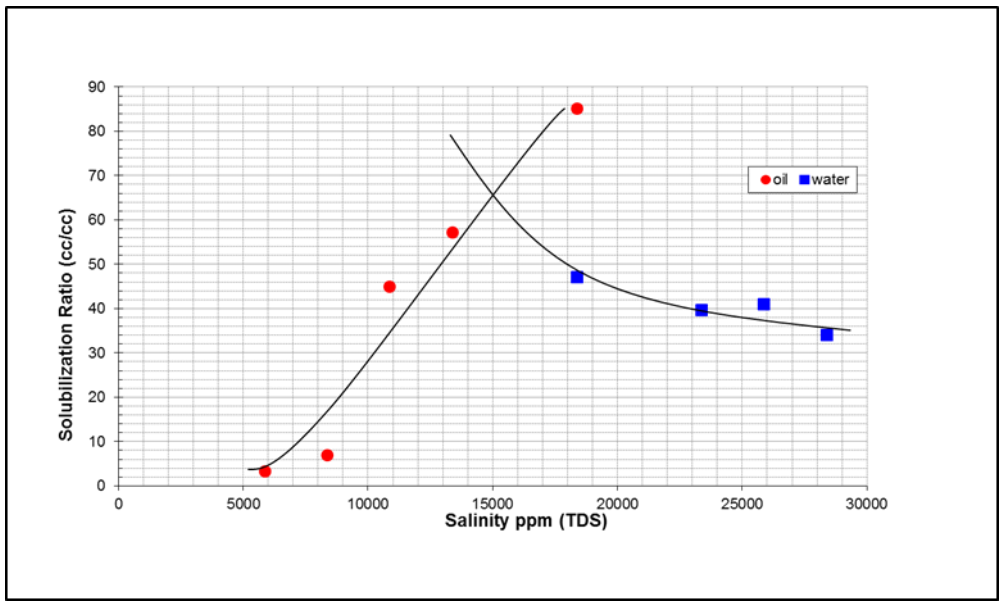

Figure 3.3: Example of surfactant solubilization plot

The point where lines for oil and water solubilization ratios intersect is called the optimum salinity. The lowest IFT is usually achieved at the optimum salinity.

Activity Diagram

One way to see whether oil is reactive is to plot the activity diagram. The reactive crude oil contains naphthenic acids which react with alkali to produce in situ soap. The produced soap is typically hydrophobic; hence, the optimum salinity tends to shift to lower salinities as the concentration of the oil in the phase behavior pipettes is increased. For non-reactive crude oils the optimum salinity does not change with the oil content. The activity diagram is the plot of oil concentration on the x-axis and total dissolved solids concentration or alkali concentration on the

y-axis. The activity diagram in Figure 3.4 illustrates how the optimum salinity is lowered as the oil concentration is increased for reactive crude oils.

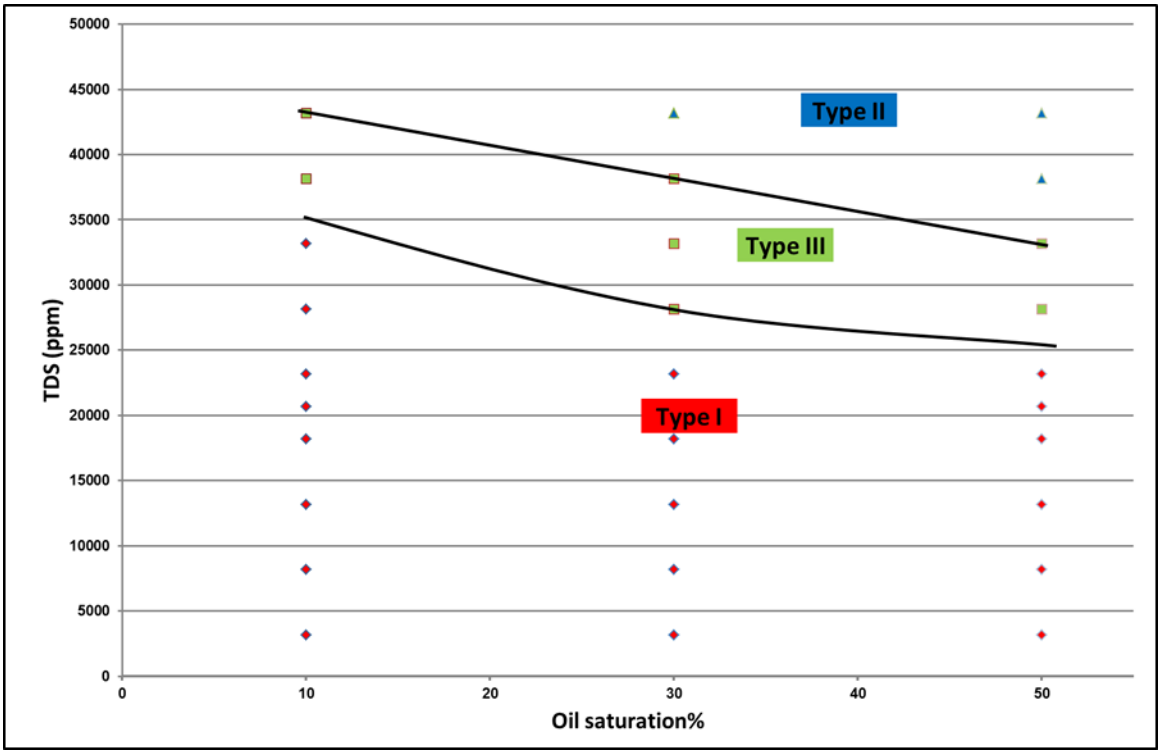

Figure 3.4: Example of activity diagram for reactive crude oil

3.3 Sandpack Equipment and Methodology

3.3.1 The Sandpack Flooding

Brine Tracer Test

Brine tracer test was performed in order to determine the pore volume of the sandpack. It involves injecting higher salinity brine compared to the formation brine. Salinity of the effluent samples were measured and plotted against injected pore volumes. In theory, the midpoint of the S-shaped curve should be equal to 1PV of the sandpack in 1D floods. For 2D floods, measured salinity was used to calculate sweep efficiencies of the quarter five-spot pattern. Many studies showed that the typical sweep efficiency in a five-spot pattern was equal to around 0.7. Using

this information, the pore volume was varied such that it matches the sweep efficiency of 0.7 at the breakthrough. The detailed description of the pore volume determination in 1D and 2D floods is presented in the calculations section.

Oil Flood

The oil flooding was conducted in order to saturate the sandpack. The sandpack was placed vertically and injected oil from the top at ~400 psi and displaced water was collected from the bottom of the sandpack. After 2-3 days the procedure was repeated in order to see whether any residual water could come out. The volume of displaced water was equal to the initial oil saturation.

In addition to oil saturation, the oil flooding was conducted to determine the oil permeability. Oil was injected at different flow rates until the pressure drop was stabilized. Then, the pressure drop for each flow rate was used to calculate the effective oil permeability at the residual water saturation.

Water Flood

After the brine tracer test and the oil flooding the waterflooding commences. For 1D floods, the waterflooding was conducted for at least 5 PV in order to ensure no oil was coming out and that pressure drop was stabilized. For 2D floods, the waterflooding was conducted for around 1PV only. The effluent samples were collected at the same time interval by using the fractional collector. The waterflood oil production was recorded, and the residual oil saturation to water was calculated by using mass balance. Lastly, the effective water permeability at the residual oil saturation to water was estimated and used to determine the end-point relative permeability to water.

Chemical Flood

The chemical flood followed waterflooding. Initially, 0.5 PV of ASP slug was injected, followed by polymer drive. The ASP slug is the same for all floods including 2D floods except small variation for the 1D flood in a steel tube experiment. The injection rates of ASP and polymer slugs were 1 ft/day for all type of floods. The effluent samples were collected using the fractional flow collector and oil cut was determined from the collected samples. The oil recovery and residual oil saturations were determined by mass balance from the effluent samples.

Effluent Analysis

The effluent analysis was done on the samples in order to see propagation of the chemical slugs and determine the surfactant retention. Furthermore, viscosity, pH, salinity and the surfactant concentration in each tube were measured.

3.3.2 SANDPACK EQUIPMENT

Steel Tube

The steel tubes provided by Autoclave Engineers^{TM} (3 ft in length and 0.67 inches in diameter) were used for the 1D displacement experiments. These tubes were used as 1D column for the reservoir sand.

Biaxial Type Core Holder

A biaxial type core holder provided by Phoenix Instruments was used to perform the sandpack floods. The reservoir sand was dry packed inside the rubber sleeve of the core holder and vacuumed for a day. Then both radial and axial stresses were applied through injecting water into the confining pressure ports. The maximum working pressure was 5000 psi. The sandpack was tested for leakage before starting the experiment.

Quarter Five-Spot Model Apparatus

A quarter five-spot cell is a cylindrical, stainless steel case designed to hold a sandpack that is 10 inches square and 1 inch thick. The cell is composed of three stainless steel plates that are bolted together. The top and bottom plates are identical and are used to hold an overburden pressure, while middle plate is used to hold sandpack. The quarter five-spot cell has confining pressure ports that are used to apply overburden pressure between rubber sleeves and top and bottom plates. The overburden pressure that can be applied was 2000 psi.

Stainless Steel Accumulator

The stainless steel accumulators provided by TEMCO™ were used as the transfer cylinders for the oil, polymer and ASP slug . They have a floating piston that separates two fluids. Vertically positioned accumulators were pumped in brine/tap water from the bottom end, and fluids on the other side of the piston would be displaced into the sandpack . These accumulators can operate at pressures up to 3750 psi.

Syringe Pumps

Teledyne™ ISCO 500D syringe pumps were used to pump fluids during the experiment. Brine was injected directly into the sandpack through the pump, however, for oil, ASP and polymer injection, pumps were used to inject brine/tap water into the stainless steel accumulator that kept fluids inside. The pumps have total 507 ml volume available inside and can operate at pressure up to 3750 psi.

Pressure Transducer

The pressure transducers from Honeywell™ were used to record pressure drops between inlet and outlet of the sandpack. The pressure measurement ranges between 0-300psi .The pressure transducers convert the measured pressure drop into voltage reading , which in turn is

sent to computer and recorded on a excel spreadsheet through Data Acquisition Card (DATAQ).In order to convert back to pressure, the calibration curve between voltage readings and pressure drop was generated before starting the experiment. The example of calibration curve is shown in the Figure 3.5.

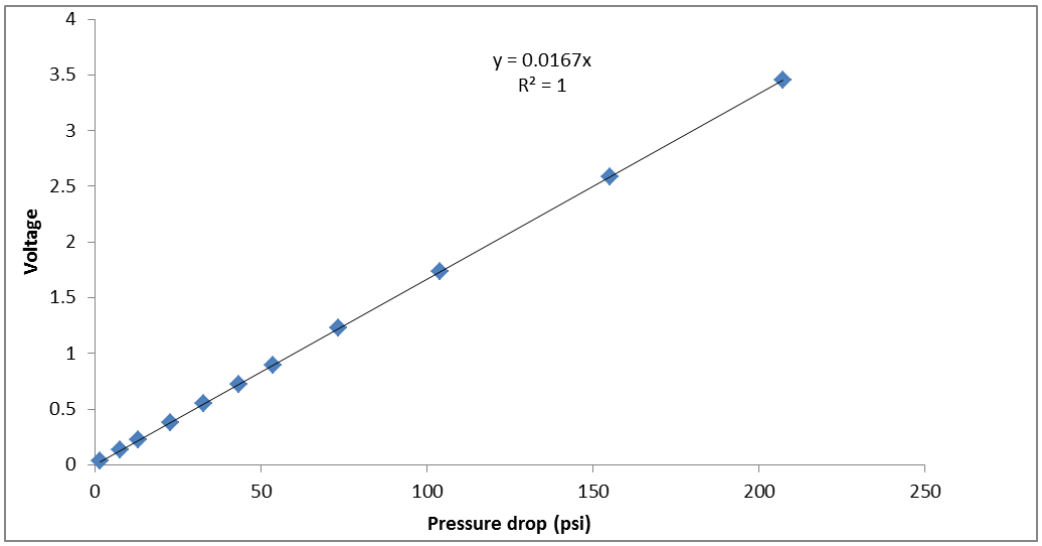

Figure 3.5: The calibration curve between voltage and pressure drop

Fraction Collector

The effluent samples from the sandpack were collected by using ISCO Retriever 500^{TM} fraction collector provided by ISCO Instruments. The fractional collector can hold up to 68 test tubes at the same time. All effluent samples were collected at the fixed time interval.

Refractometer

A portable refractometer RF12, provided by Extech Instruments, was used to measure refractive indices of the effluent samples and bulk solutions. The calibration curve between refractive index and salinity was generated for conversion from refractive indices to salinities of brine and aqueous phase of the effluent samples.

Rheometer

The viscosities of oil, brine, polymer, and ASP slugs were measured by using AR-G2 rheometer provided by TA instruments. The rheometer can measure viscosities using several different geometries such as cone and plate and concentric cylinders. The 2^o cone and plate geometry was used to measure viscosities of solutions. The required sample size was about 0.6 ml. The sample is loaded on a peltier plate, and the rheometer rotates cone which contacts fluid on plate. The torque required to rotate the fluid at that particular speed is converted to a viscosity value. The minimum torque that can be applied was about 0.003 $\mu N.m$ and the maximum torque was about 200 $\mu N.m$. In general, viscosities obtained at 0.01 s^{-1} shear rates and above were considered accurate.

High Performance Liquid Chromatograph (HPLC)

The UltiMate^{TM} 3000 HPLC by Dionex was used to measure the dynamic surfactant retention in the effluent samples after sandpack flooding. HPLC can separate different components of a sample by using chromatographic process. Furthermore, HPLC measures retention time of each separated components. The calibration samples that were prepared from the batch ASP solution were measured. Later, a calibration curve between the surfactant retention time and its concentration was generated. The calibration curve was used to get surfactant concentration in the effluent samples.

pH Meter

The Oakton waterproof pH meter was used to measure pH of the effluent samples and batch solutions. It can measure pH of solutions with +/- 0.01accuracy, and it can also measure

temperature of the solutions up 50 °C. The pH meter is calibrated with pH 4, 7, 10 buffer solutions every time before measuring pH of the effluent samples.

Handheld UV Lamp

A handheld UVL-56 ultraviolet lamp provided by Analytik Jena Company was used to better distinguish interfaces between free oil and microemulsions. It emits long wave ultraviolet light at 365 nm wavelength.

Filter Press

A stainless steel OFITE filter press was used to filter stock solutions of oil, polymer, and ASP. Polymer and ASP solutions were filtered by using 1.2 μm Millipore hydrophilic cellulose filter paper at 15 psi argon gas pressure. Oil and brine stocks were filtered by using 1.2 μm and 0.45 μm filter paper respectively.

3.3. 3 SANDPACK FLOOD IN A STEEL TUBE AND CORE HOLDER.

Sandpack Preparation in a Steel Tube

The steel tube sandpack packing started with wetting reservoir sand thoroughly. Then, wetted sand was packed in to 3 feet long steel tube while adding some brine. Extra brine was added in order to get rid of trapped air. While packing, the steel tube was tapped often in order to dislodge air and ensure tight packing. Excess water was drained from the bottom and after capping the steel tube was flooded from the bottom connection port in order to ensure no air was trapped inside the dead volume zone.

Sandpack Preparation in a Core Holder

The core holder was dry packed. Dry reservoir sand was poured into the core holder while at the same time the core holder was being vacuumed from the bottom. The sandpack was

regularly tapped from outside during the whole process. After capping the core holder, it was vacuumed for one day before proceeding with the experiment.

3.3.4 SANDPACK FLOOD IN A 2D QUARTER FIVE-SPOT PATTERN

2D Quarter Five-Spot Pattern Description

Figure 3.6 shows a sketch of the quarter five-spot sand pack and the picture of the actual quarter 5-spot sand pack. The flooding area is rectangular shape with 10”×10”×1”. It is covered on top and bottom with a rubber sheet where confining pressure can be applied. The sandpack is encased with steel.

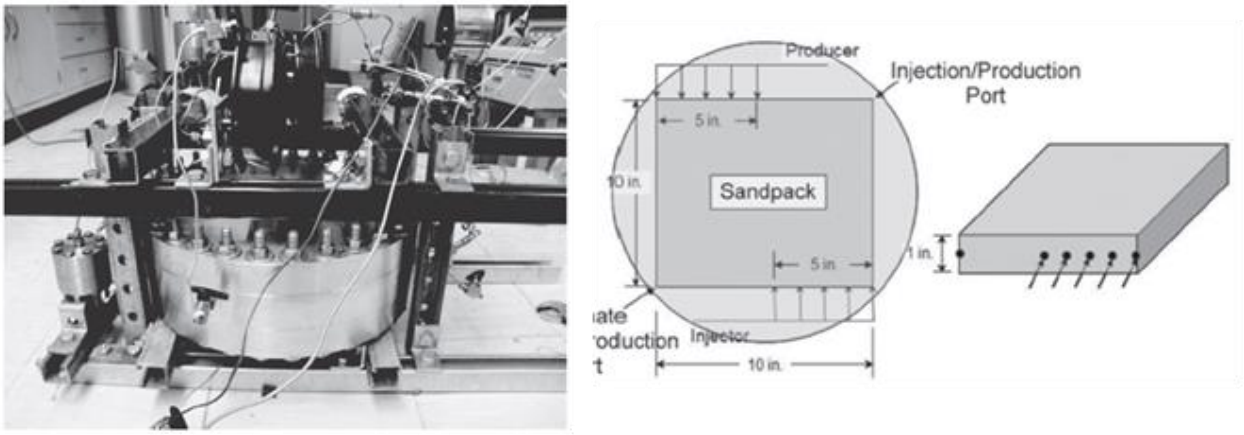

Figure 3.6: A quarter five-spot pattern (Kumar, 2013)

2D Quarter Five-Spot Sandpack Preparation

The quarter five-spot pattern was wet packed. The reservoir sand was wetted with excess water and mixed at the same time in order to dislodge trapped air inside the reservoir sand. Then, water wetted sand was spread in small quantities inside the square shaped slot for sand while adding excess of water. Further, extra sand was scraped off from top of the sandpack, and the circular rubber sleeve was put on top of the sandpack. Subsequently, the top steel plate was screwed on. The bottom and top rubber sleeves were used to separate the sandpack and the

overburden liquid. The Figure 3.7 shows the top plate and the square shaped slot filled with sand on top of which the rubber sleeve was placed.

Figure 3.7: Top steel plate and middle plate with the sandpack

After closing the five-spot pattern, overburden pressure of 1300 psi was applied. For that purpose top and bottom plates have two injection ports each. Injection ports are used to inject liquid into the hollow space between the rubber sleeves and the inside surface of the plates. Then, the side valves of the 5-spot were opened so that excess amount of water can be leaked out. The compression of the sand from bottom and top ensures creation of tighter sandpack.

3.3.5 SANDPACK FLOOD CALCULATIONS

Pore Volume and Porosity Estimation in a 1D Flood

The sandpack pore volume in a 1D flood was determined by conducting brine tracer test. The brine salinity that was two times of the formation salinity was injected into the 1D sandpack. The injection was carried out until the effluent samples' salinity was equal to injection brine salinity. Then, the brine salinity was normalized and plotted against injected pore volumes. In

theory, for the homogenous 1D sandpack the normalized salinity plot should be S shaped and the midpoint of the S-shaped curve should be equal to the sandpack pore volume. Obtained pore volume was divided by total volume to get porosity of the sandpack. The Figure 3.8 shows a typical plot.

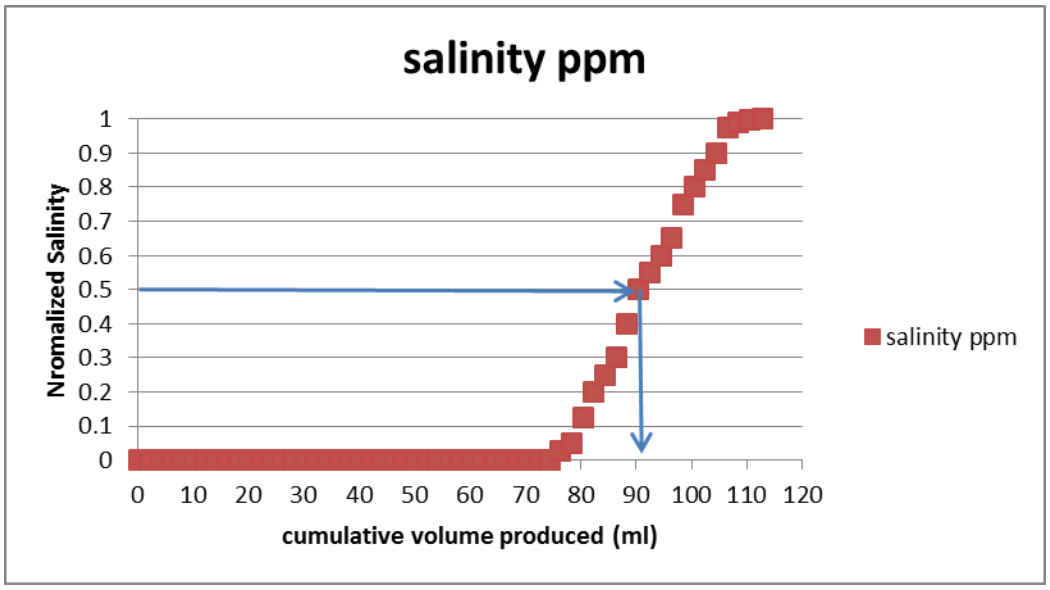

Figure 3.8: Example of estimation of 1D sandpack pore volume

Pore Volume and Porosity Estimation in a 2D Flood

A quarter five-spot pore volume can be estimated with two methods. First, after wet packing the reservoir sand inside the five-spot pattern, the amount of water that would be expelled due to applying overburden pressure was subtracted from the total water that was added during wet packing the sandpack. Obtained value should be equal to the pore volume of the sandpack. This method is less accurate than the second method which is conducting a brine tracer test in the 2D sandpack. It involves determining sweep efficiency in the miscible flood of the homogenous five-spot pattern. Sweep efficiency is calculated as follows

$$E_A = \int_0^{t_D} (1 - \frac{C_D}{C_{D_o}}) dt_D \qquad (3.5)$$

where, E_A is the sweep efficiency of the sandpack, t_D is the injected pore volumes, C_D is the normalized salinity at the outlet, and C_{D_o} is the normalized salinity at the inlet which is equal to one.

Habermann (1960) estimated sweep efficiencies for a five spot patterns and found out that the sweep efficiency at breakthrough was typically equal to 0.7 during miscible floods. Furthermore, from Brigham et al., (1965) it was found that breakthrough occurs close to 0.72 PV during the miscible flood.Lastly, the sweep efficiency of the brine flood must not exceeed 1.0 close to the end of the tracer test. Thus, the pore volume was adjusted until the curve of sweep efficiency matched the sweep efficiency at the breakthrough (E_{Abt}) which must be close to 0.7 and the final sweep efficiency (E_{Afinal}) which must be close to value 1.0. Figure 3.9 shows the example of brine tracer test done on the quarter five-spot pattern, it can be seen that E_{Abt} and E_{Afinal} matched reuired values of 0.7 and 1.0 respectively.

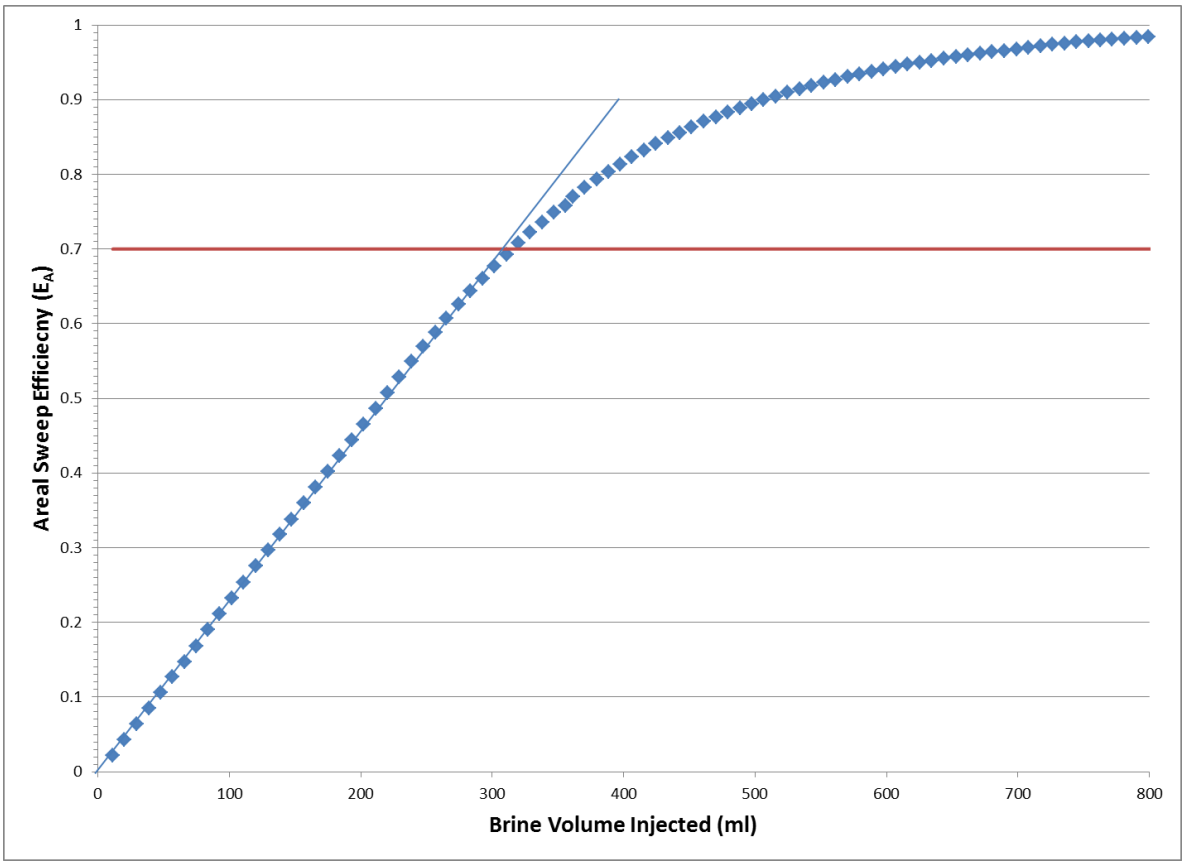

Figure 3.9: An example of pore volume determination in a quarter five-spot pattern

Absolute Water (Brine) Permeability

In order to get absolute water permeability, pressure drop was measured during single phase brine flow when the sandpack was fully saturated by brine only. Absolute brine permeability in 1D flood was calculated by using Darcy's law

$$k_{w@Sw=100\%} = \frac{q_w \mu_w L}{A \Delta P} \tag{3.6}$$

where, $k_{w@Sw=100\%}$ is the absolute water permeability, q_w is the water flow rate, μ_w is the water viscosity, L is the sandpack length, A is the cross-sectional area perpendicular to the flow, and ΔP is the pressure drop across the sandpack.

Effective Oil Permeability

The effective oil permeability was calculated during oil flood when water saturation was at the residual value. The oil flow rate was varied until pressure drop is stabilized at each new oil flow rate. The effective oil permeability at the residual water saturation was calculated as follows

$$k_{o\_eff} = \frac{q_o \mu_o L}{A \Delta P} \tag{3.7}$$

where, k_{o_eff} is the effective oil permeability, q_o is the oil flow rate, μ_o is the oil viscosity, L is the sandpack length, A is the cross-sectional area perpendicular to the flow, and ΔP is the pressure drop across the sandpack.

Effective Water Permeability after Waterflood

Effective water permeability was calculated at the end of the waterflood when no oil was being produced and pressure drop stabilized across the sandpack at the constant flow rate. The effective water permeability at the residual oil saturation to the water was calculated as follows

$$k_{w\_eff} = \frac{q_w \mu_w L}{A \Delta P} \tag{3.8}$$

where, k_{w_eff} is the effective water permeability, q_w is the water flow rate, μ_w is the water viscosity, L is the sandpack length, A is the cross-sectional area perpendicular to the flow, and ΔP is the pressure drop across the sandpack.

End Point Oil/Water Relative Permeability

The endpoint oil relative permeability was determined by dividing the effective oil permeability at the residual water saturation by the base permeability. The base permeability was chosen to be the absolute water permeability. The end-point oil relative permeability at the residual water saturation was calculated as follows

$$k_{ro} = \frac{k_{o\_eff}}{k_{w@Sw=100\%}} \tag{3.9}$$

where, k_{ro} is the end-point oil relative permeability at the residual water saturation, k_{o_eff} is the effective oil permeability, and $k_{w@Sw=100\%}$ is the absolute water permeability.

The end-point water relative permeability was calculated in the similar way by dividing the effective water permeability at the residual oil saturation to water by the absolute water permeability

$$k_{rw} = \frac{k_{w\_eff}}{k_{w@Sw=100\%}} \tag{4.0}$$

where k_{rw} is the end-point water relative permeability at the residual oil saturation, k_{w_eff} is the effective water permeability, and $k_{w@Sw=100\%}$ is the absolute water permeability.

Initial Oil Saturation

Initial oil saturation was calculated from the mass balance. At high pressure drop (~400psi) oil was injected into the sandpack that was initially fully saturated with the formation brine, and the displaced water was collected until no water would come out. The initial oil saturation estimated by

$$S_{oi} = \frac{V_{water\_produced}}{V_p} \tag{4.1}$$

where S_{oi} is the initial oil saturation, $V_{water\_produced}$ is the volume of produced that is also equal to volume of oil in the sandpack, and V_p is the pore volume of the sandpack

Cumulative Oil Recovery

Cumulative recovery was estimated from the oil recovered in the effluent samples. De-emulsifier was added to the effluent samples so that oil solubilized in the microemulsion would be separated from the microemulsion. The oil recovery was estimated as follows

$$N_p = \frac{\Sigma V_{oil}}{V_p} \tag{4.2}$$

where, N_p is the cumulative oil produced, V_{oil} is the effluent oil volume in the produced sample, and V_p is the pore volume of the sandpack

Oil Cut

Oil cut, which is a fraction of oil in the total volume produced, was estimated from the oil produced at the outlet, and defined as

$$f_o = \frac{V_{oil}}{V_{oil} + V_{water}} \tag{4.3}$$

where, f_o is the oil cut in the effluent sample produced, V_{oil} is the effluent oil volume in the produced sample, V_{water} and is the effluent water volume in the produced sample,

CHAPTER 4: RESULTS

The objective of this work was to find an ASP formulation that works with a reservoir oil of 100 cp viscosity, and show its effectiveness in 1D and 2D (quarter five-spot pattern) floods. The volumetric sweep efficiency becomes one of the major factors in viscous oil recovery in addition to factors that affect 1-D ASP floods.

Initially, a specific ASP formulation was suggested by the company. This formulation was tested along with modifications to this formulation. Two 1-D sandpack ASP floods were conducted with the original and modified ASP designs. The principal difference between the two designs was the mobility control during the flood.

4.1 Original Formulation

4.1.1 ASP Formulation #1 for Reactive Crude Oil

A specific surfactant formulation was initially provided by a company. At that time, they had done preliminary work on microemulsion phase behavior and selected specific surfactant, alkali, and co-solvent. Furthermore, they also selected HPAM polymer concentration.

Final ASP injection formulation included 1% Alfoterra surfactant provided by Sasol, 1% isobutanol (IBA) alcohol as a co-solvent, 1.75% sodium carbonate (Na_2CO_3), and synthetic reservoir brine (3164 ppm). Figure 4.1 shows solubilization plot of the surfactant formulation. Salinity was varied by changing Na_2CO_3 concentration. The optimum salinity was determined to be around 15,000 ppm of alkali concentration. The solubilization ratio are quite high and equal to 60 at optimum salinity, however, the equilibration time was about a month.

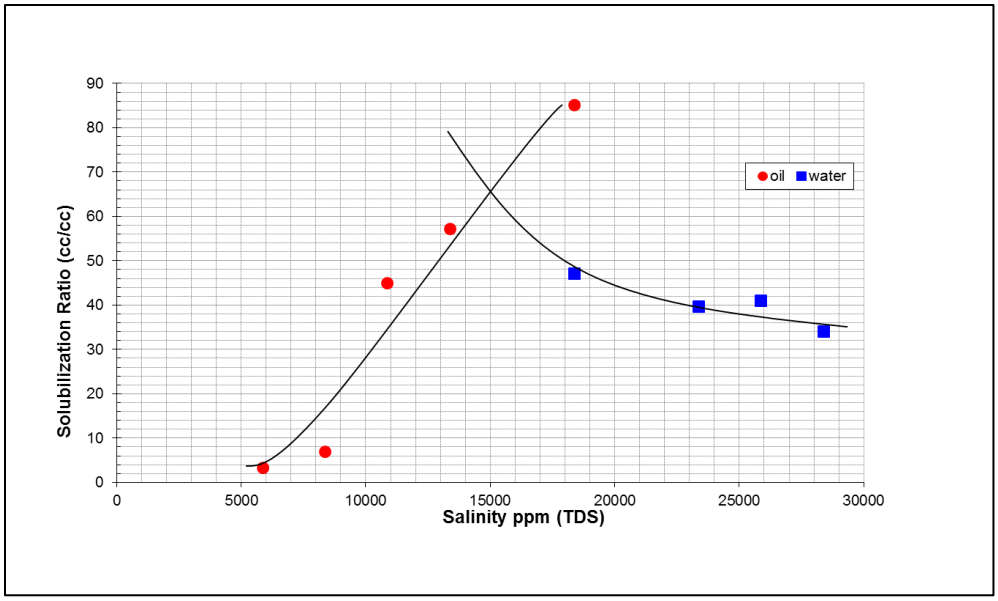

Figure 4.1: Solubilization plot for ASP#1 formulation

4.1.2 1D ASP#1 SANDPACK FLOOD

Tracer Test and Brine Flood

After carefully wet-packing reservoir sand into 3ft long steel tube, the sandpack tracer test was performed, where at first 10,000 ppm NaCl brine was injected until salinity did not change. Next, salinity of 20,000 ppm NaCl brine was injected and effluent salinities were measured by using a refractometer. The volume produced where normalized concentration equals 0.5 indicates the pore volume of the sandpack.

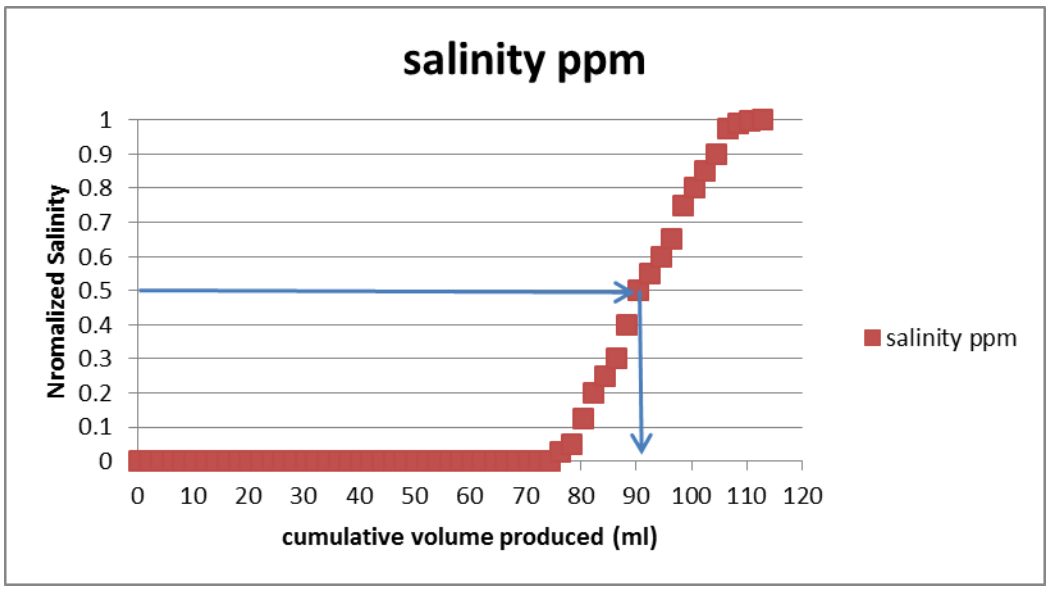

Figure 4.2: Tracer rest for ASP#1 sandpack flood

Figure 4.2 shows that the sandpack pore volume was equal to 90.38 ml, and thus, by dividing pore volume by total volume of the steel tube porosity was determined to be equal to 43.4%

In order to get absolute brine permeability, the sandpack was flooded with the SRB. After obtaining brine permeability from pressure drop data, the sandpack was saturated with the reservoir oil at a pressure drop of ~400 psi. After a couple days, oil was injected again to dislodge any residual water that was left inside. At the end, the initial oil saturation of 84% was obtained before the waterflooding. Furthermore, oil flood was performed to get the effective oil permeability at the residual water saturation. Table 4.2 lists brine and oil permeabilities and other sandpack properties obtained. 1D ASP sandpack flooding apparatus is sketched in Figure 4.3.

Table 4.1: Properties of reservoir sand sandpack

ASP#1 Sandpack Properties and Initial Condition:	
Outcrop:	reservoir sand
Mass:	311 gm
Porosity:	0.435
Length:	3 ft
Diamter:	0.67 in
Area:	0.352 in^2
Temperature:	25 ^oC
Overburden Pressure:	None
Brine Permeability:	7.66 D
Oil Permeability:	8.04 D
Pore Volume:	90.38 ml

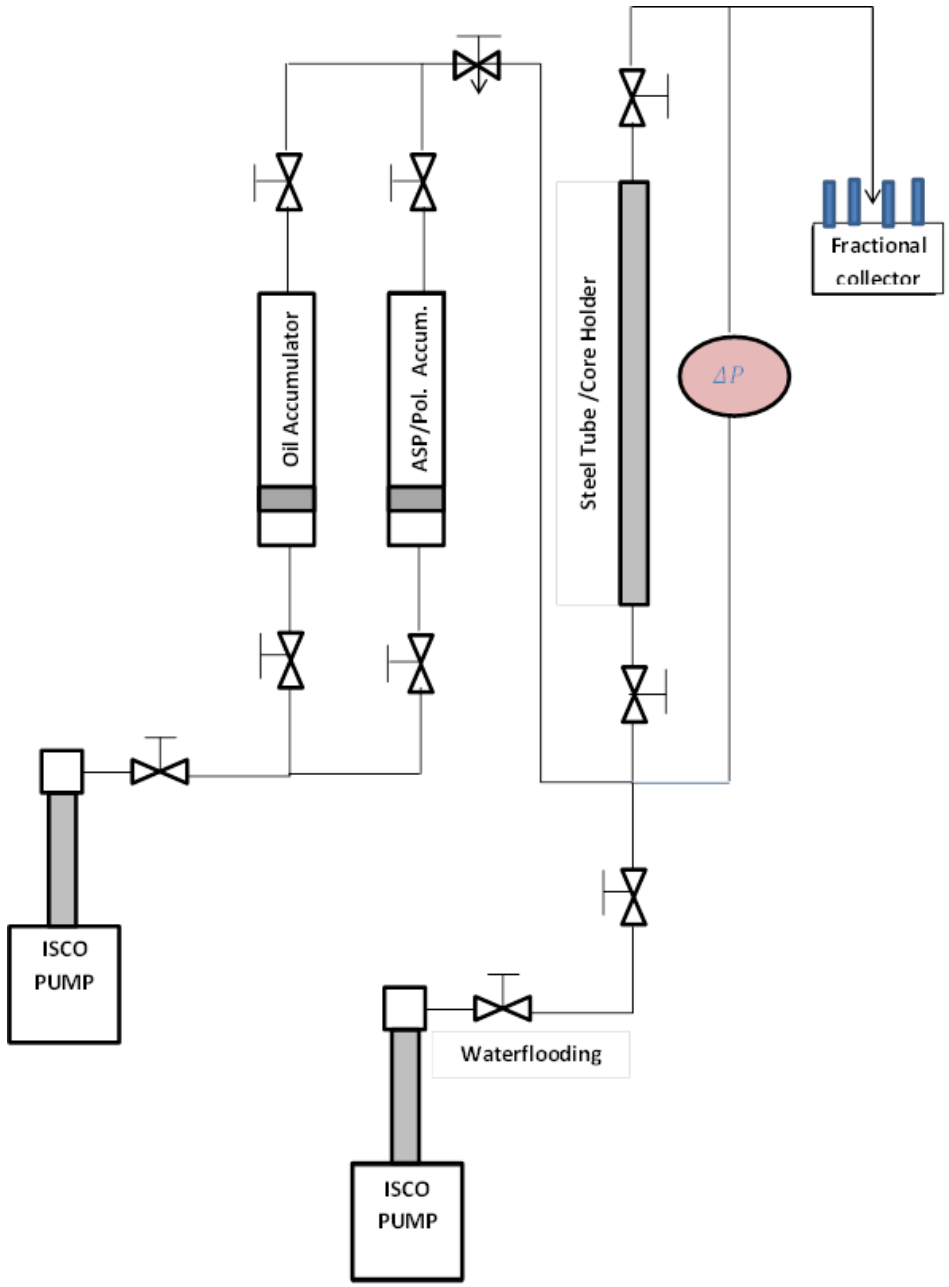

Figure 4.3: 1D ASP sandpack flood apparatus

ASP#1 Sandpack Waterflood

The sandpack was waterflooded with SRB brine for at least 5 PV; no oil was coming out at the end. Frontal velocity of the waterflood was to **10 ft/day**. Thus, the end point relative

permeabilities for oil flood and water flood, residual water saturation to oil, and residual oil saturation to water from both oil flood and waterflood were obtained. The effluent data were used to get relative permeability curves, but most importantly, apparent viscosity and total relative mobility of the oil/water bank. Table 4.3 shows the flow properties and Figure 4.4 shows constructed relative permeability curves calculated from the Corey model.

Table 4.2: Mobility control requirement parameters for ASP#1

Mobility control requiremnent parameters for ASP#1			
Parameter	Definition	Value	Basis
K_{rw}^{o}	End point water relative permeability	0.0251	Obtained from waterflood
K_{ro}^{o}	End point oil relative permeability	1	Obtained from oil flood
n_w	Fractional flow exponent water	2	Assumed for water wet
n_o	Fractional flow exponent oil	2	Assumed for water wet
S_{wr}	Residual water saturation to oil	0.16	Calculated from mass balance
S_{or}	Residual water saturation to water	0.4	Calculated from mass balance
μ_w	Water viscosity	0.9	Measured in rheometer
μ_o	Oil viscosity	100	Measured in rheometer

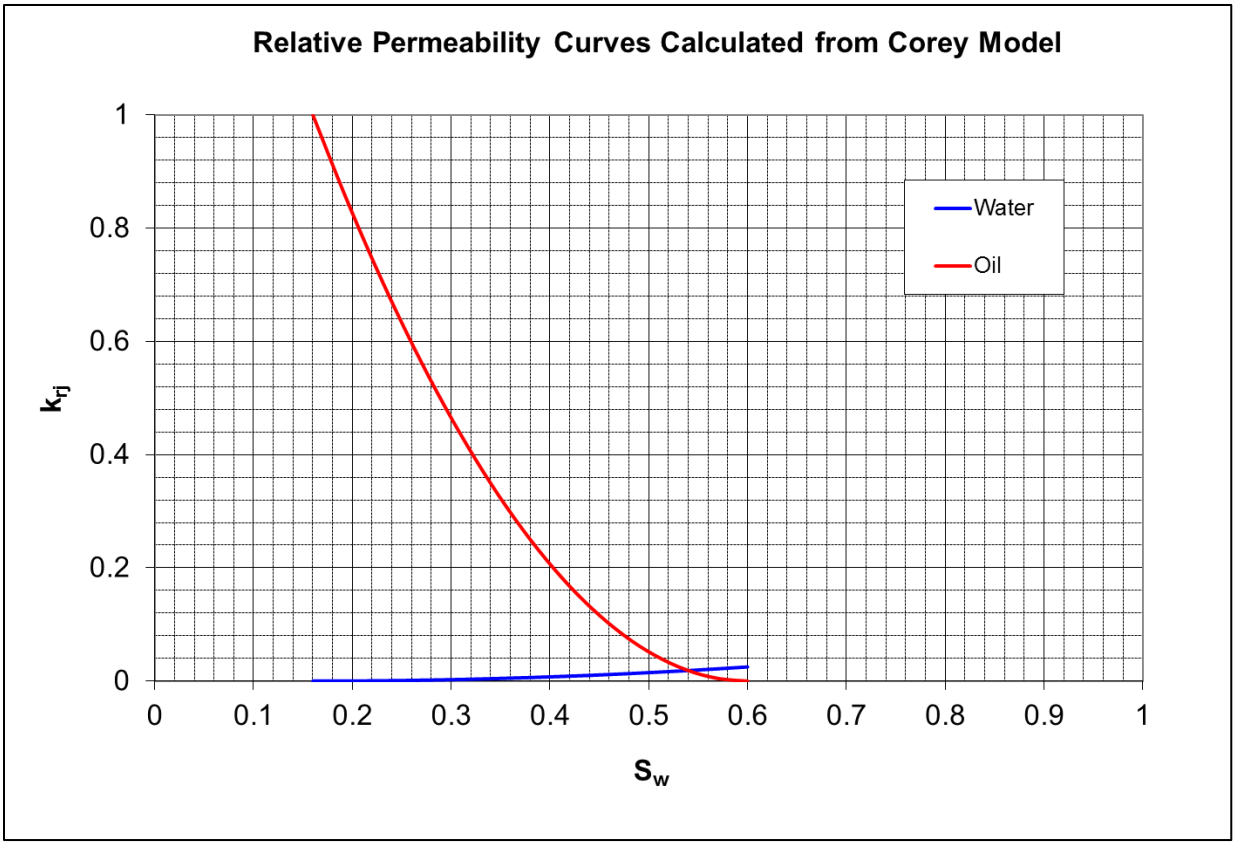

Figure 4.4: Relative permeability curves for ASP#1

ASP#1 Mobility Control Requirements and Design

From the relative permeability data, total relative mobility and apparent viscosity curves were constructed. Figure 4.5 shows that the minimum total relative mobility was calculated to be ~0.0073 cp^{-1}, and thus, the maximum apparent viscosity of the oil bank was ~136 cp, which is equal to the reciprocal of the minimum point for the total relative mobility. Therefore, ASP and polymer drive slugs must have a viscosity around 136 cp for a stable displacement of oil/water bank.

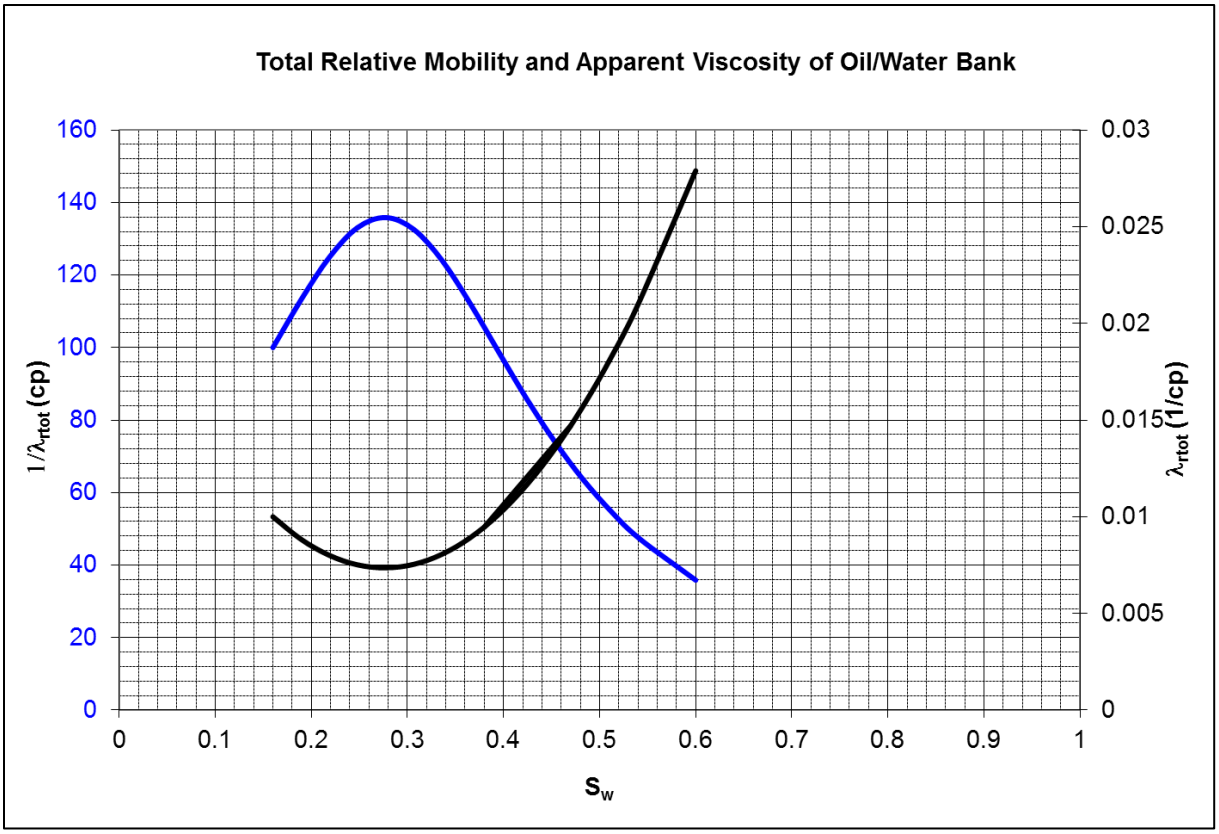

Figure 4.5: Total relative mobility and apparent viscosity of oil/water bank for ASP#1

The original formulation had polymer (HPAM 3630S) concentrations of 3000 ppm and 2000 ppm in ASP slug and the polymer drive, respectively. Figures 4.6 shows viscosity versus concentration of polymer behavior at fixed salinity of around 13,000 ppm which includes 1% Na_2CO_3 and SRB brine.

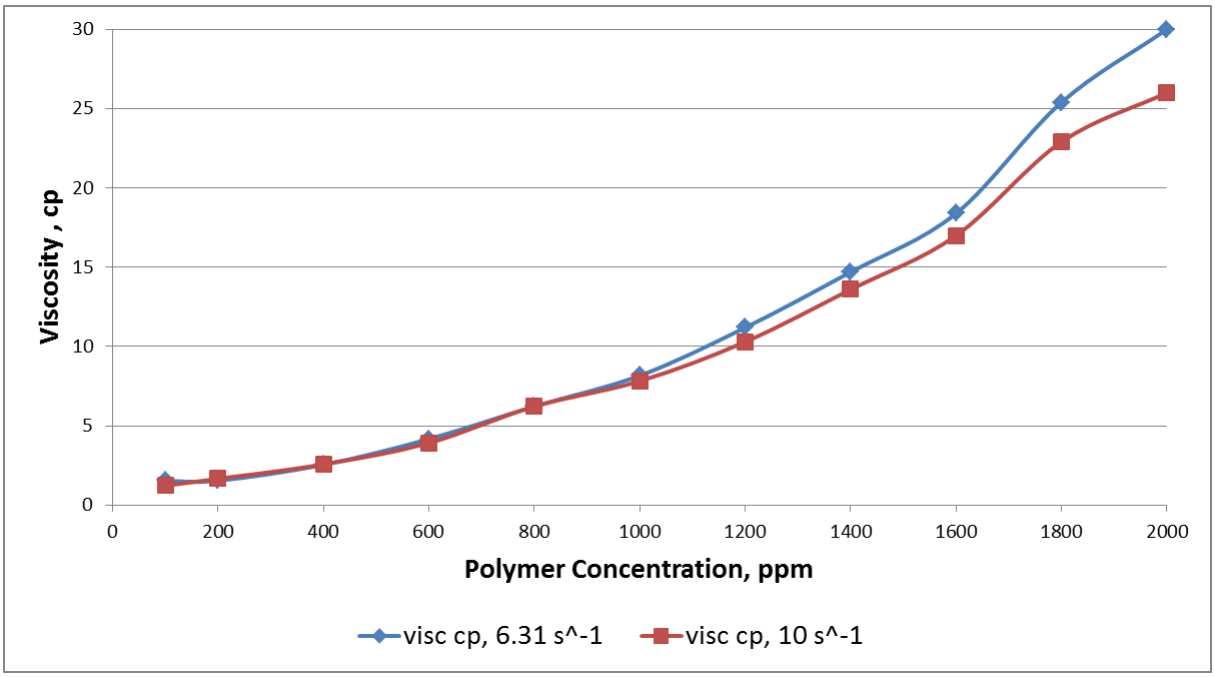

Figure 4.6: Viscosity vs. concentration of HPAM 3630S for ASP#1

At 2000 ppm polymer concentration, the polymer drive viscosity was around 30 cp at 6.31 s^{-1} shear rate. Figure 4.7 shows final ASP slug and polymer drive viscosities at different shear rates. At 3000 ppm polymer concentration viscosity of ASP slug at 6.31 s^{-1} shear rate was around 90 cp. The mobility control would be adverse with the original formulation, since both ASP slug and polymer drive viscosity is low compared to the required 136 cp viscosity required for a stable flood.

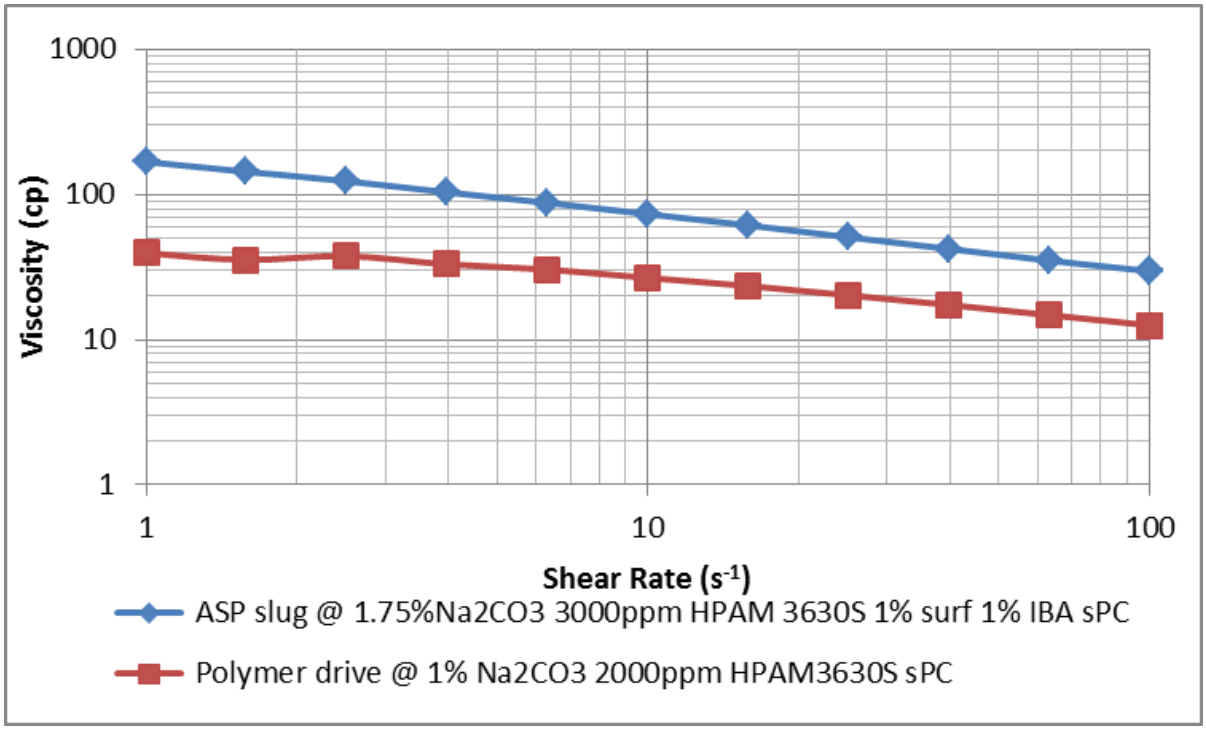

Figure 4.7: Viscosity for ASP slug and polymer drive vs. shear rate for ASP#1

ASP#1 Chemical Flood

Chemical floods involve injection of ASP slug and polymer drive as well as chase water. Salinity of ASP slug was chosen to be a little higher than the optimal salinity due to oil being reactive. Furthermore, salinity of polymer drive was chosen to be 0.6 fraction of ASP slug salinity. The main reason was that it would create salinity gradient which was proven to be more favorable flooding strategy compared to a constant salinity flood. The sizes of ASP slug and polymer drive were chosen to be 0.5 PV and 2 PV respectively. Lastly, the injection rate for both ASP slug and polymer drive was chosen to be around 1 ft/day which is a typical injection rate in fields.

Table 4.3:ASP#1 flood design properties

ASP#1 Flooding Desgin		
Slug Components:	ASP slug:	Polymer Drive
PV injected:	0.5	2
[HPAM 3630S] ppm	3000	2000
[surf#1], wt%	1% Alfoterra	----
[Cosolvent], wt. %	1% IBA	----
ppm Na2CO3	17500	10000
TDS ppm	20664	13164
Frontal velocity, ft/day	1.04	1.04
Viscosity at 6.310 s^{-1} & room temp	87.7	30.46
Viscosity at 10 s^{-1} & room temp	73.43	26.7
Oil Viscosity, s^{-1}	100	100

The most important thing in assessing correctly the performance of ASP is the amount of residual oil saturation. In general, a laboratory scale ASP flood to be considered successful, the final oil saturation must be around 5% or less after tertiary recovery for light oils. For viscous oils the final oil saturation might be a little higher since viscosity of oil is significantly higher.

Table 4.5 shows the summary of ASP #1 sandpack flood. The waterflood recovered 52% of the original oil in place (OOIP) and decreased oil saturation from an initial oil saturation of 84% to 40.3 %. The chemical flood including the second waterflood recovered additional 31% of OOIP and increased the overall recovery to 83% of OOIP. The chemical flood decreased oil saturation from 40.3% to 14.4%. Nevertheless, tertiary recovery was able to recover only 64% of the remaining oil in place (ROIP).

Table 4.4: ASP#1 summary

Soi=84%			
5.2 PV	WF I recovery,ml:	Recovery, % OOIP	So
	39.32	52%	40.3%
0.5PV	ASP slug recovery, ml:		
	0.84	1%	39.3%
2PV	PolymerDrive, ml:		
	19.471	26%	17.4%
5.1 PV	WF II recovery, ml:		
	3.1	4%	14.4%
12.8PV	Total:	83%	14.4%
7.6 PV	ASP+polymer+WFII:	Tertiary Recovery, % ROIP	
	23.411	64%	14.4%

Figure 4.8 shows cumulative oil recovery, oil cut, oil saturation and pressure drop versus pore volumes injected. At the end of waterflood, no oil was coming out and pressure drop had stabilized. Maximum pressure drop per foot during the whole flood reached 8.81 psi/ft. This pressure drop is considered high for field application where normally 1-3 psi/ft pressure drop is observed. Oil cut reached maximum value of 65**%**.

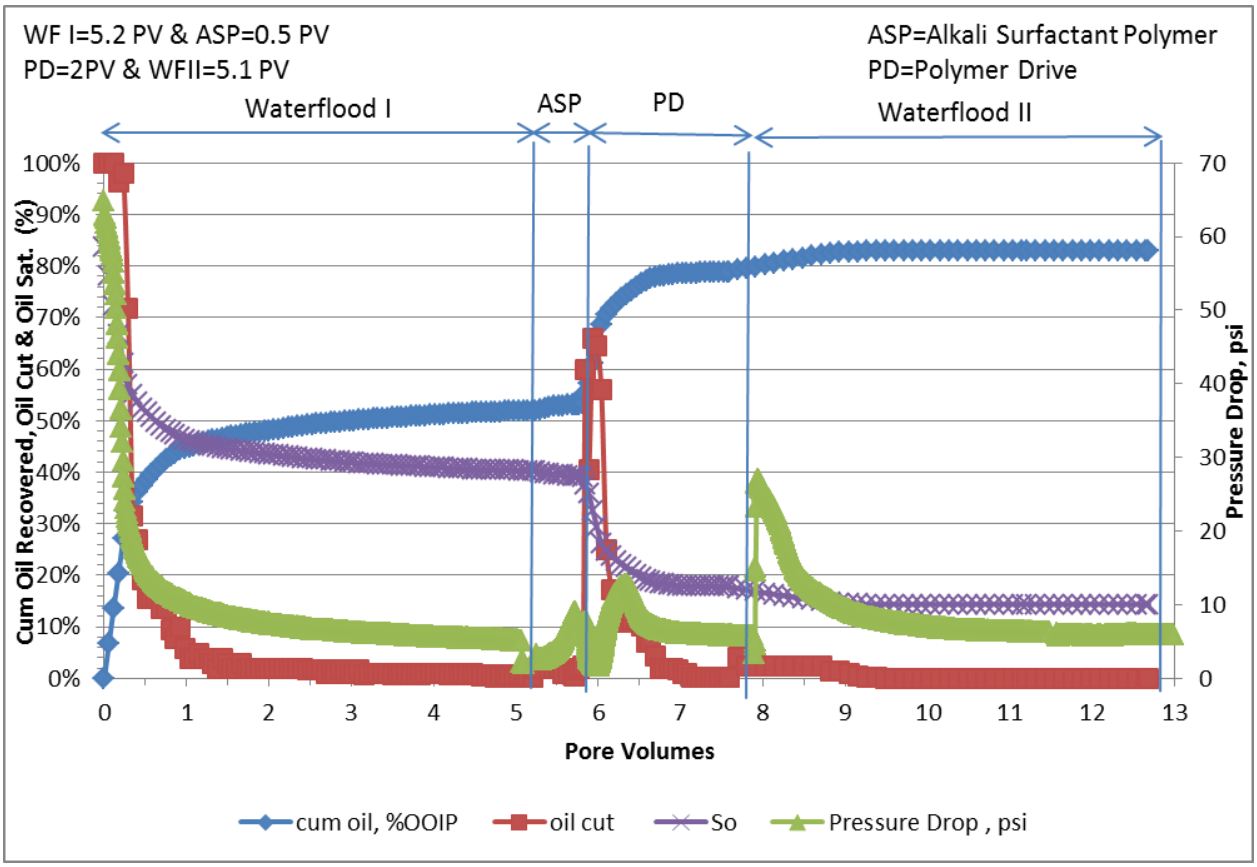

Figure 4.8: ASP#1 Cum. oil, oil cut, oil sat., and pressure drop vs. pore volumes

ASP#1 Effluent Analysis

Figure 4.9 shows the effluent surfactant concentration. Between 6 and 7 PV, only a small amount of surfactant came out. Then major surfactant slug came out at the beginning of 8 PV injection and reached a maximum surfactant concentration at the beginning of 9 PV injection. Thus, surfactant came out mostly after the oil bank.

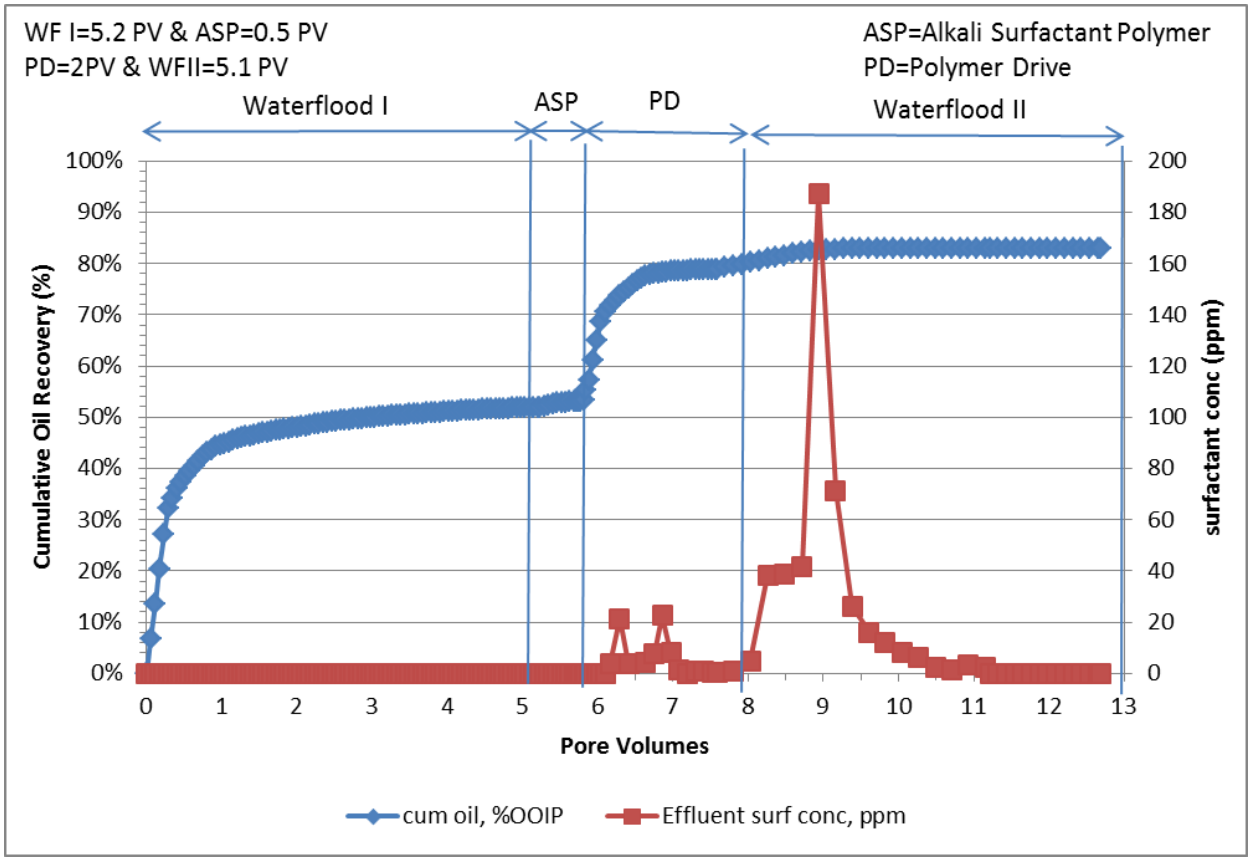

Figure 4.9: Surfactant concentration in effluent and cum oil

Figure 4.10 shows that pH increased promptly after oil cut reached the peak and started to decrease which means that alkali was following the oil bank.

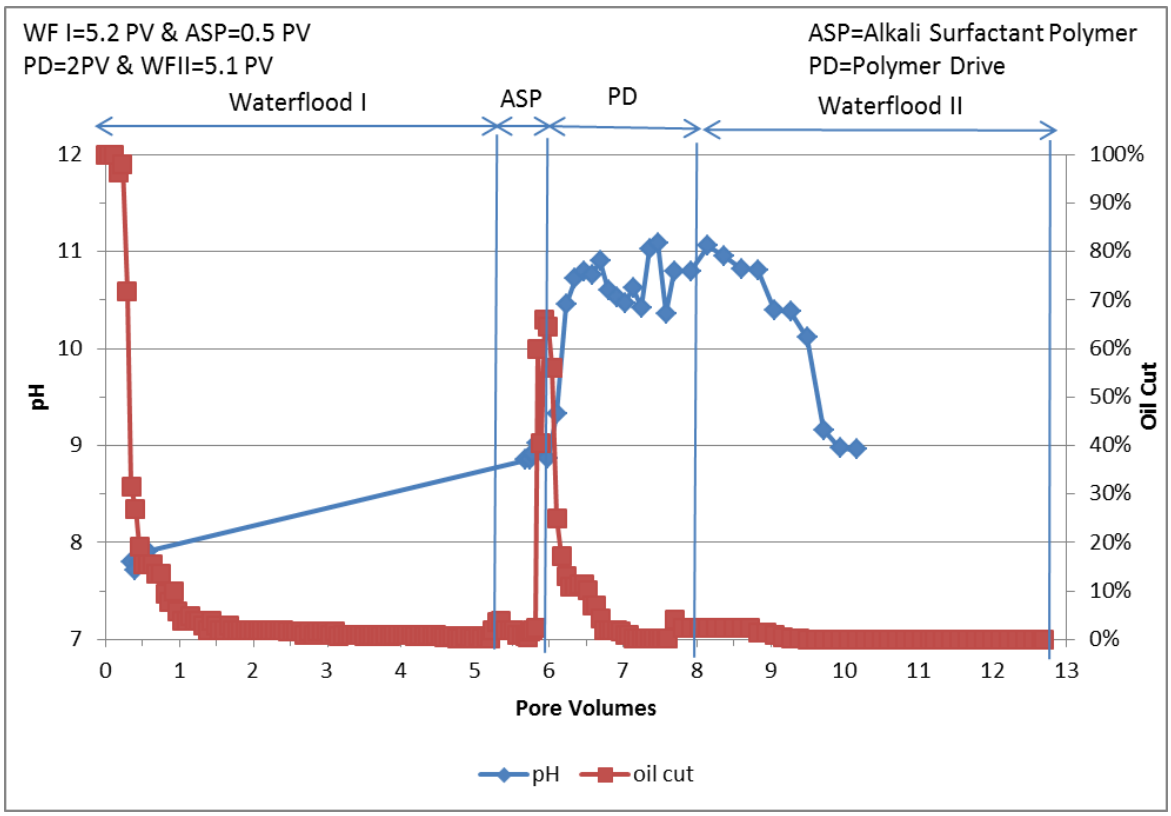

Figure 4.10: Oil cut and pH vs. pore volumes

Similar to pH, Figure 4.11 shows that total salinity reached the producer after the oil cut reached the peak and started to decrease.

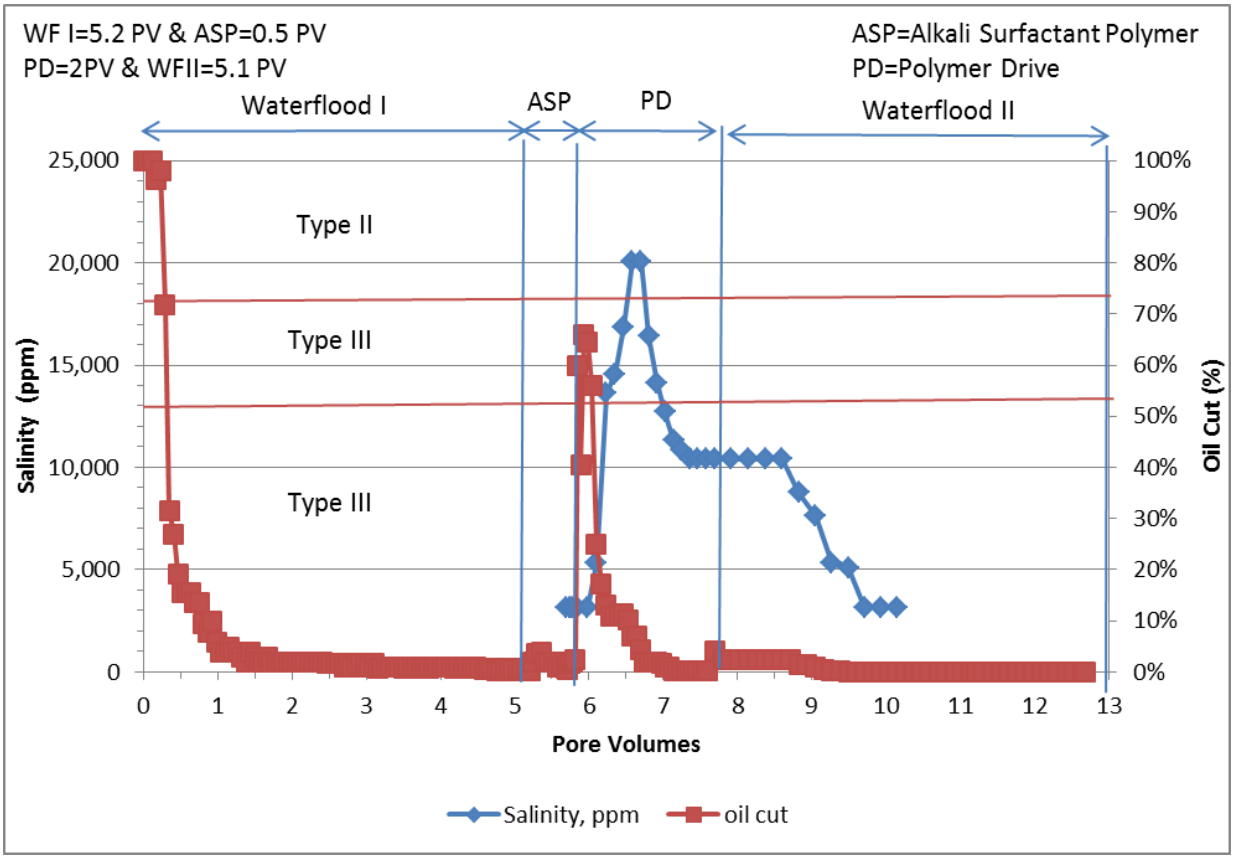

Figure 4.11: Oil cut and salinity vs. pore volumes

In addition to pH and total salinity slug, viscosity of the effluent samples increased shortly after oil cut reached its peak and started to decrease as shown in Figure 4.12.

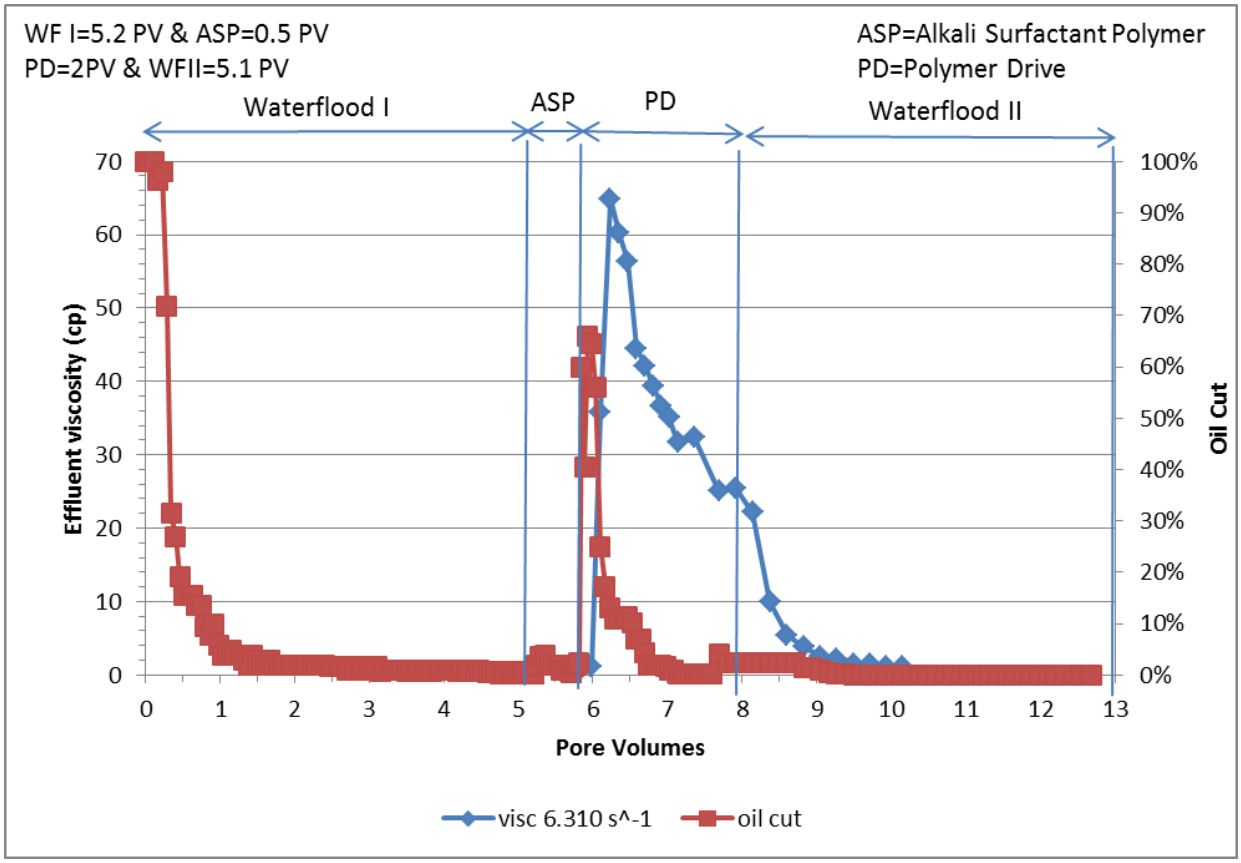

Figure 4.12: Oil cut and effluent viscosity vs. pore volumes

Figure 4.13 shows surfactant slug lagged behind the oil bank. Calculated surfactant retention (surfactant adsorption + surfactant trapping) was equal to 1.42 mg/g of rock which is very high value. Most of the surfactant gets trapped due to adverse mobility ratio.

.

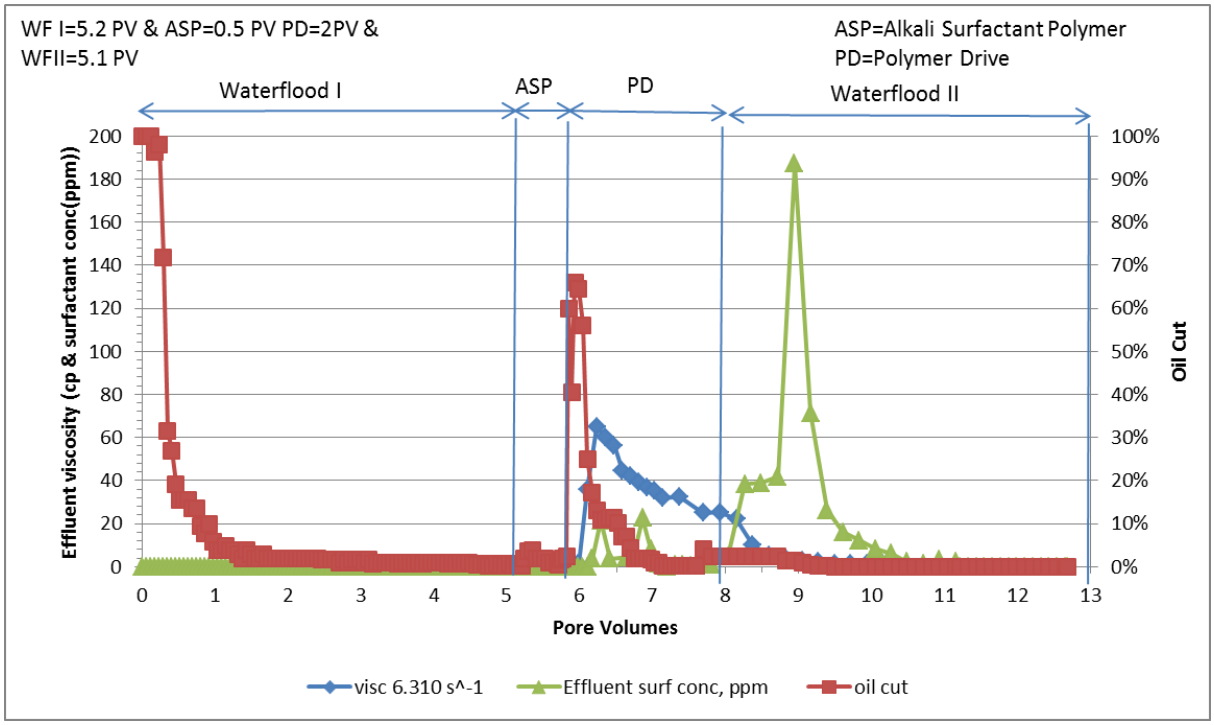

Figure 4.13: Effluent surfactant conc., viscosity and oil cut vs. pore volumes

Figures 4.14 and 4.15 show the surfactant concentration, salinity, pH and viscosity of the aqueous effluent. Surfactant slug came out a lot later compared to other slugs even though dispersion was minimal since sandpack was 3ft long. Main surfactant slug came out after breakthrough of other slugs. It can be seen in Figure 4.14 that surfactant slug lags from salinity and polymer slugs by at least 2 PV. That is the main reason of very high surfactant retention. Surfactant mostly gets trapped. Furthermore, a low IFT was probably not achieved in ASP#1 flood because most of the surfactant was staying in Type I region. Surfactant never reacted fully with oil and most of the surfactant stayed in the aqueous phase.

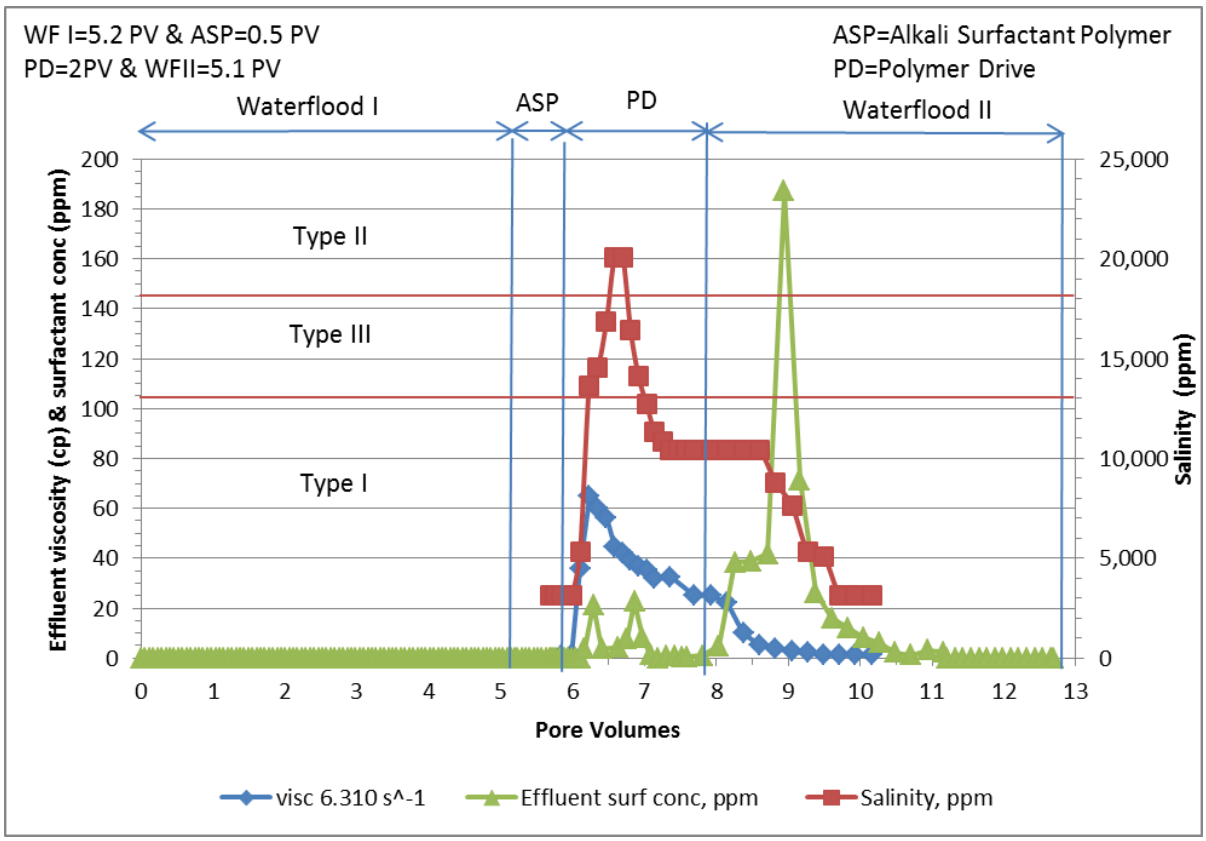

Figure 4.14: Effluent salinity, surfactant and viscosity vs. pore volumes

Significant surfactant retardation can be observed in the Figure 4.15, while pH and viscosity waves propagate together.

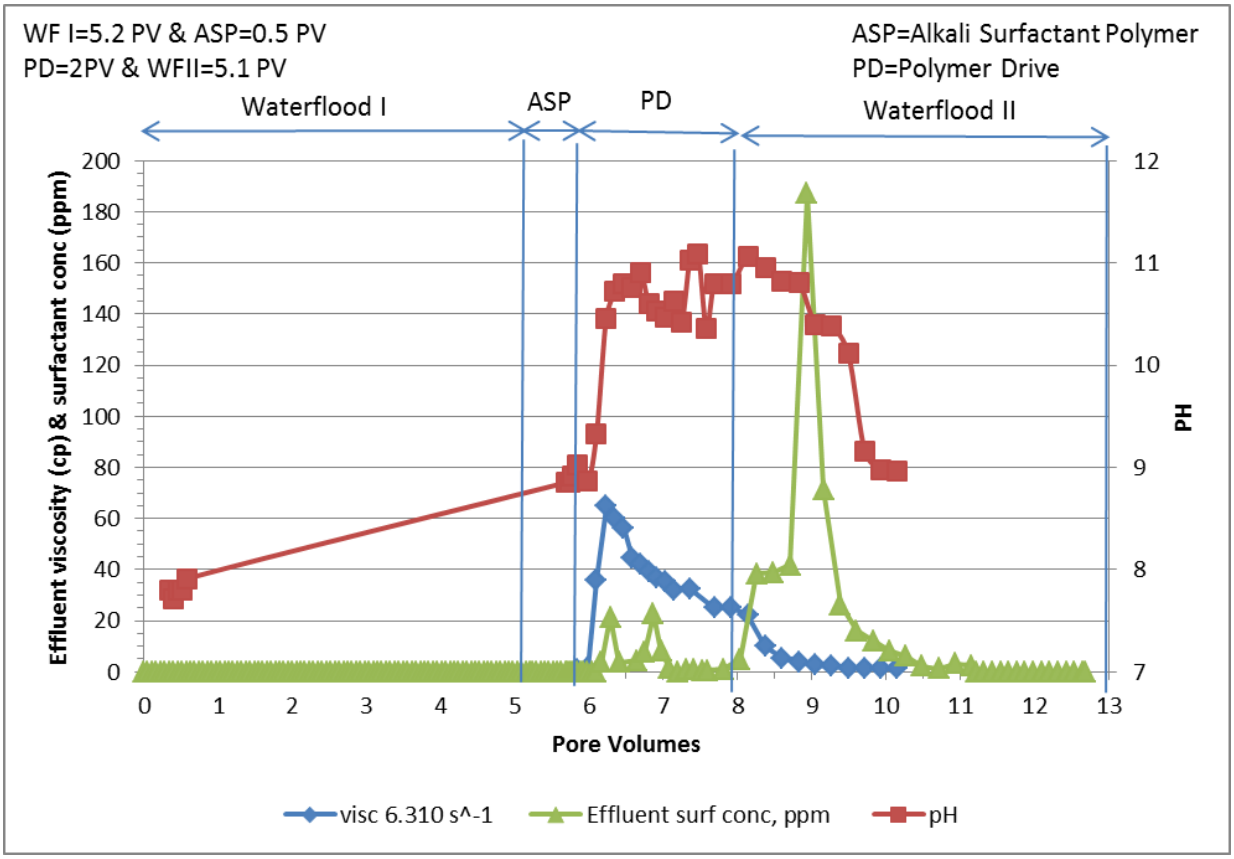

Figure 4.15: Effluent pH, surfactant conc. and viscosity vs. pore volumes

4.2 1D ASP#2 Sandpack Experimental Results and Methodology

There was a need to improve the formulation used in ASP#1 sandpack flood. One of the issues with ASP#1 formulation was that it had long equilibration time as well as formation of viscous emulsion at elevated salinities in Type II region. Thus, a more robust ASP formulation was needed.

4.2.1 ASP Formulation #2 for Reactive Crude Oil

In order to improve the surfactant formulation, we had to perform a systematic study of the microemulsion phase behavior. Figure 4.16 shows a simplified flowchart for microemulsion

phase behavior methodology presented by Solairaj (2011). Since we already had a working formulation that needed slight modification in its equilibration time and flow ability, the main components were the same as in the ASP#1 formulation. Furthermore, we wanted to improve the mobility ratio in ASP#2 formulation.

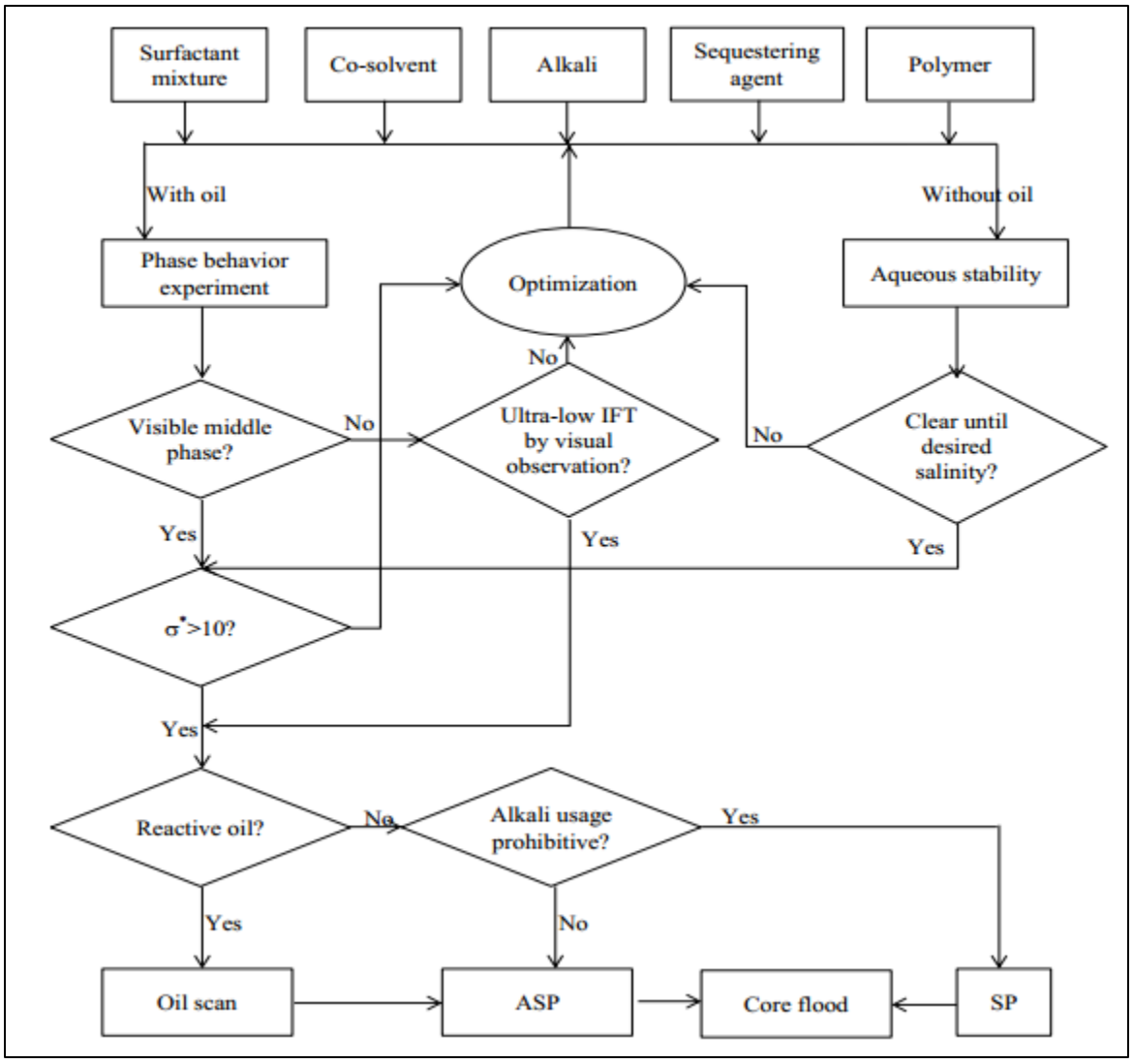

Figure 4.16: Generalized ASP phase behavior flow chart (Solairaj et al., 2011)

Several successful formulations were found which had better flow ability and equilibration times. Mainly they were mixtures of Alfoterra™ surfactant and Enordet™ surfactant. Mixture of

Alfoterra and Enordet at 3:1 ratio respectively was chosen as the main surfactant solution. Aqueous stability tests showed that the surfactant solution in brine is clear at the desired salinity, as shown in Figure 4.17. Figures 4.18-4.23 show phase behavior tests that were performed with oil concentrations of 50%, 30%, 10%, respectively. It was identified that optimum salinity increased as oil concentration decreased, which is an indication of an oil being active.

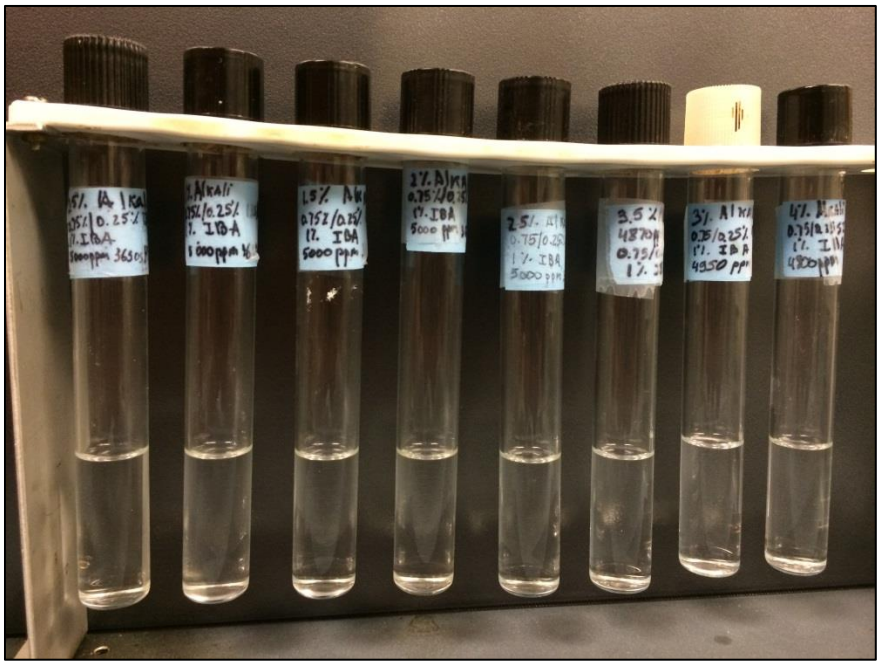

Figure 4.17: ASP#2 aqueous stability

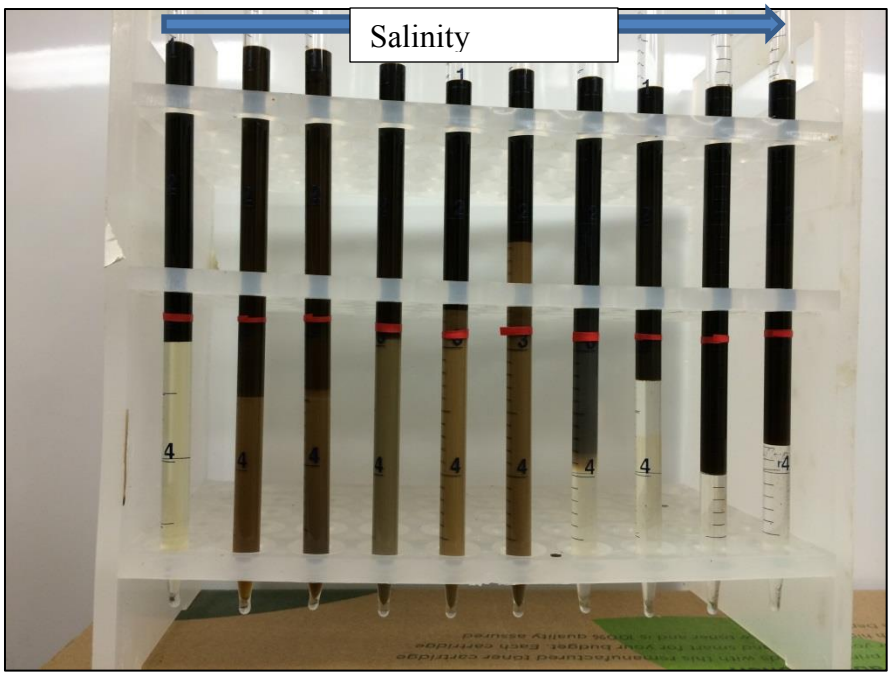

Figure 4.18: ASP#2 phase behavior for So=50%

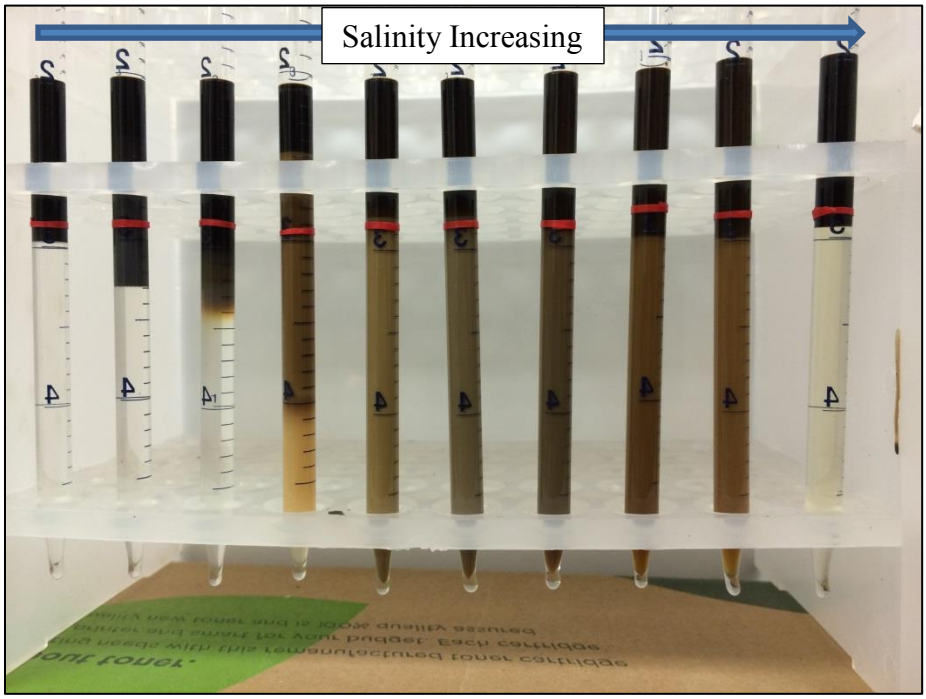

Figure 4.19: ASP#2 phase behavior for So=30%

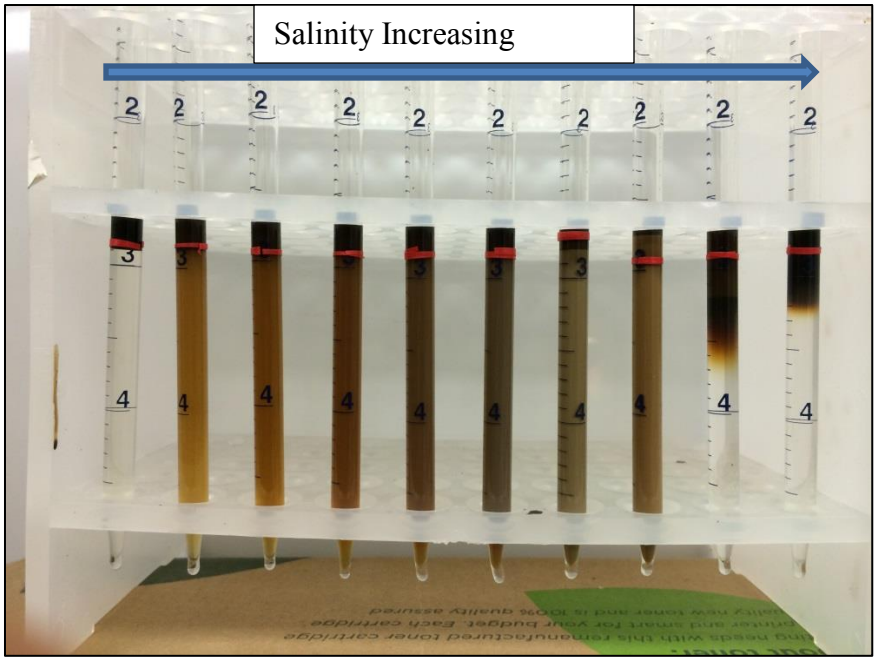

Figure 4.20: ASP#2 phase behavior for So=10%

Since Enordet Internal Olefin Sulfonate is a more hydrophilic surfactant compared to Alfoterra surfactant, its addition causes the optimum salinity to increase significantly compared to ASP#1 formulation. The optimum salinity was around 27,000 ppm concentration of sodium carbonate (Na_2CO_3) at an oil concentration of 50% or water oil ratio of 1. The solubilization ratio at the optimum salinity decreased compared to ASP#1 formulation, but the equilibration time and the overall flow ability of microemulsion improved significantly. Figure 4.21 shows the solubilization plot for ASP#2 formulation.

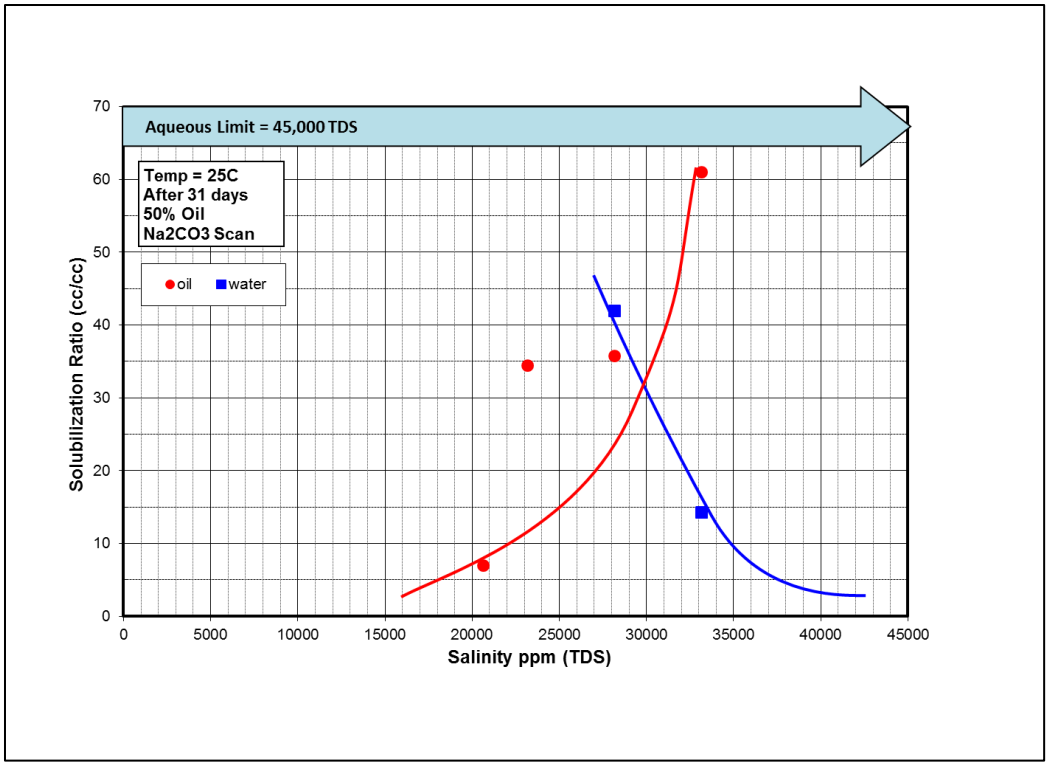

Figure 4.21: ASP#2 solubilization plot for So=50%

Figure 4.22 shows that optimum salinity at oil concentration of 30% was equal to 30,000 ppm of sodium carbonate.

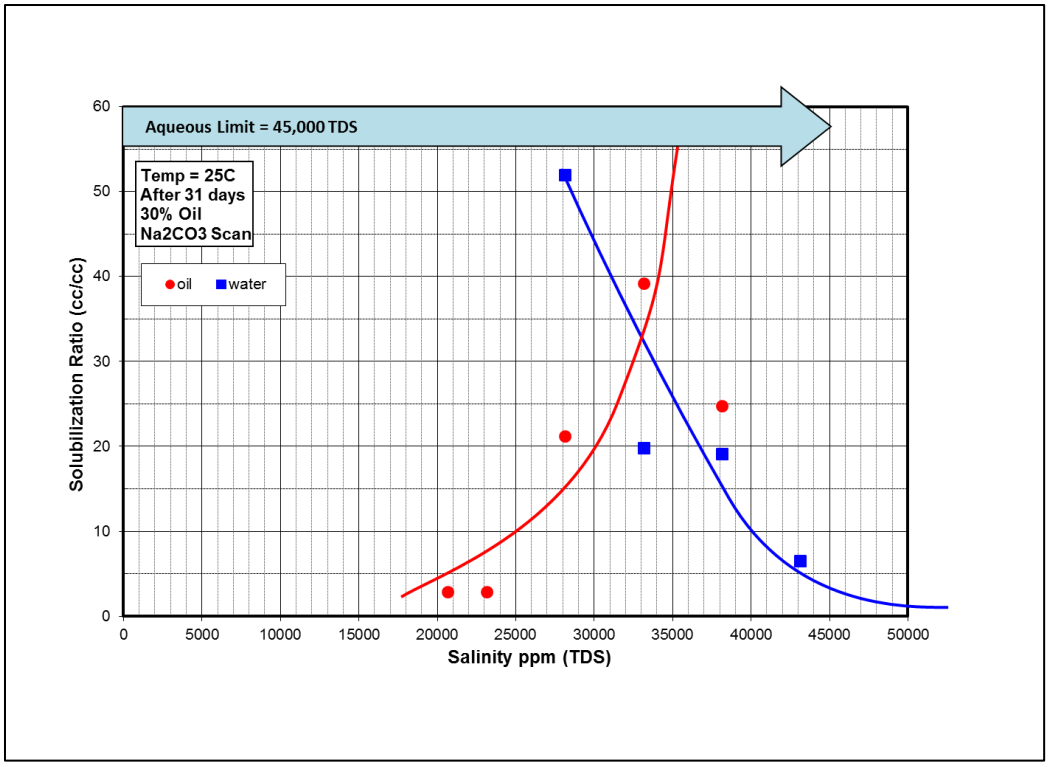

Figure 4.22: ASP#2 solubilization plot for So=30%

Lastly, Figure 4.23 shows that optimum salinity at oil concentration of 10% was equal to 37,000 ppm of sodium carbonate. Thus, as oil concentration decreased optimum salinity increased. Such behavior of optimum salinity is usually exhibited by reactive oils due to generation of in situ soap when alkali reacts with naphthenic acids in reactive oil. The generated soap is usually more hydrophobic than synthetic surfactant; thus, it tends to decrease optimum salinity as oil concentration is increased.

.

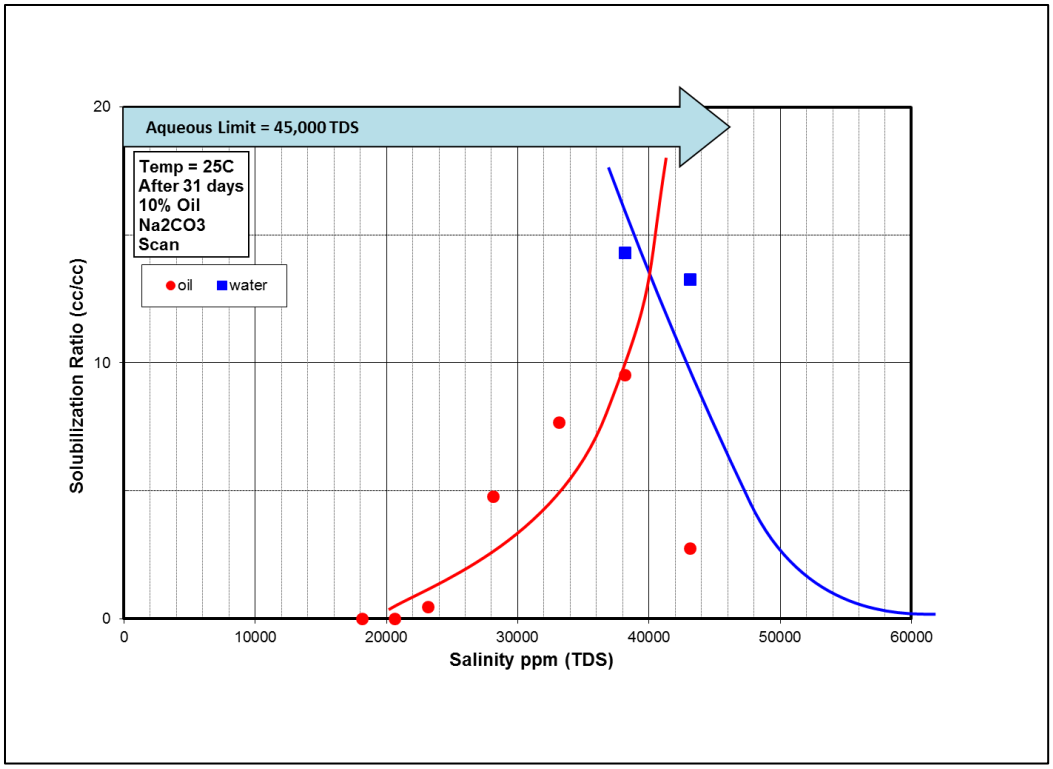

Figure 4.23: ASP#2 solubilization plot for So=10%

Alkali Test

Alkali test is another method to qualitatively evaluate whether oil is reactive or not. Figure 4.24 shows results from alkali test where only sodium carbonate in small increments was added to brine and oil mixture in order to see whether solubilization of water or oil would occur. Reactive oils generally produce highly hydrophobic soap. As it can be seen in Figure 4.24, especially up to 0.5% alkali concentration, significant water solubilizes for the most test samples. That is qualitative indication of oil being active and generating hydrophobic soap just by reaction with alkali.

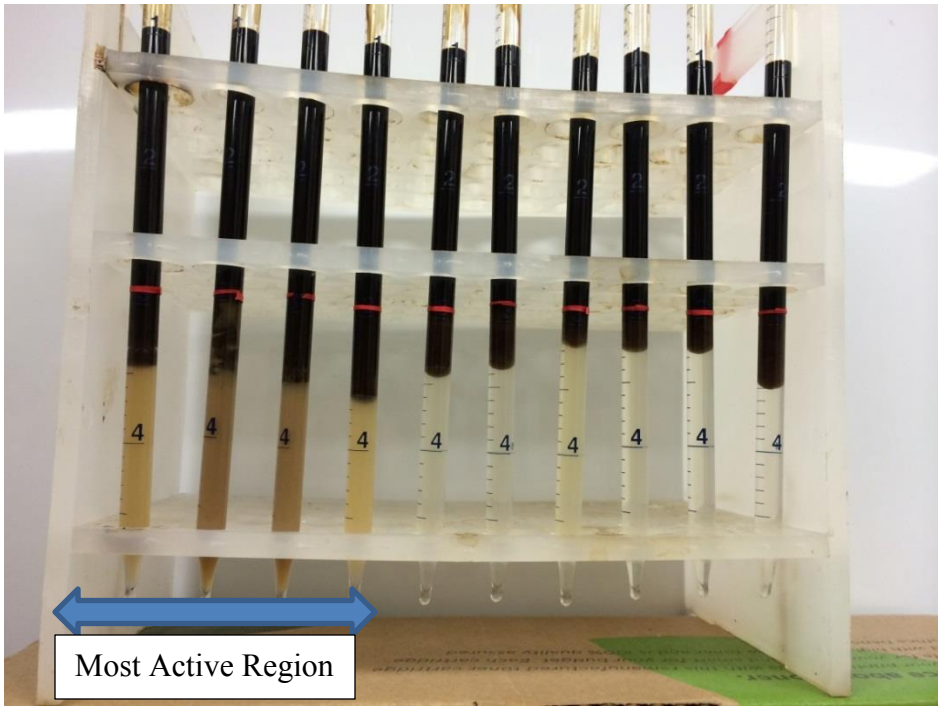

Figure 4.24: Alkali test for reservoir oil

ASP#2 Activity Diagram

Generally, for inactive oils optimum salinity does not change with oil concentration. Thus, the activity diagram, which is phase behavior for different oil saturations plotted together, will have a line with zero slope. If oil is active it will have a negative slope. In general negative slope is preferred if we plot phase behavior result versus increasing oil saturation. Having negative slope on the activity diagram ensures that surfactant slug will hit type III region salinity. Figure 4.25 shows the activity diagram, which was constructed from the phase behavior tests for So=50%, So=30%, and So=10%. It has a negative slope which is indication of oil being active and favorable for ASP flood.

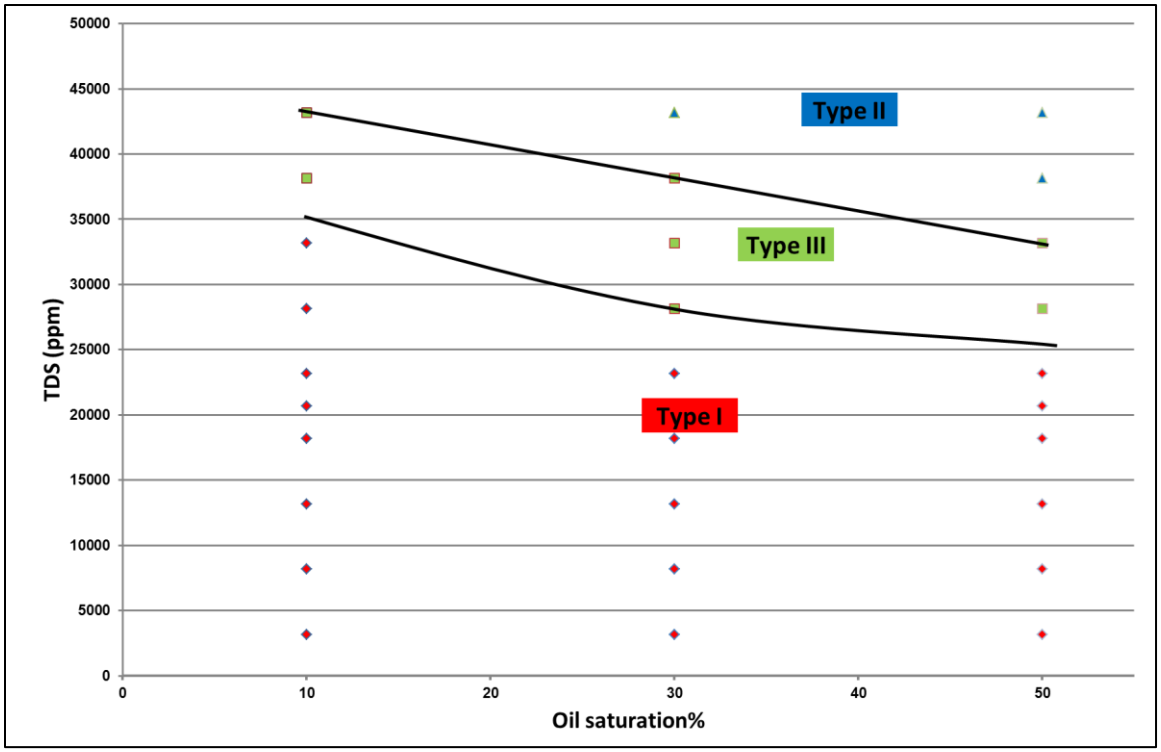

Figure 4.25: ASP#2 activity diagram

Dynamic IFT Measurements between ASP and Reservoir Oil

Interfacial tension (IFT) was measured with the final ASP formulation and reservoir oil. As it can be seen from Figure 4.26, the IFT goes to ultra-low values and is consistent with estimation from solubilization ratio and IFT relationship through Huh's equation (1979).

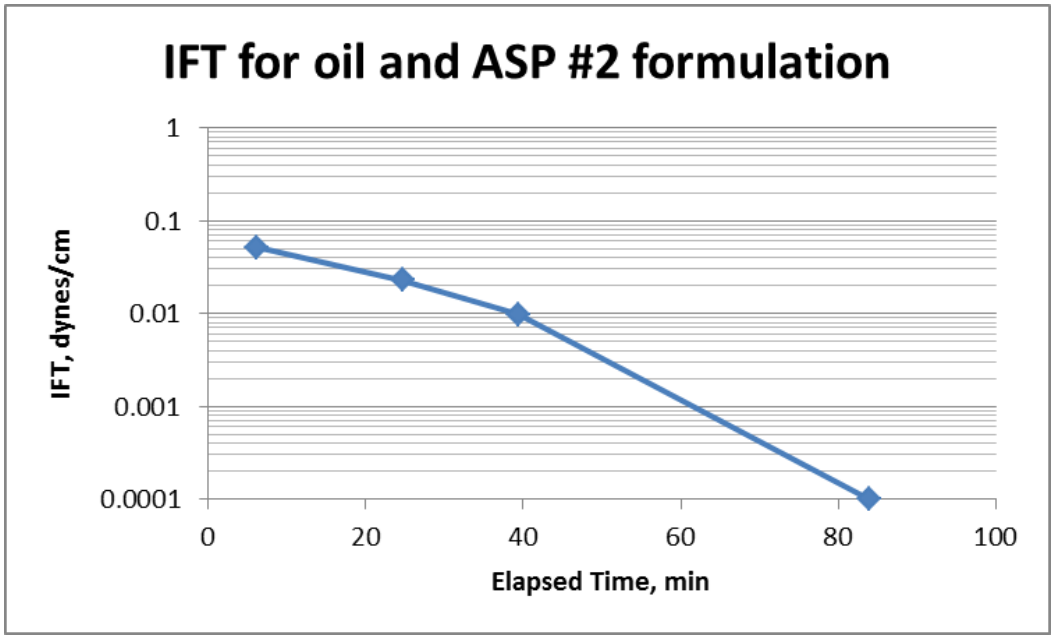

Figure 4.26: ASP#2 dynamic IFT measurement

Microemulsion Viscosity

Larger samples of oil-brine-surfactant mixtures were equilibrated so that microemulsion viscosities for different salinity region can be measured. In Type I region, viscosities of water-external microemulsion were measured, in Type II region viscosities of oil-external microemulsion were measured, and in Type III viscosities of middle phase microemulsion were measured. Figure 4.27 shows that viscosity increases and peaks within the Type III region with viscosities three times the oil viscosity. Further optimization work can be done by increasing co-solvent concentration to decrease the microemulsion viscosity.

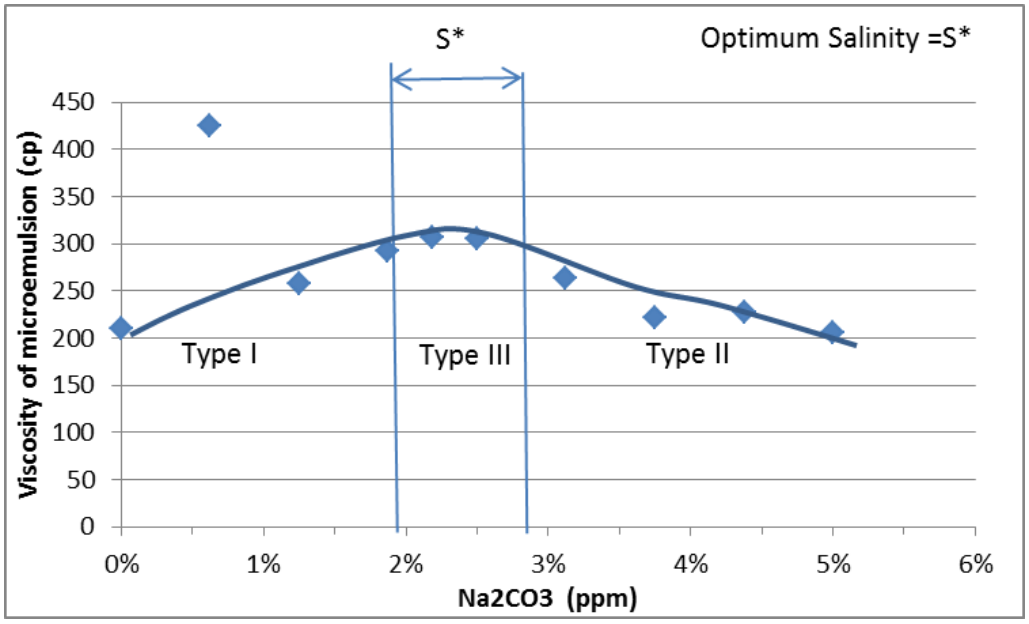

Figure 4.27: ASP#2 Microemulsion viscosities for So=50% and at 6.31 s^{-1}

ASP#2 Salinity Gradient Design

Salinity gradient is a very important parameter that needs to be planned carefully in order to ensure a successful flood. For active oils that have negative slope in the activity diagram, it is desirable to inject ASP slug at an over-optimum salinity followed by a polymer drive at an under-optimum salinity. Furthermore, having a salinity gradient ensures passing through a Type III region of ultra-low IFT, and ending with a salinity of Type I region at the end of the surfactant bank which ensures that surfactant stays in the aqueous phase. Lastly, having a gentle slope in the activity diagram helps to increases the duration of time spent in type III region of ultralow IFT. In Figure 4.28, the dotted line represents the salinity gradient. It is designed so that salinity first would be raised above optimum salinity value and followed by polymer drive with lower salinity approximately 70% of ASP slug salinity as a rough estimate.

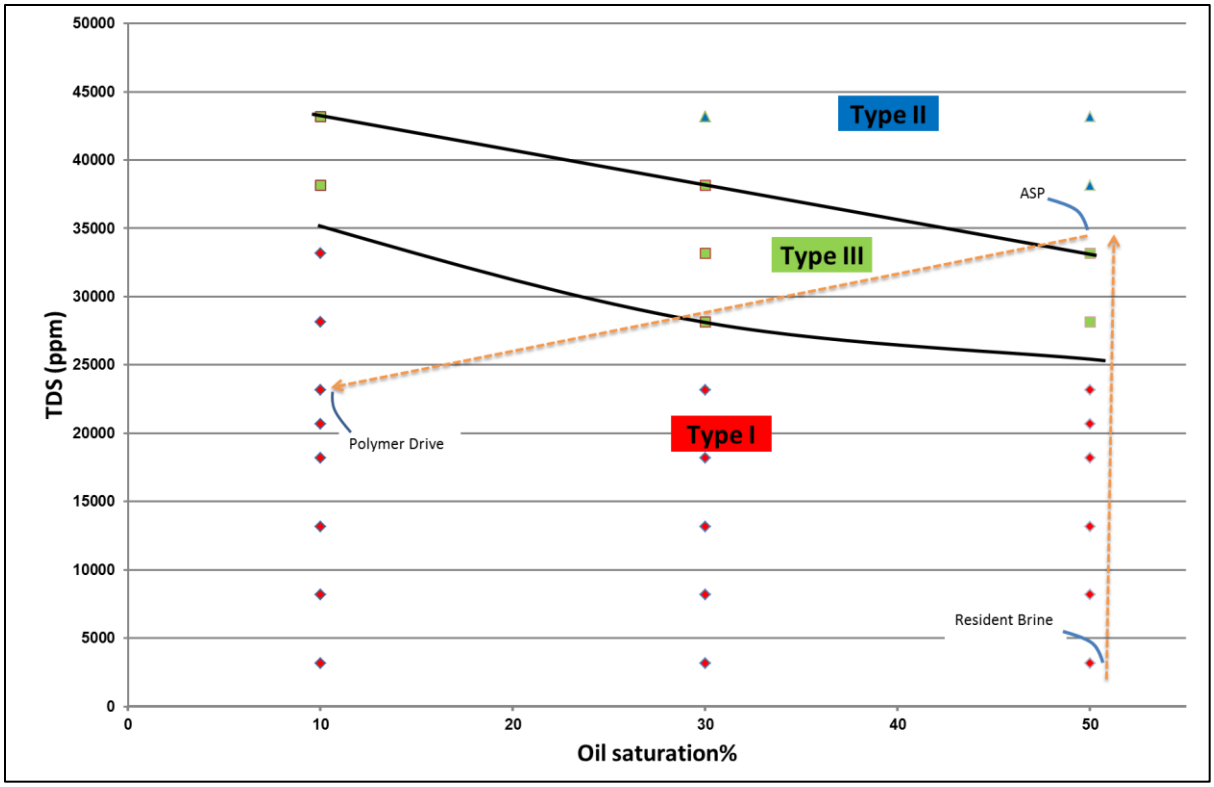

Figure 4.28: ASP#2 salinity gradient design

4.2.2 ASP#2 SANDPACK FLOOD

The main difference between ASP#1 and ASP#2 was that confining pressure of **1500 psi** was used in ASP#2. As seen in Table 4.6, permeability of the same reservoir sand changed significantly after applying 1500 psi overburden stress in ASP#2; permeability went down from ~8 Darcy in unconfined ASP#1 to ~2 Darcy in a 1500 psi confining pressure in ASP#2 sandpack for the same reservoir sand used. Furthermore, ASP#2 sandpack was much shorter compared to 3ft steel bar sandpack. That adds bigger dispersion to the ASP#2 flood due to inverse proportionality of dispersion to length.

Table 4.5: ASP#2 sandpack properties

ASP#2 Core Properties:	
Outcrop:	reservoir sand
Mass:	297 gm
Porosity:	0.354
Length:	6 in
Diamter:	1.5 in
Area:	1.767 in^2
Temperature:	25 ^oC
Overburden Pressure:	1500 psi
Brine Permeability:	2.21 D
Oil Permeability:	3.15 D
Pore Volume:	61.57 ml

ASP#2 Waterflood

The sandpack was waterflooded with softened reservoir brine (SRB) for at least 5 PV and until no oil was coming out. Frontal velocity of the waterflood was to **1 ft/day** (**10ft/day** for ASP#1). Thus, the end point relative permeabilites for oil flood and waterflood, residual water saturation to oil, and residual oil saturation to water from both oil flood and waterflood were obtained as shown in Table 4.7. The data were used to get relative permeability curves and most importantly, apparent viscosity and total relative mobility of the oil/water bank. Table 4.7 shows obtained data and Figure 4.29 shows constructed relative permeability curves calculated from Corey Model.

Table 4.6: Mobility control parameters for ASP#2

Mobility control requiremnent parameters for ASP#2			
Parameter	Definition	Value	Basis
K_{rw}^o	End point water relative permeability	0.0424	Obtained from waterflood
K_{ro}^o	End point oil relative permeability	1	Obtained from oil flood
n_w	Fractional flow exponent water	2	Assumed for water wet
n_o	Fractional flow exponent oil	2	Assumed for water wet
S_{wr}	Residual water saturation to oil	0.18	Calculated from mass balance
S_{or}	Residual water saturation to water	0.343	Calculated from mass balance
μ_w	Water viscosity	0.9	Measured in rheometer
μ_o	Oil viscosity	100	Measured in rheometer

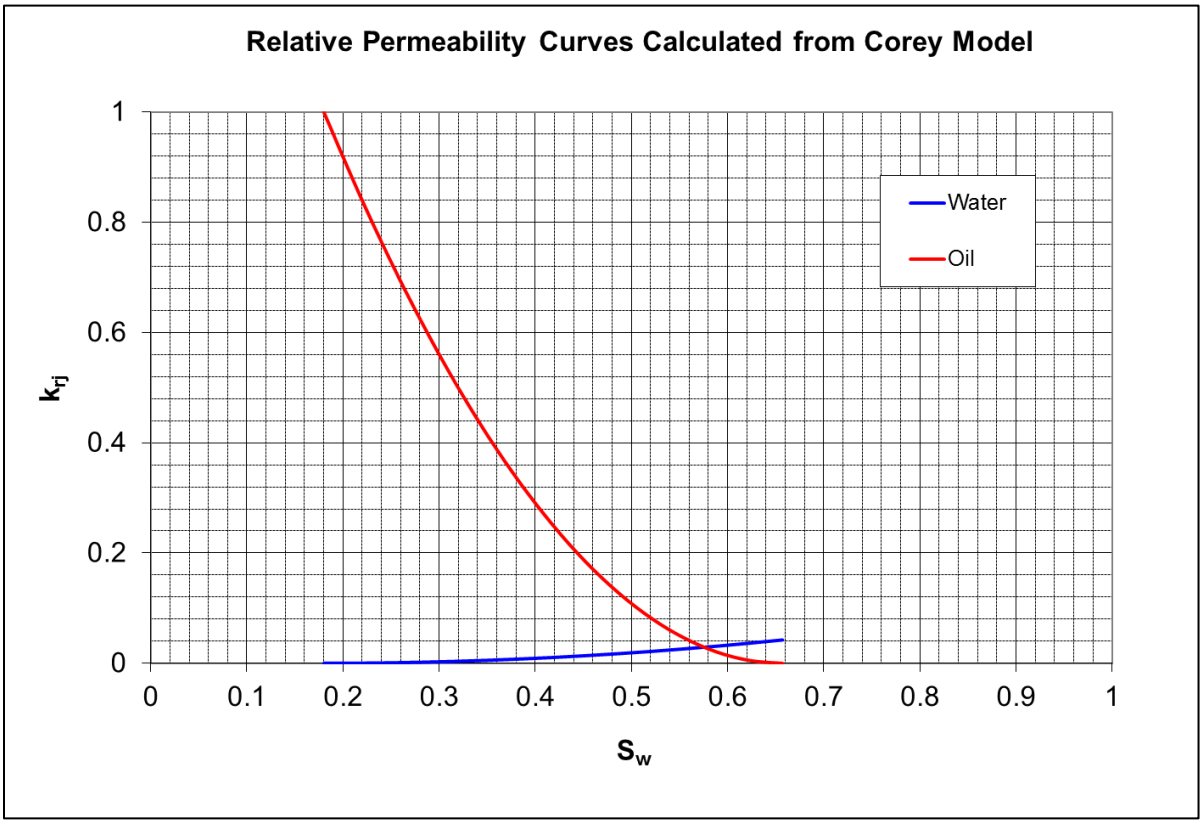

Figure 4.29: Relative permeability curves for ASP#2

ASP#2 Mobility Control Requirements

From the relative permeability data total relative mobility and apparent viscosity curves were constructed. Figure 4.30 shows that the minimum total relative mobility was calculated to be ~0.0083 cp^{-1}, and thus, the maximum apparent viscosity of oil bank was ~120 cp, which is equal to the reciprocal of the minimum point for total relative mobility. Therefore, ASP and polymer drive slugs must have around 120 cp viscosity for a stable displacement of oil/water bank.

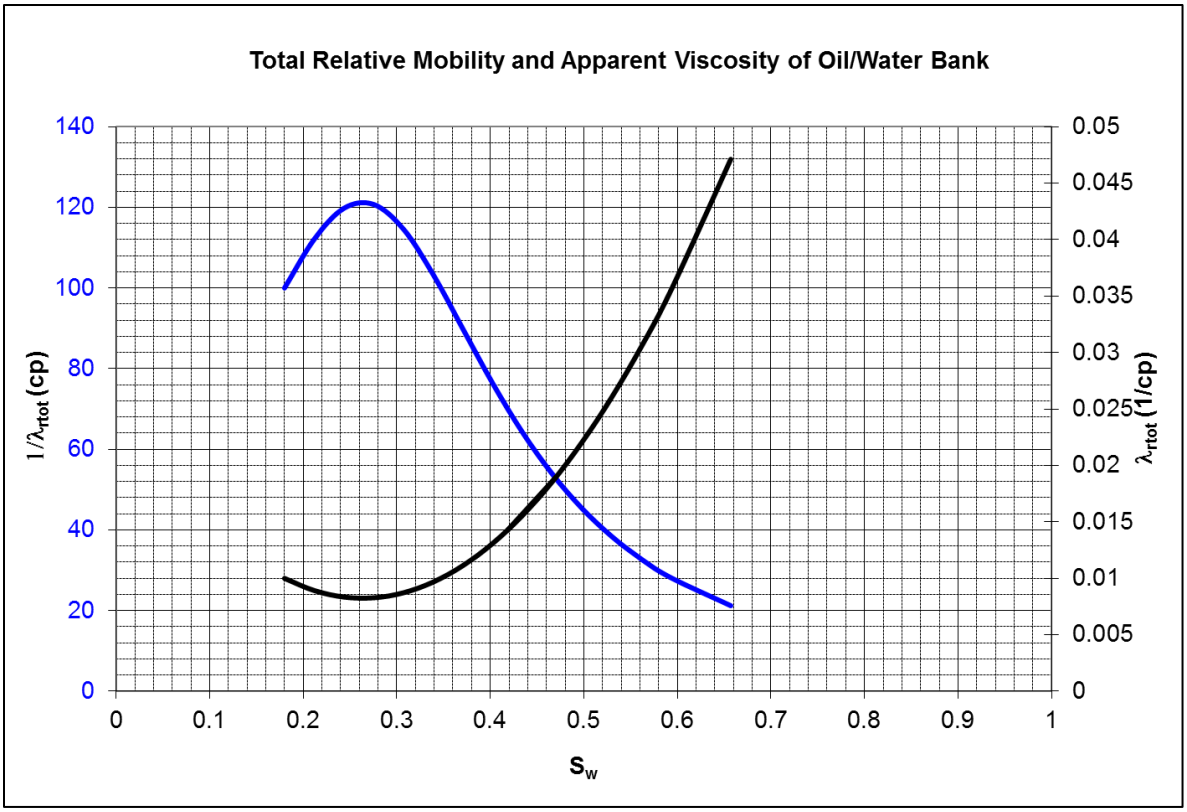

Figure 4.30: Apparent viscosity and total relative mobility of oil/water bank for ASP#2

Figure 4.31 shows that viscosities of ASP slug, polymer drive I, polymer drive II are all above minimum required viscosity in order to have stable displacement of oil bank. Furthermore, the slug viscosities were intentionally higher than required minimum viscosity for a stable flood. The main reason was that microemulsion viscosity was 2-3 times viscosity of oil; thus, the maximum apparent viscosity of oil/water bank was less than microemulsion viscosity around optimum salinity region.

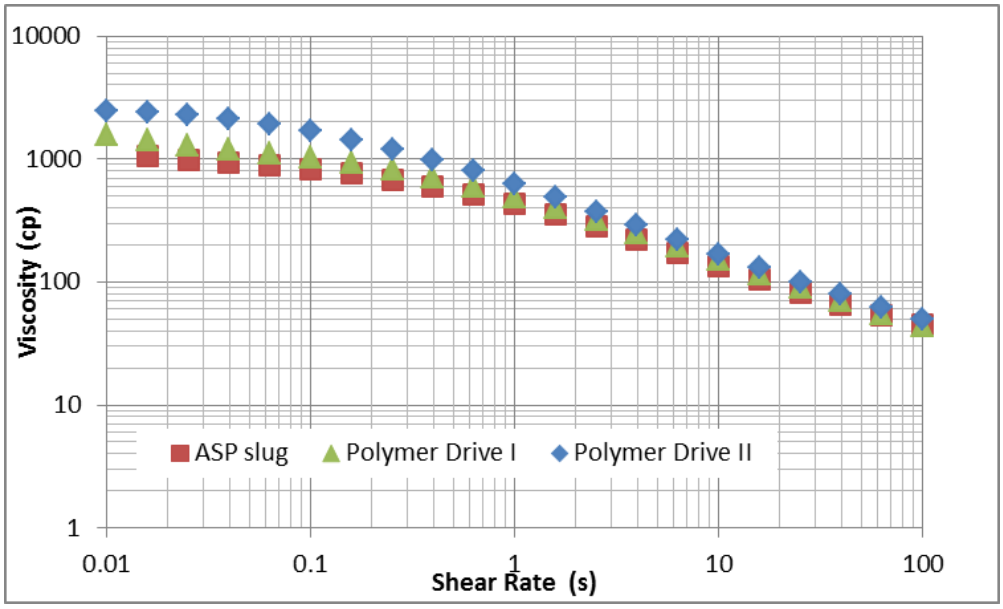

Figure 4.31: ASP slug, polymer drive viscosities for ASP#2

ASP#2 Chemical Flood

The chemical flood involved injection of ASP slug, polymer drive I and polymer drive II as well as chase waterflood in order to check whether more residual oil would come out after polymer drive. Table 4.8 shows flooding design. Salinity of ASP slug was chosen to be a little higher than the optimal salinity due to oil being reactive. Nevertheless, salinity of final ASP slug was also equal to Type III region salinity at 10% oil concentration. Salinity of polymer drive had the same salinity as ASP slug because it was used to extend the duration of over optimum salinity zone. That was done due to high dispersion in a shorter sandpack that was used in ASP#2 flooding compared to a steel tube sandpack that was used for ASP#1 experiment. Furthermore, salinity of polymer drive II was chosen to be 0.7 fraction of ASP slug and polymer drive I salinities. The main reason was that it would create salinity gradient which was proven to be more favorable flooding strategy compared to constant salinity flood. The sizes of ASP slug, polymer drive I (PD I) and polymer drive II (PD II) were chosen to be 0.5 PV,0.3 PV and 1.3 PV

respectively. Lastly, the injection rate for both ASP slug and polymer drive was chosen to be around 1ft/day which is a typical injection rate in actual fields.

Table 4.7: ASP#2 sandpack flood design

ASP#2 Flooding Desgin			
Slug Components:	ASP slug:	Polymer Drive I	Polymer Drive II
PV injected:	0.5	0.3	1.3
[HPAM 3630S] ppm	4750	5050	4750
[surf#1], wt%	0.75% Alfoterra	----	----
[surf#2], wt%	0.25% Enordet IOS	----	----
[Cosolvent], wt. %	1% IBA		
ppm Na2CO3	32500	32500	22750
TDS ppm	35664.5	35664.5	25914.5
Frontal velocity, ft/day	1	1	1
Viscosity at 6.310 s^{-1} & room temp	172.9	194.6	220.4
Viscosity at 10 s^{-1} & room temp	134.4	150.6	168.9
Oil Viscosity, s^{-1}	100	100	100
pH	11.92	11.91	11.8

Summary of ASP#2 Flood

Table 4.9 shows summary of ASP #2 sandpack flood. Waterflood recovered 58% of original oil in place (OOIP) and decreased oil saturation from initial oil saturation of 82% to 34.3 %. Chemical flood including the second waterflood recovered extra 35% of OOIP and increased overall recovery to 93% of OOIP. Furthermore, chemical flood decreased oil saturation from 34.3% to 5.9%. Tertiary recovery was able to recover 84% of remaining oil in place (ROIP). To conclude, ASP#2 sandpack flood in viscous oil is considered to be a successful flood.

Table 4.8: ASP#2 sandpack flood summary

Soi=82%			
5.2 PV	WF I recovery,ml:	Recovery, % OOIP	So
	29.3416	58%	34.3%
0.5PV	ASP slug recovery, ml:		
	0.425	1%	33.6%
0.3 PV	Polymer Drive I, ml:		
	11.15	22%	13.6%
1.3PV	Polymer Drive II, ml:		
	6.26	12%	5.9%
2PV	WF II recovery, ml:		
	0	0%	5.9%
9.3 PV	Total:	93%	5.9%
4.1 PV	ASP+PDI+PDII+WFII:	Tertiary Recovery , % ROIP	
	17.835	84%	5.9%

From Figure 4.32, the maximum pressure drop per foot was equal **to 12 psi/ft,** which would be unsustainable in the field. It is possible to decrease pressure drop by adding better co-solvent so that microemulsion phase viscosity at optimum salinity will decrease, and thus, decreasing overall pressure drop. Oil cut rose to ~75% and water cut accordingly decreased from 100% to ~25%. The oil/water bank thickness was around 0.5 PV. Furthermore, mobility ratio between oil/water bank and chemical slug was less than ~0.66 as it can be estimated from the division of the pressure drop for oil/water bank by the pressure drop at the end of polymer flood II.

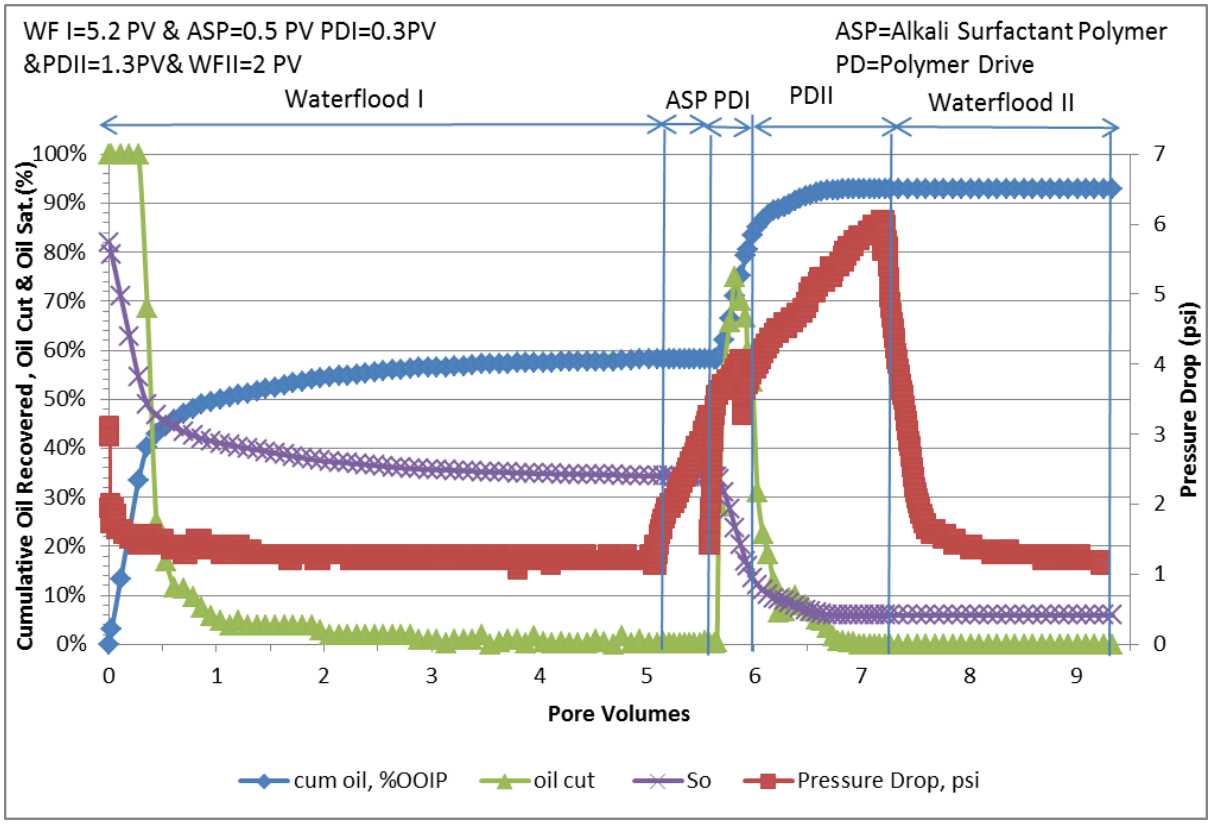

Figure 4.32: Cum. oil, oil cut, oil sat. and pressure drop vs. pore volumes

ASP#2 Effluent Analysis

Figure 4.33 shows effluent surfactant concentration obtained from HPLC analysis & cum oil recovery. ASP#2 Surfactant retention (surfactant adsorption+surfactant trapping) was calculated to be 0.87 mg/g of rock. High surfactant retention was due to forming viscous microemulsion. Furthermore, as shown in Figure 4.38, addition of extra polymer drive I slug that had same salinity as ASP slug might have forced surfactant slug slightly overstay in Type II region; thus, it cause loss of significant surfactant in residual oil. The surfactant retention can be decreased through decreasing microemulsion viscosity by adding better more branched co-solvent and removing extra polymer drive I from the injection scheme.

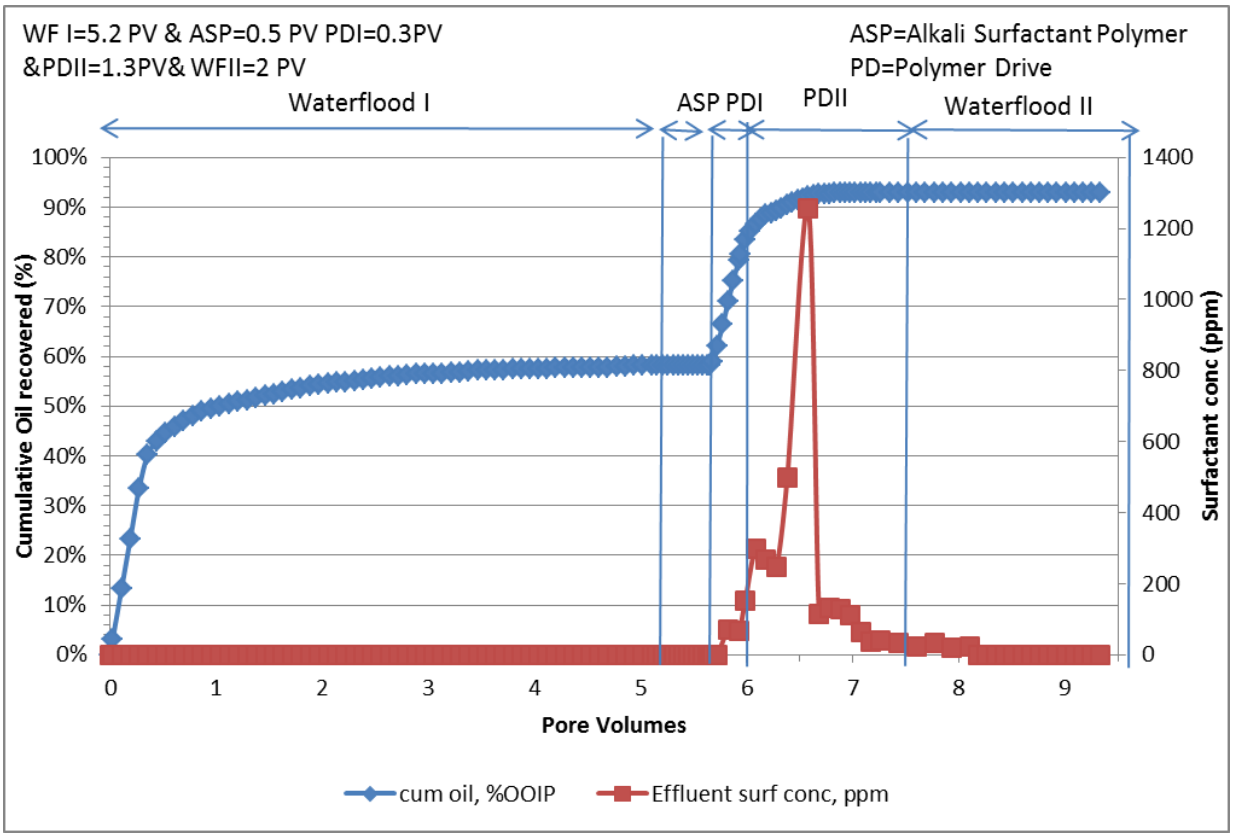

Figure 4.33: Effluent surfactant concentration, cum. oil vs. pore volumes

Figure 4.34 shows that salinity increased promptly after oil cut reached the peak and started to decrease which means that alkali was following the oil/water bank.

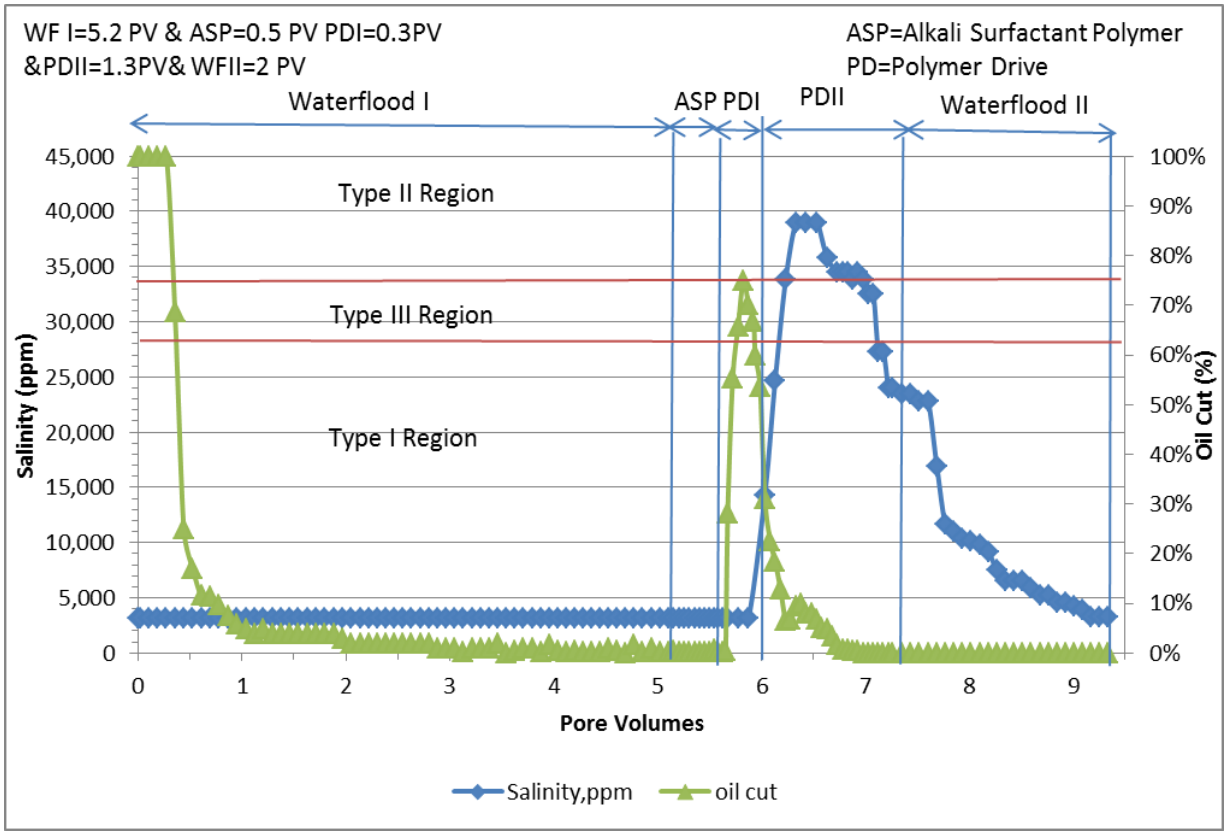

Figure 4.34: Oil cut, salinity slug vs. pore volumes

In addition to salinity slug, pH and viscosity of the effluent samples increased shortly after oil cut reached its peak and started to decrease as shown in Figures 4.35 and 4.36.

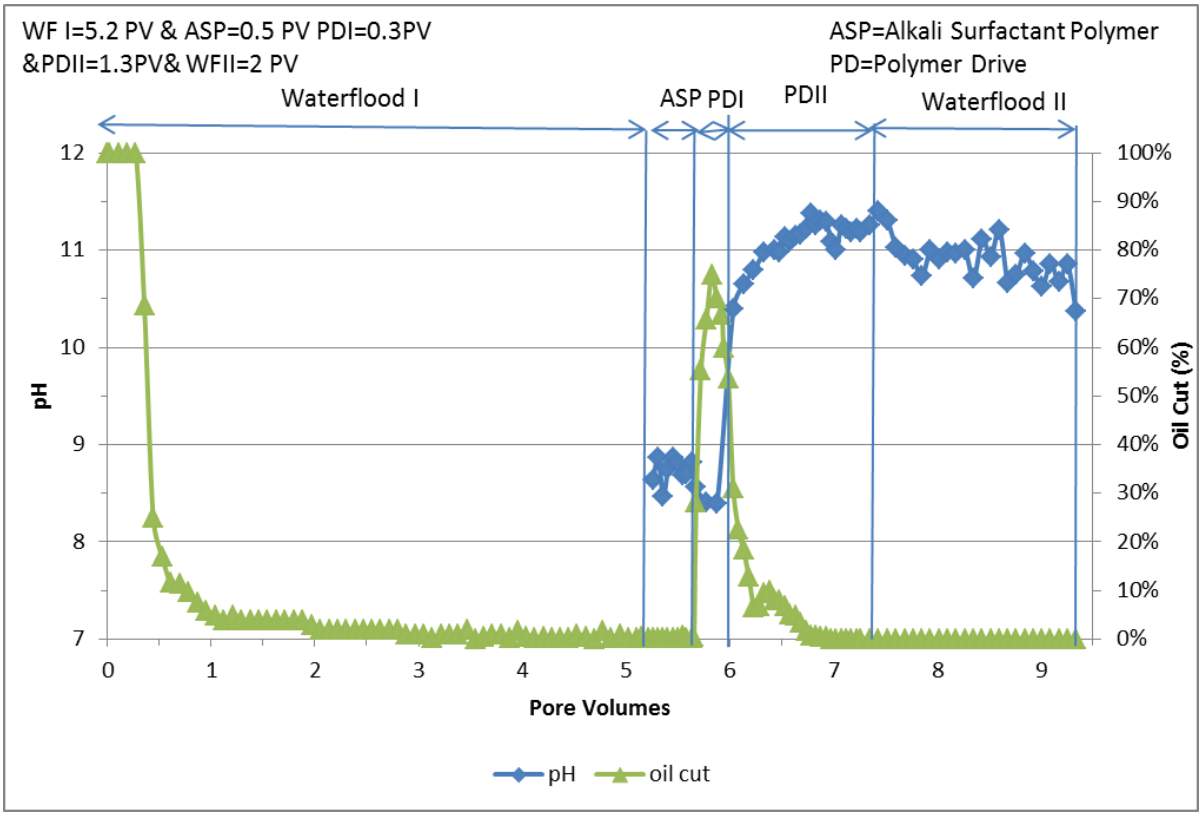

Figure 4.35: Oil cut, pH vs. pore volumes

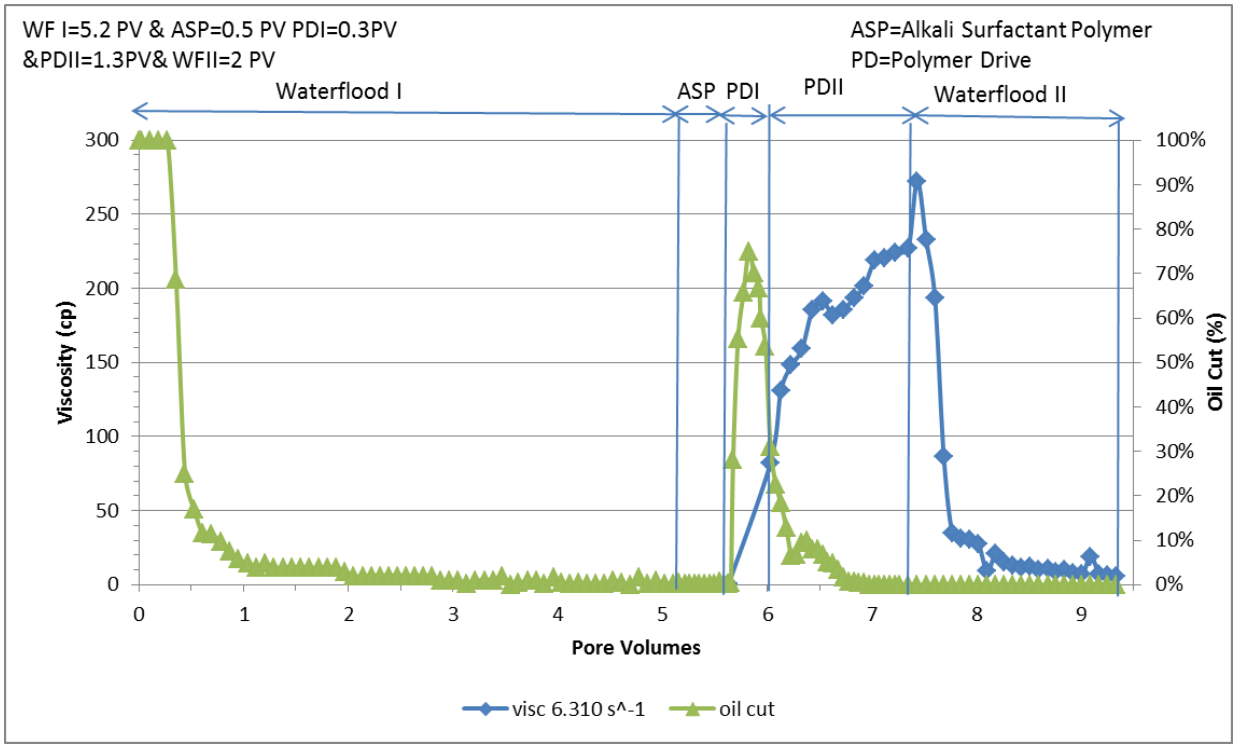

Figure 4.36: Oil cut, viscosity vs. pore volumes

Figure 4.37 shows that surfactant slug had two peaks. Smaller peak came out promptly after oil cut reached the peak and started to decrease, and larger surfactant peak came out with small delay which means that some surfactant got trapped.

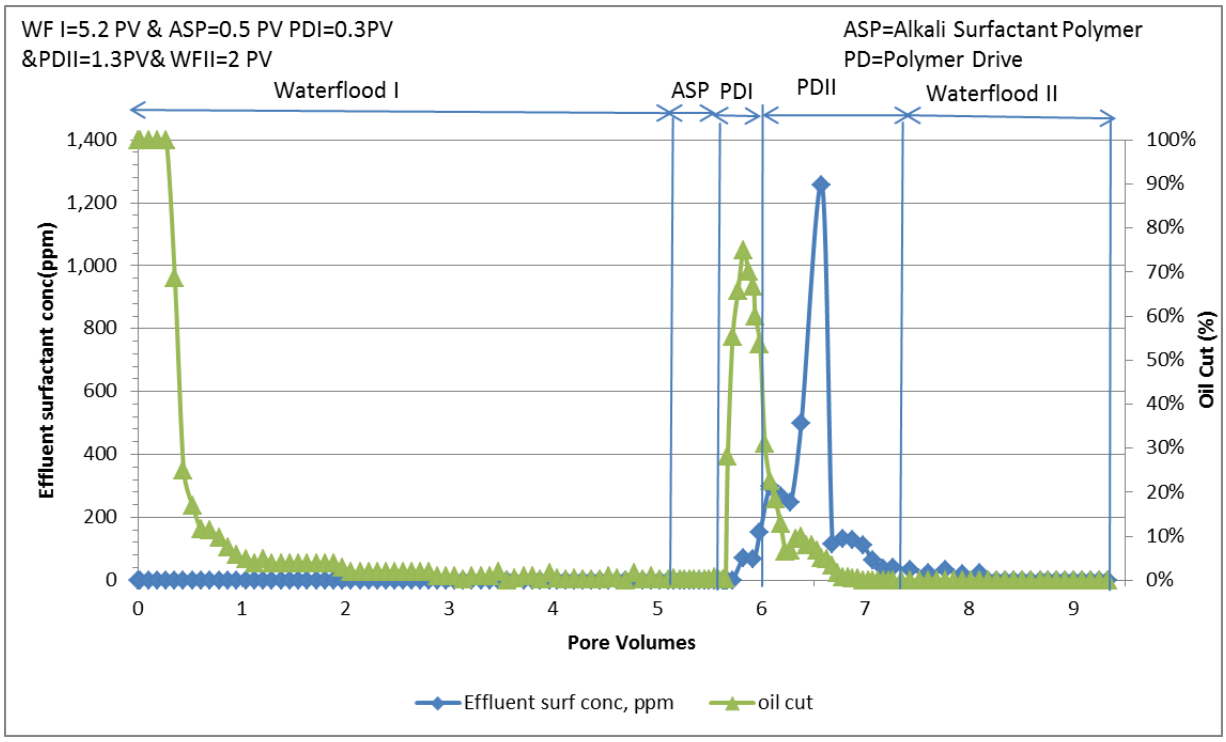

Figure 4.37: Oil cut, effluent surfactant concentration vs. pore volumes

Figures 38 and 39 show plots of salinity, pH, and surfactant concentration and viscosity slugs plotted. It can be seen that retardation of surfactant is not big and all fronts travel together. This ensures that surfactant slug passes through required ultralow IFT region. Even though surfactant retention showed high value, surfactant slug propagated much better compared to ASP#1.

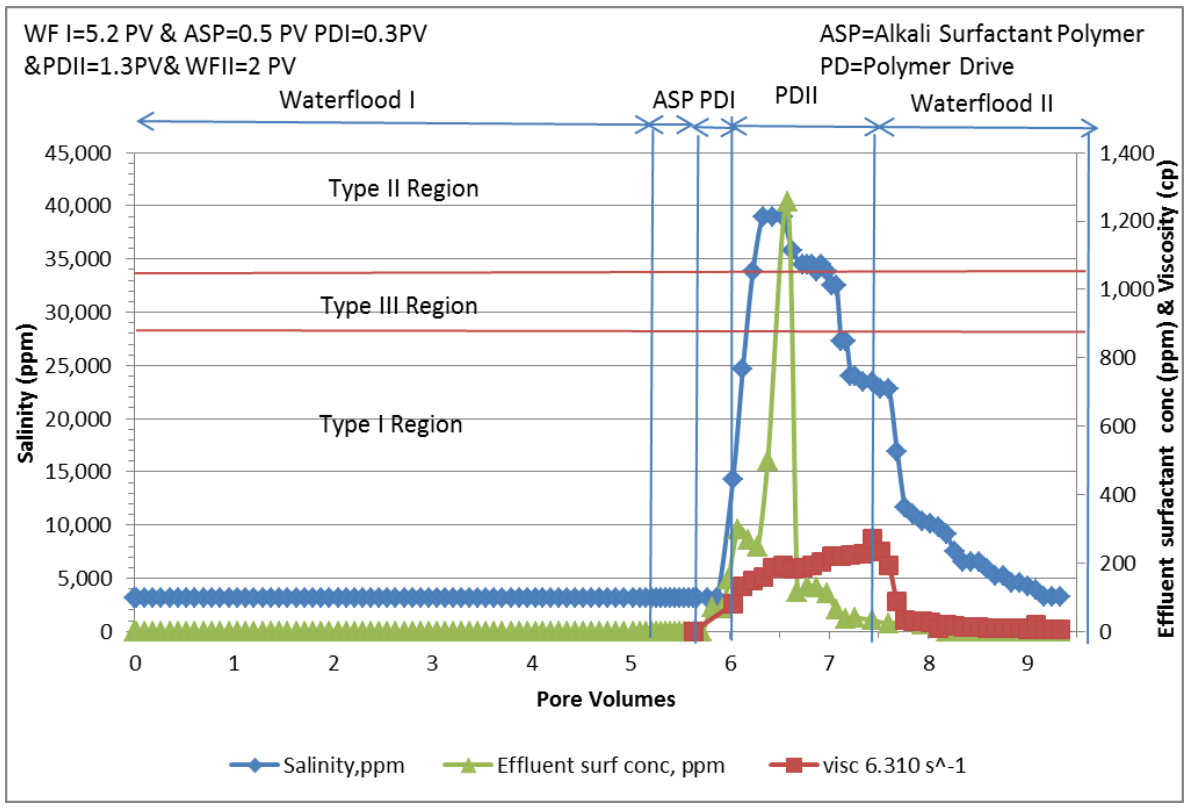

Figure 4.38: Effluent surfactant conc., salinity, viscosity vs. pore volumes

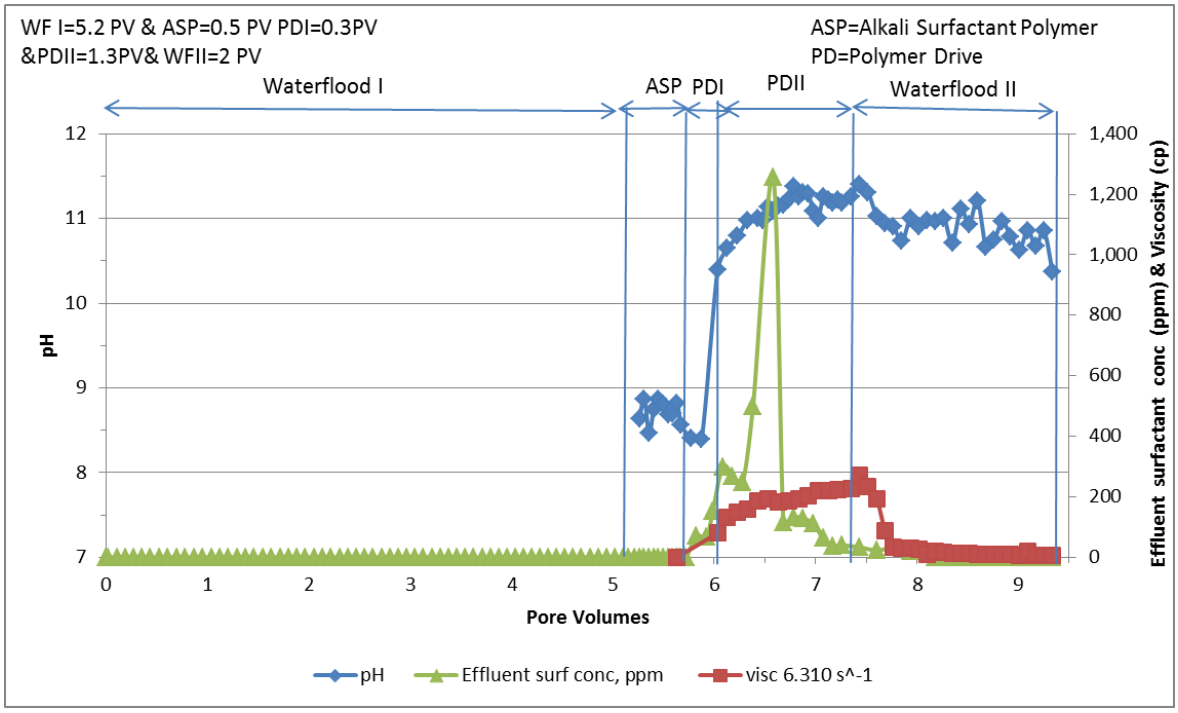

Figure 4.39: Effluent surfactant conc., pH, viscosity vs. pore volumes

Validation of Results

Figure 4.40 shows sand extracted from the sandpack after the experiments ASP#1 and ASP#2. Sand in the left jar was extracted after ASP#2 stable sandpack flood, while sand in the right jar represents sand extracted after ASP#2 unstable sandpack flood. ASP #2 stable flood clearly recovered more oil because sand is of lighter color and visually free of oil; contrary to that, unstable ASP#1 flood clearly left a lot of oil in the sandpack after the experiment was finished.

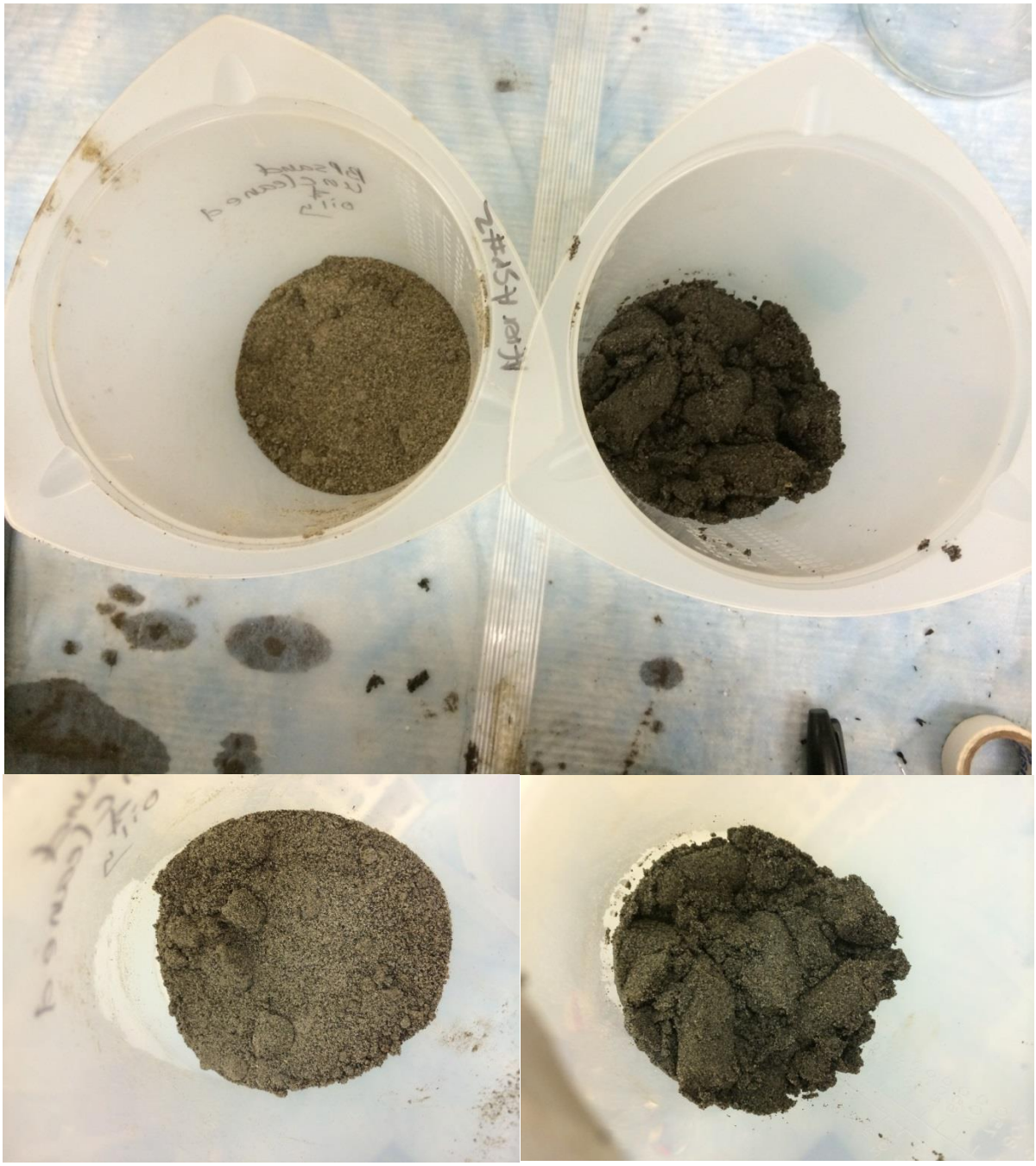

Figure 4.40: Comparison of the sands after the ASP#1 and ASP#2 sandpack flood experiments

4.3 2D Quarter Five-Spot Sandpack Experimental Results

First ASP5spot#1 2D quarter 5-spot pattern flood was conducted under stable conditions and second ASP5spot#2 2D quarter 5-spot pattern flood was conducted under unstable condition.

4.3.1 2D Quarter Five-Spot Sandpack Preparation and Flooding Procedure

Figure 4.41 shows a sketch of the quarter 5–spot sand pack and the picture of the actual quarter 5-spot sand pack. The flooding area is rectangular shape with 10”×10”×1”. It is covered on top and bottom with a rubber sheet where an overburden pressure can be applied. The pack is encased in steel.

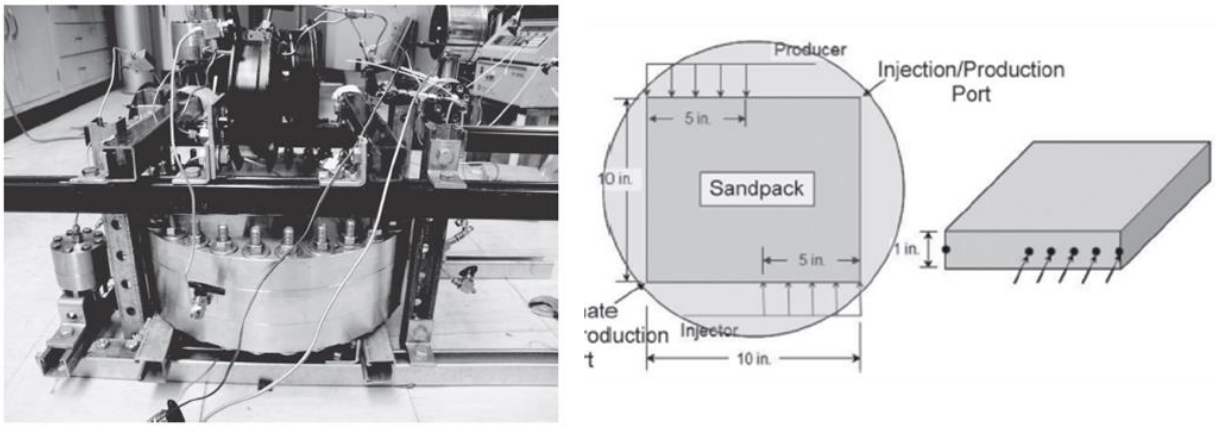

Figure 4.41: Top views of the quarter 5-spot pattern and actual picture of quarter 5-spot pattern

The quarter five–spot pattern was wet packed. After closing the quarter five-spot pattern, an overburden pressure of 1300 psi was applied. Then, the side valves of the quarter five -spot were opened so that excess amount of water can be leaked out. The formation brine in the model was displaced with a brine of different salinity. The effluent conductivity was measured which

can be translated to the salinity. The brine pore volume of the model was calculated from the effluent salinity.

Once the quarter five-spot pattern was completely saturated with the injection brine, oil was injected into the sandpack. Softened reservoir brine was used for waterflooding as it was done before for 1D ASP floods. The initial oil saturation was calculated from material balance. Then ASP slug and polymer drive solutions were injected followed by injection of SRB brine. Oil recovery, water cut and pressure drop were monitored. Figure 4.42 shows 2D ASP quarter five-spot pattern sandpack flooding diagram.

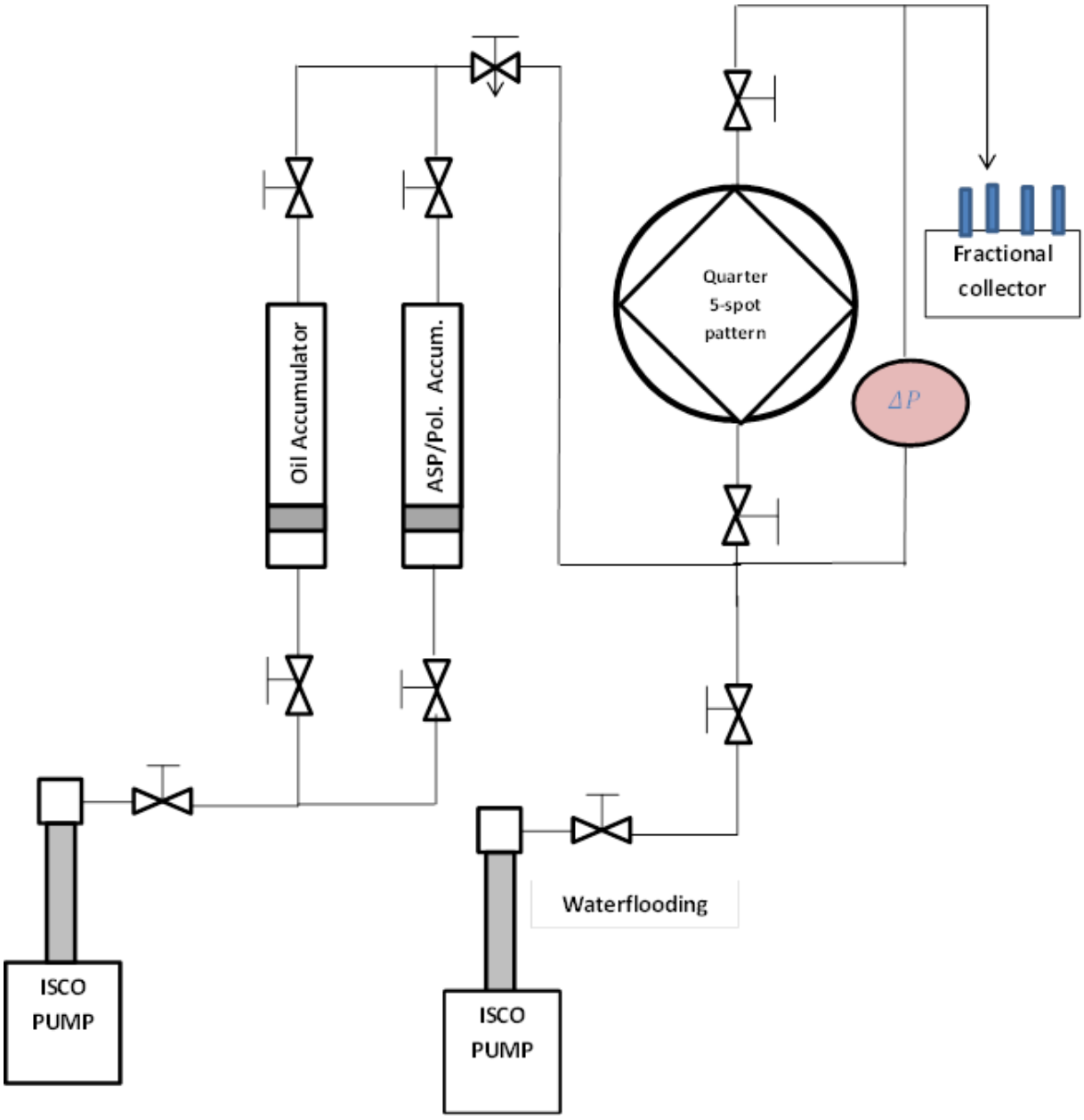

Figure 4.42: 2D ASP sandpack flood diagram

4.3.2 ASP5SPOT#1 2D QUARTER FIVE-SPOT SANDPACK FLOOD

Pore Volume Determination by Brine Tracer Test

Figure 4.43 shows the plot of brine tracer test performed on a quarter five -spot sandpack in order to determine its pore volume.As shown in Figure 4.44, for quarter five-spot patterns the sweep efficiency was estimated to be between 68% -72% at the breakthrough by Dyes et al. (1954), Habermann (1960) and many others. It can be seen from Figure 3 that sweep efficiency at the breakthriough usually occurs at around 68% . Furthermore, from Brigham et al. (1965) it was found that breakthrough occurs close to 0.72 PV during the miscible flood. Figure 4.45 shows sweep eficiency plot for this experiment. The breakthrough occurred at around 385 ml injected brine tracer which is supposed to be equal to 0.72 PV accroiding to Brigham et al. (1965). Thus, it was estimated that the quarter five-spot pattern sandpack had a pore volume of 535 ml.

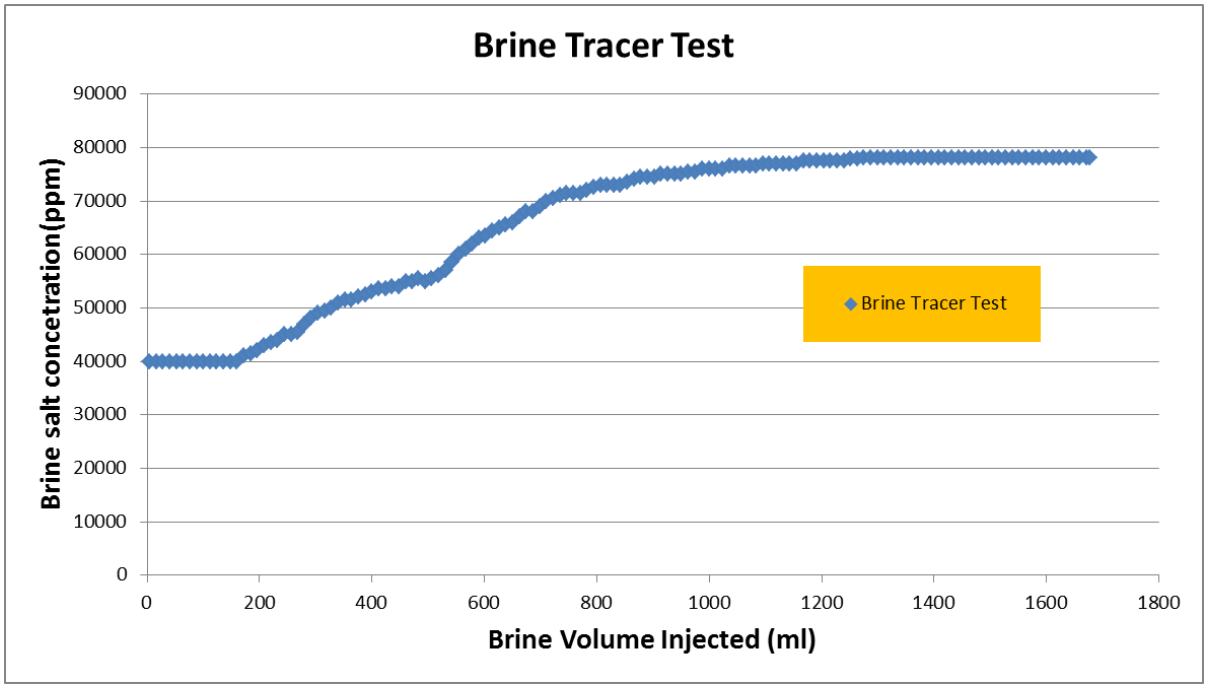

Figure 4.43: Brine tracer test for 2D sandpack

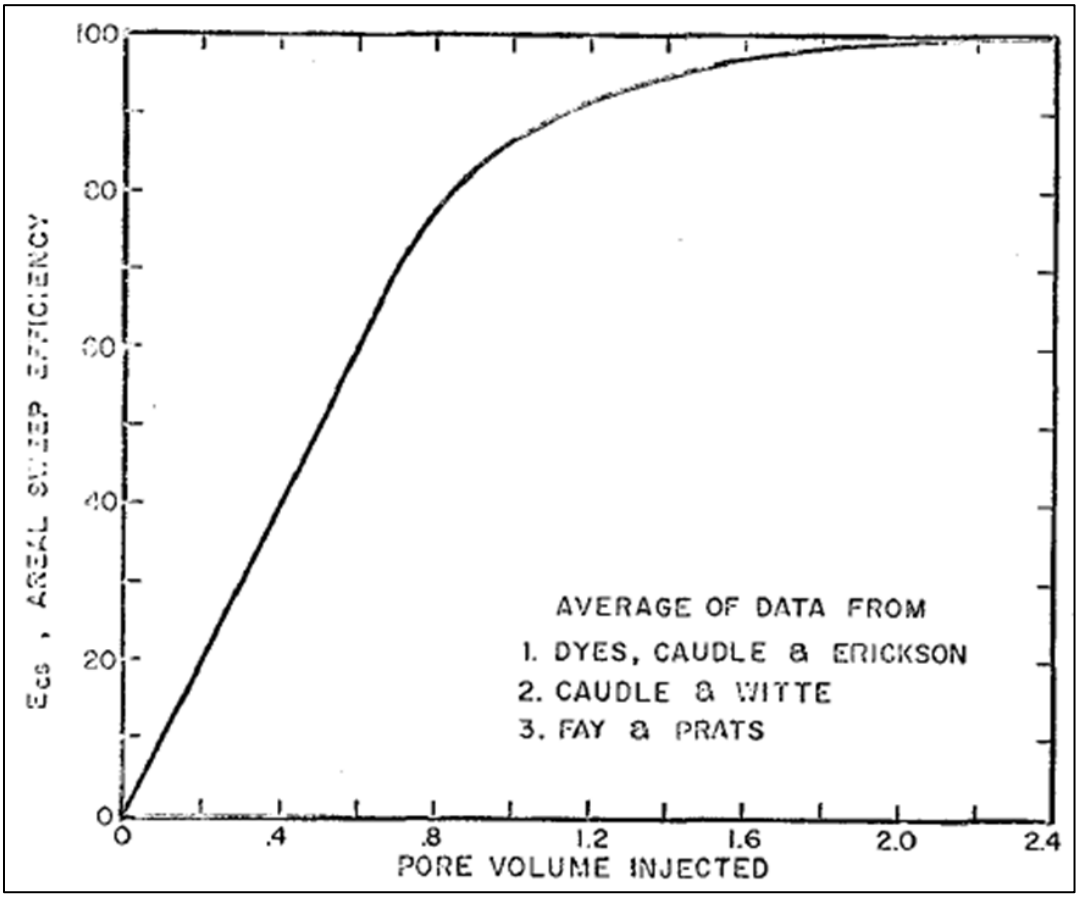

Figure 4.44: Five-spot sweep efficiency data for mobility ratio =1 (Dyes, 1954)

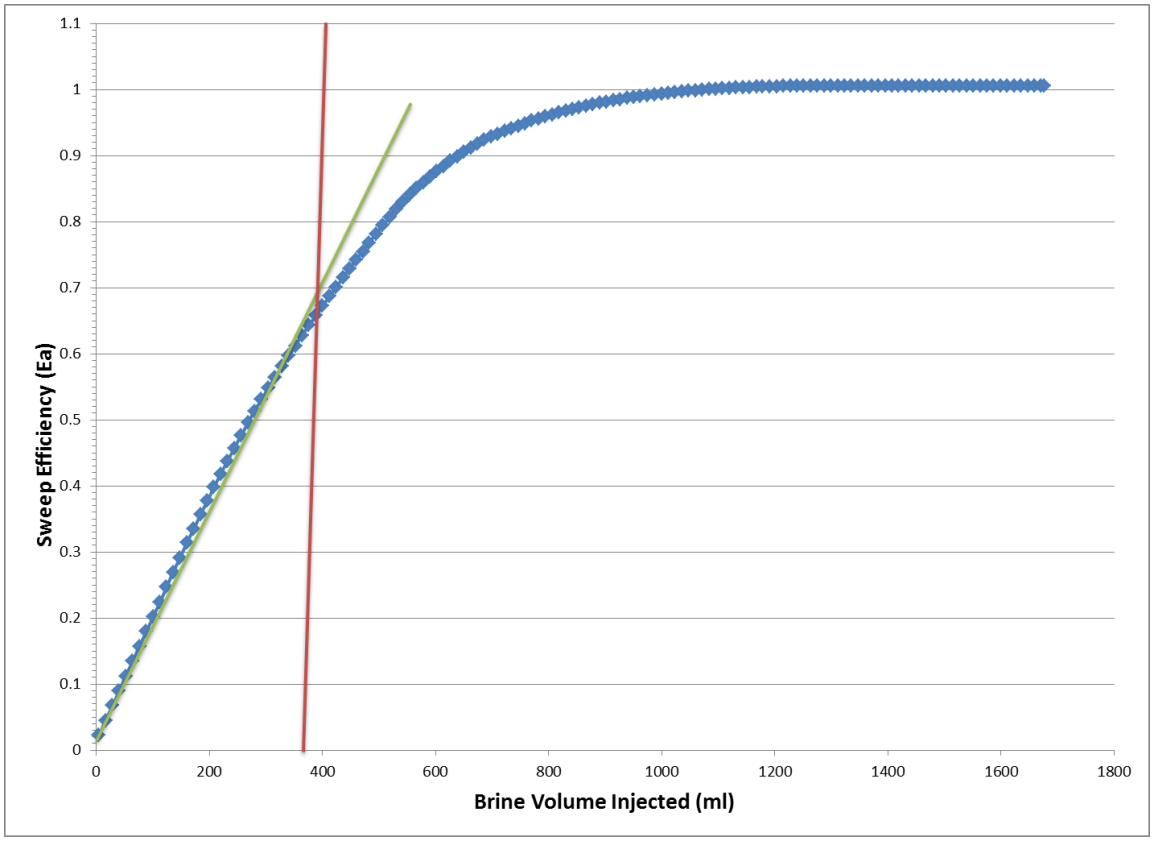

Figure 4.45: Pore volume determination for a quarter five-spot pattern

ASP5spot#1 Quarter Five-Spot Sandpack Properties

Table 4.10 shows the initial properties of the sandpack before flooding started.Porosity was detremined through tracer test and was equal to 32.6 %. Overburden pressure of 1300 psi was applied to the sandpack. Inititial oil satuuration was equal to 88% . Experiments were performed at the room temperature.

Table 4.9: ASP5spot#1 quarter five-spot sandpack properties

ASP5spot#1 Sandpack Properties:	
Outcrop:	reservoir sand
Porosity:	0.326
Dimensions:	10×10×1 inch^3
Temperature:	25 ^oC
Overburden Pressure:	1300 psi
Pore Volume:	535 ml
OOIP:	470 ml
Soi:	88%

ASP5spot#1 Flood Design

Table 4.11 represents overall ASP5spot#1 flooding design. There was one big difference compared to ASP#2 in 1D flood; we did not employ Polymer Drive I. The main reason was that according to ASP#2 flood in 1D flood it seems that we overstayed in overoptimum salinity zone too long due to employing extra polymer drive (PDI) which had the same salinity as ASP slug. We think that overstaying in overoptimum region for too long caused the surfactant retantion to be high .Other than that, all flooding design properties remained exactly same as in 1D ASP#2 flood described earlier.

Table **4.10**: ASP5spot#1 flood design

ASP5spot#1 Flooding Desgin			
Slug Components:	ASP slug:	Polymer Drive I	Softened Reservoir Brine (SRB)
PV injected:	0.48	1.05	4.2
[HPAM 3630S] ppm	4750	4750	----
[surf#1], wt%	0.75% Alfoterra	----	----
[surf#2], wt%	0.25% Enordet IOS	----	----
[Cosolvent], wt. %	1% IBA		----
ppm Na2CO3	32500	22750	----
TDS ppm	35664.5	25914.5	3164
Frontal velocity, ft/day	0.8	0.8	0.8
Viscosity at 10 s^{-1} & room temp	180	180	1
Oil Viscosity, s^{-1}	100	100	100
pH	11.21	11.1	7.82

Figure 4.46 shows viscosities of the slugs and reservoir oil. This time we had viscosity of both ASP and Polymer slugs to be equal to ~180 cp at 10 s^{-1} shear rate.

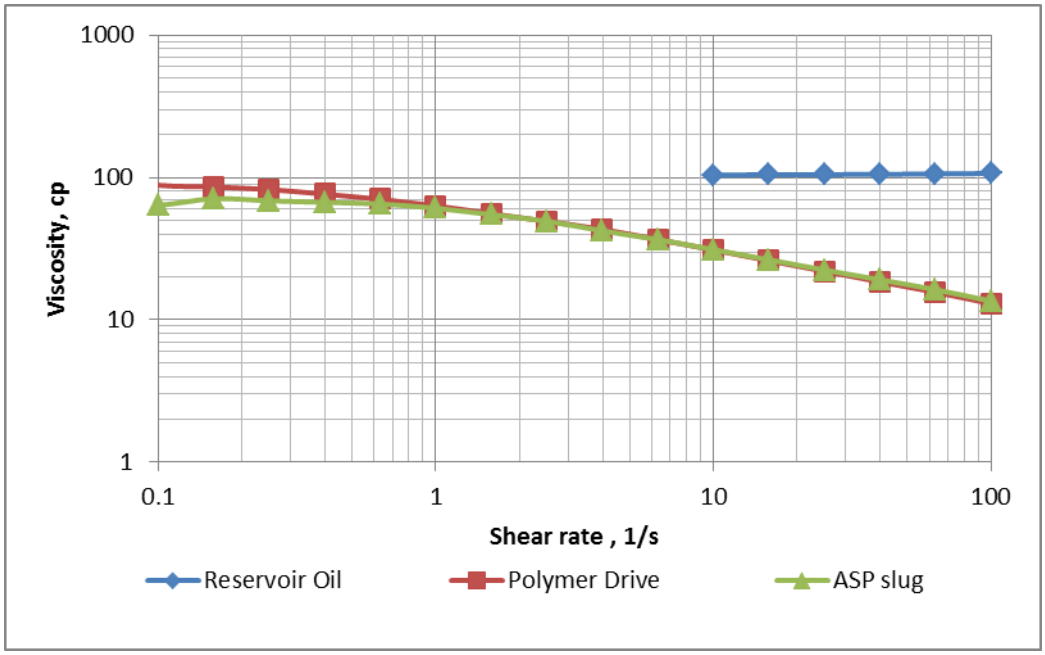

Figure 4.46: Viscosities of ASP, polymer slug, and reservoir oil

Salinity Gradient Design for ASP5spot#1 Flood

Figure 4.47 illustrates the salinity gradient design that was employed in the 5-spot flood. According to that design 5-spot sandpack was waterflooded for 1PV followed by 0.5 PV of ASP and 1 PV of polymer slug, and finally finished with second waterflood in order to see whether there is any remaining oil left after tertiary recovery.

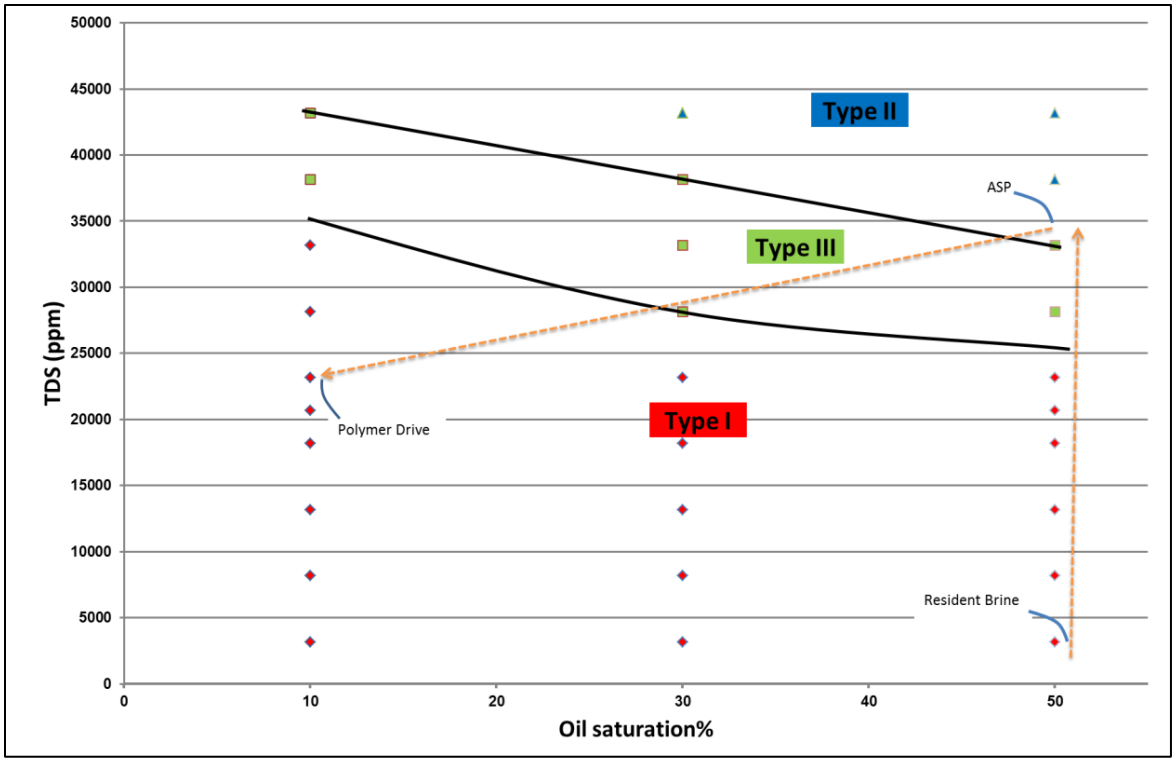

Figure 4.47: Salinity gradient design for ASP5spot#1 flood

Summary of ASP5spot#1 Flood Results

Table 4.12 shows summary of ASP5spot #1 sandpack flood. Waterflooding recovered 52% of original oil in place (OOIP) and decreased oil saturation from initial oil saturation of 88% to 42.1%. Chemical flooding including second waterflooding recovered extra 48% of OOIP and increased overall recovery to 98.7% of OOIP. Furthermore, chemical flooding decreased oil saturation from 42.1% to 1.2%. Tertiary recovery was able to recover 97% of remaining oil in place (ROIP). To conclude, stable ASP5spot#1 sandpack flooding in viscous oil showed excellent results.

Table 4.11: Summary of ASP5spot#1 flood results

Soi=88%			
1.14PV	Waterflood I,ml:	Recovery, % OOIP	So
	244.25	52%	42.1%
0.48PV	ASP slug recovery, ml:		
	25.85	6%	37.1%
1.05PV	Polymer Drive , ml:		
	190.525	41%	1.7%
3.06PV	Waterflood II, ml:		
	3.2	1%	1.2%
TOTAL:	TOTAL:	TOTAL:	TOTAL:
5.73 PV	463.825	98.7%	1.2%
1.53PV	ASP+PD:	Tertiary Recovery , % ROIP	
	219.575	97%	1.2%

Figure 4.48 shows cumulative recovery, pressure drop, and oil cut and saturation for the flood. Oil cut reached a high value of 80% and stayed there for around ~0.4 PV. Oil cut shape shows that flood was stable. Surfactant breakthrough occurred at ~2 PV of total injection time when oil cut started falling down and 0.9 PV after the start of surfactant injection time. The final oil saturation at the end of flood was 1.2%. Maximum pressure drop was reached at the end of polymer drive injection and was equal to 30 psi, which in turn equals to 25 psi/ft across the quarter five-spot pattern. Furthermore, mobility ratio between oil/water bank and chemical slug was around ~0.66, as it can be estimated from the division of the pressure drop for the oil bank by the pressure drop at the end of polymer flood.

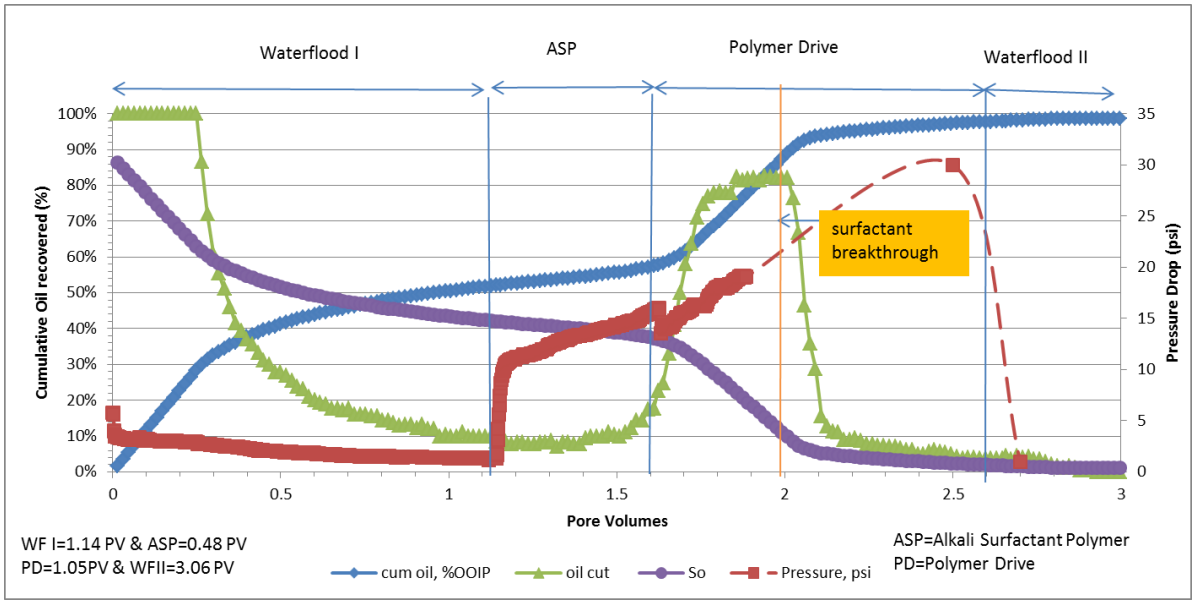

Figure 4.48: Cumulative oil recovery, oil cut, oil saturation and pressure drop

Effluent Analysis

Effluent analysis was performed on the collected samples. Total salinity, pH and viscosity of each sample were measured. Figures 4.49-4.51 show that salinity, pH and viscosity slugs come out promptly after oil cut goes down without much delay. Measured pH increased when surfactant breakthrough occurred at around 2 PV and stayed at around ~11 for at least 1 PV. Total salinity also increased at the surfactant breakthrough and reached around 33,000 ppm. Viscosity slug also increased immediately after surfactant breakthrough and reached about 200-230 cp values at 6.31 s^{-1} shear rate.

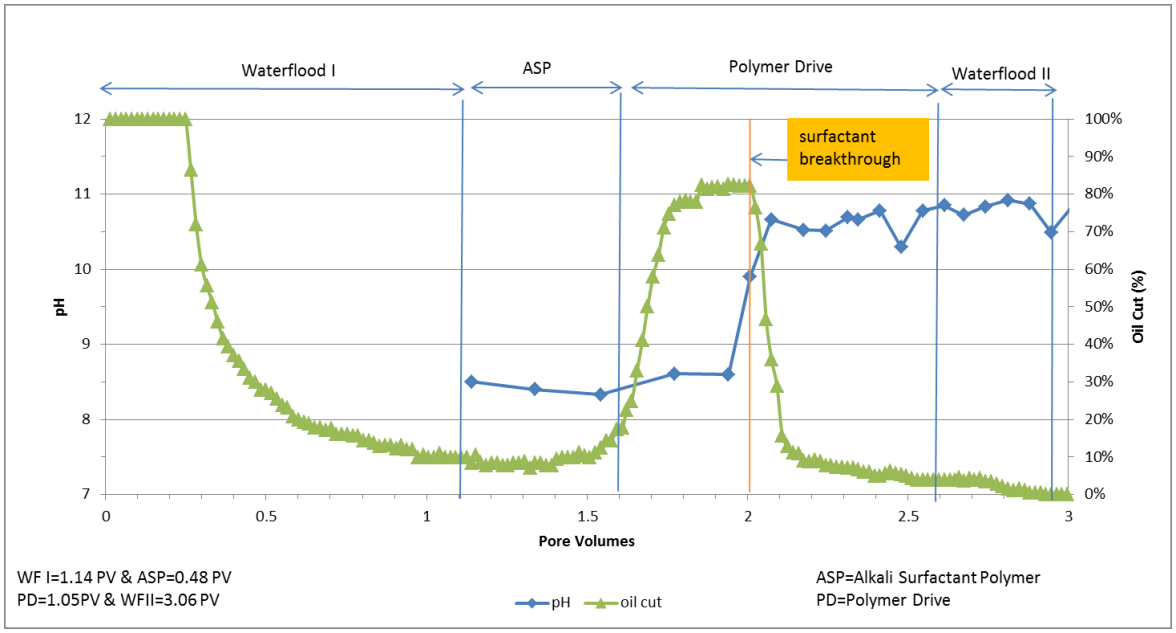

Figure 4.49: Oil cut and effluent pH

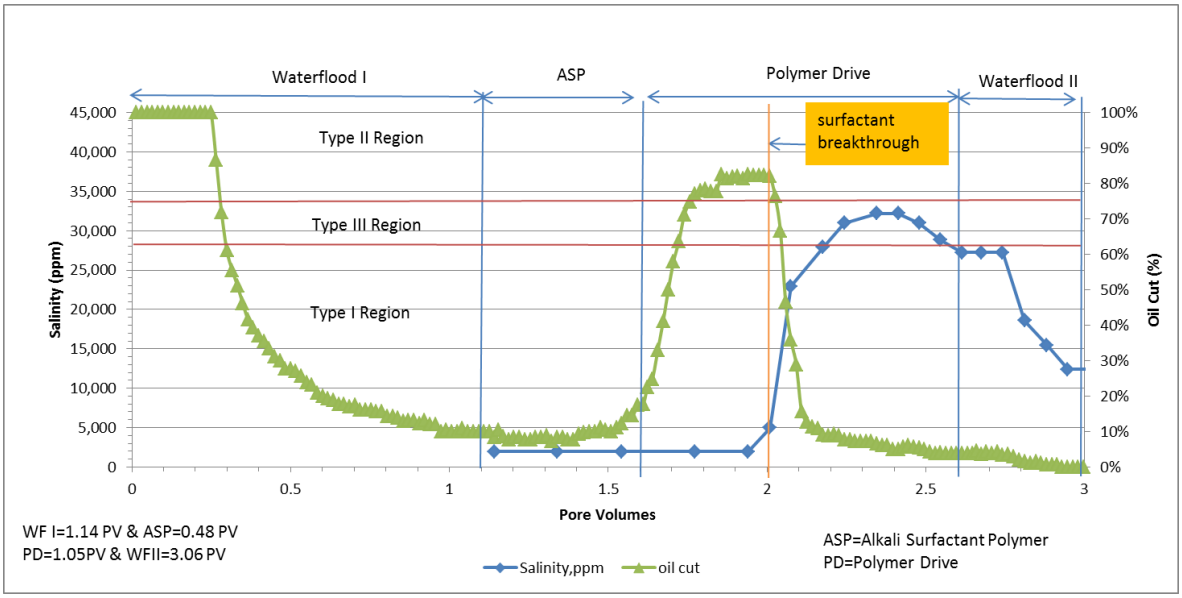

Figure4.50: Oil cut and effluent salinity

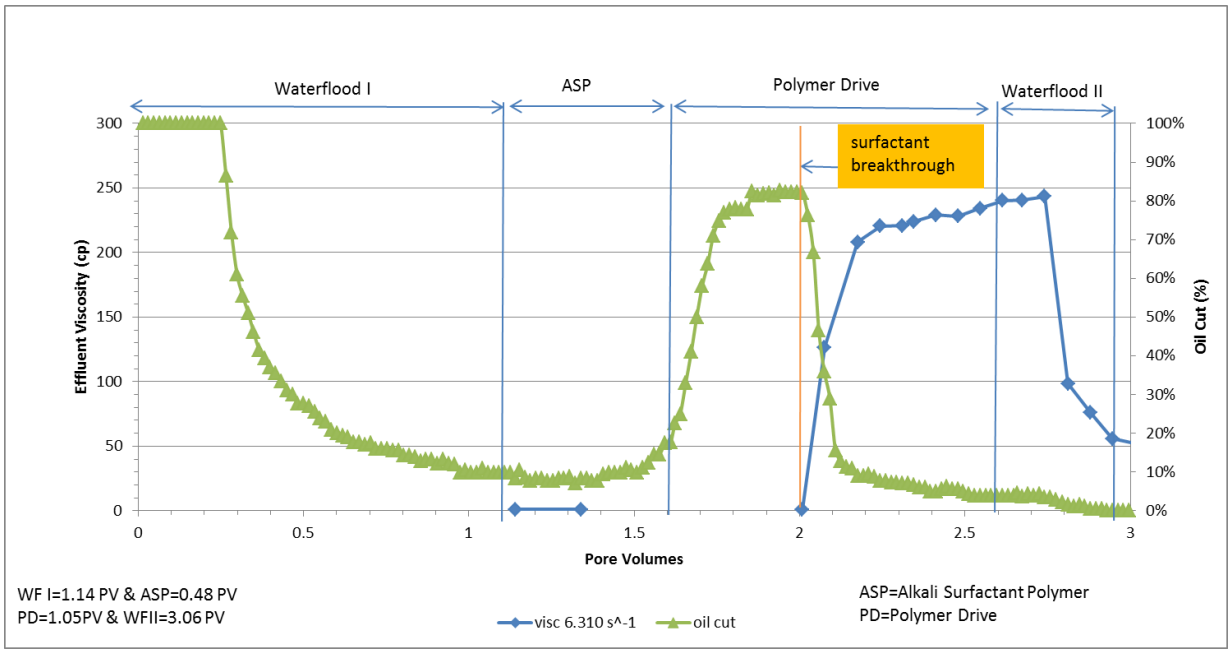

Figure 4.51: Oil cut and effluent viscosity at 6.31 s^{-1} shear rate

Figures 4.52 through 4.54 show salinity, viscosity and pH slugs compared to each other. There is not much lag between the slugs and they all start increasing after surfactant breakthrough.

.

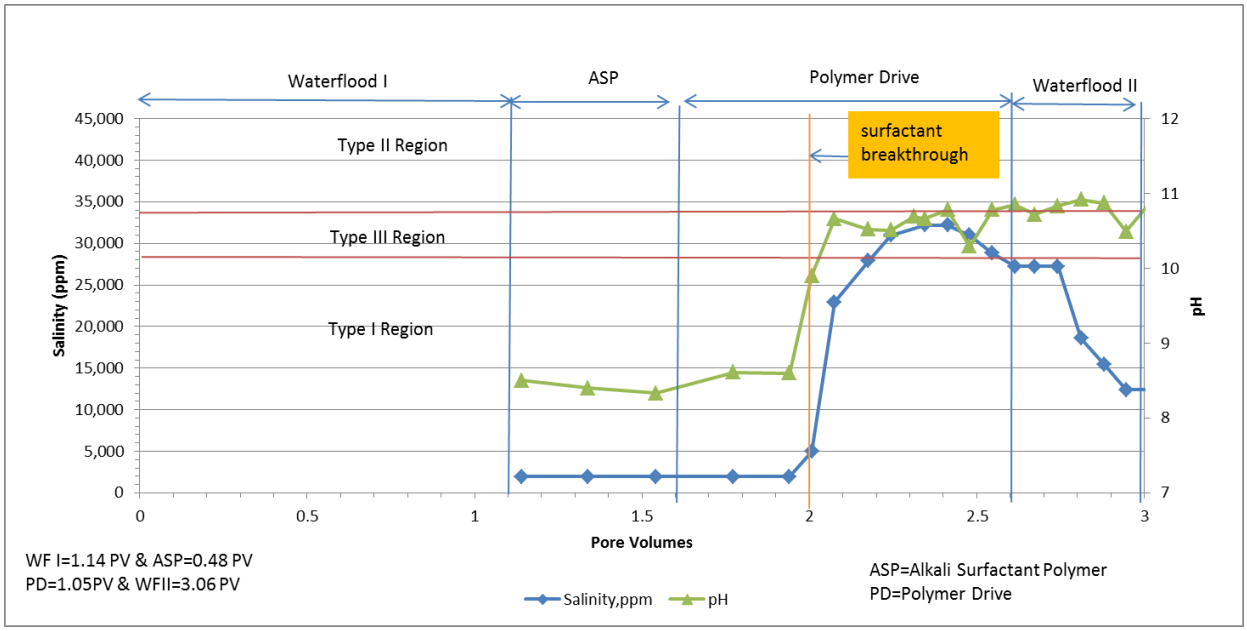

Figure 4.52: Effluent salinity and pH

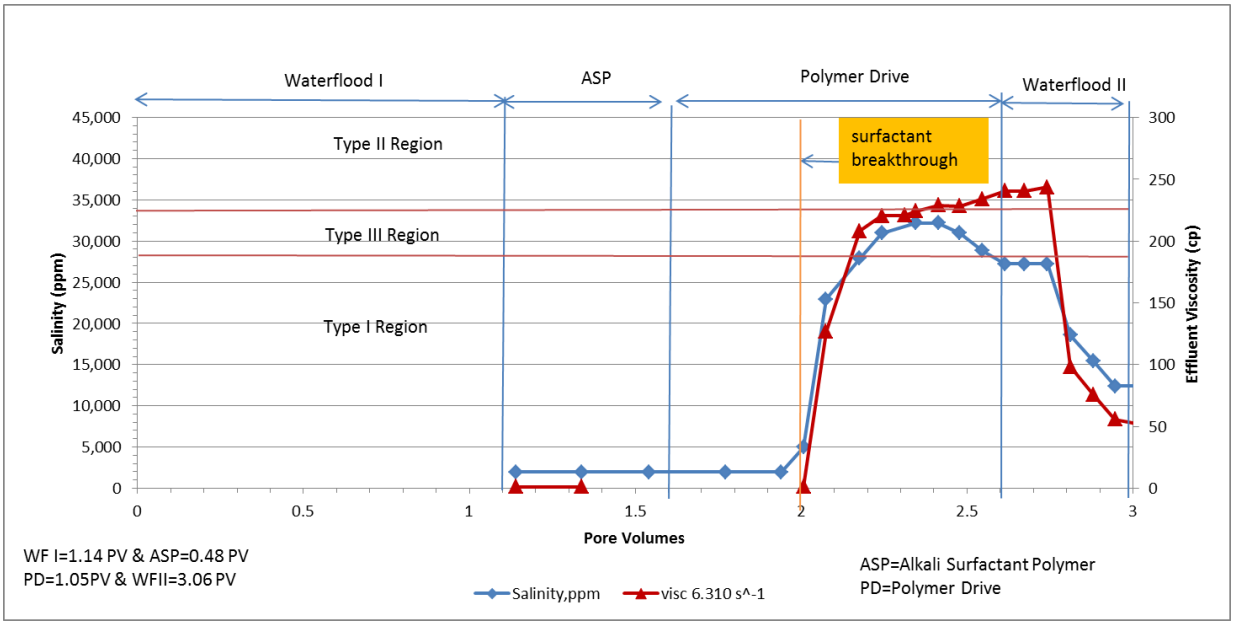

Figure 4.53: Effluent salinity and viscosity at shear rate 6.31 s^{-1}

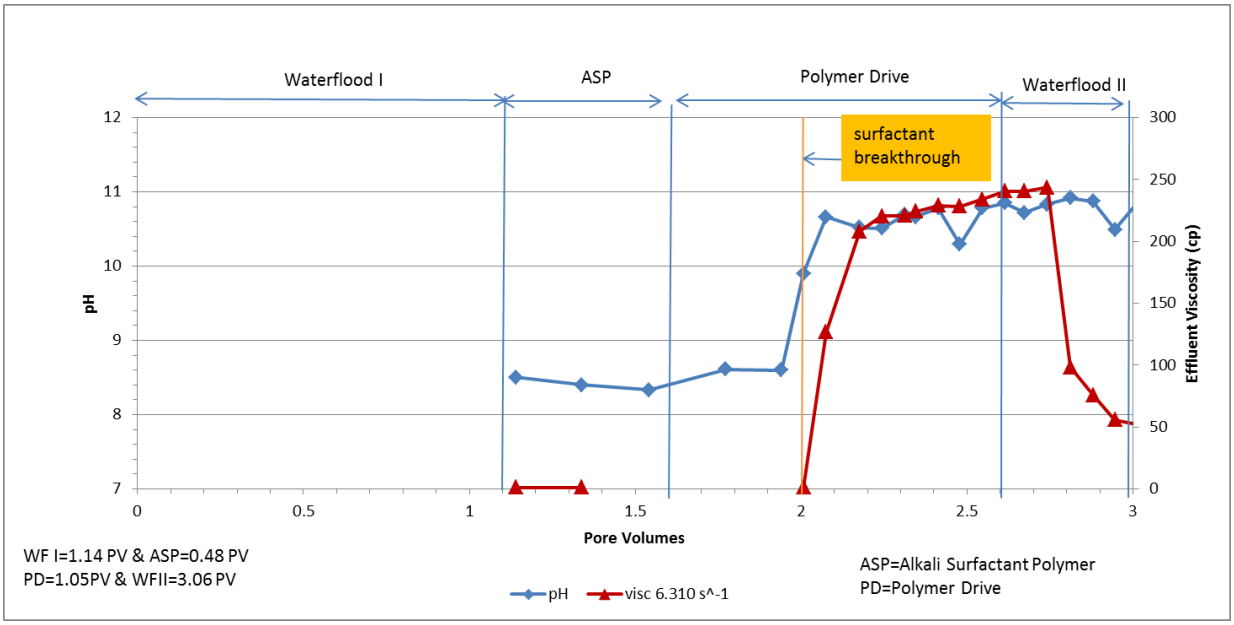

Figure 4.54: Effluent pH and viscosity at 6.31 s^{-1} shear rate

Surfactant Effluent Analysis

Surfactant concentration in the aqueous phase for each effluent sample was measured. Figures 4.55 to 4.58 show the salinity, surfactant concentration, pH, viscosity and oil cut of the effluent samples. In all Figures surfactant slug travels together with other slugs and there is no delay. Furthermore, surfactant retention was computed to be ~ 0.58 µg/gm of rock. Considering flood was in 2D pattern surfactant retention was relatively low, furthermore, surfactant retention in 2D pattern was lower compared to ASP#2 sandpack flooding in 1D. The main reason was that surfactant slug fell directly into Type III region salinity and very stable nature of flood.

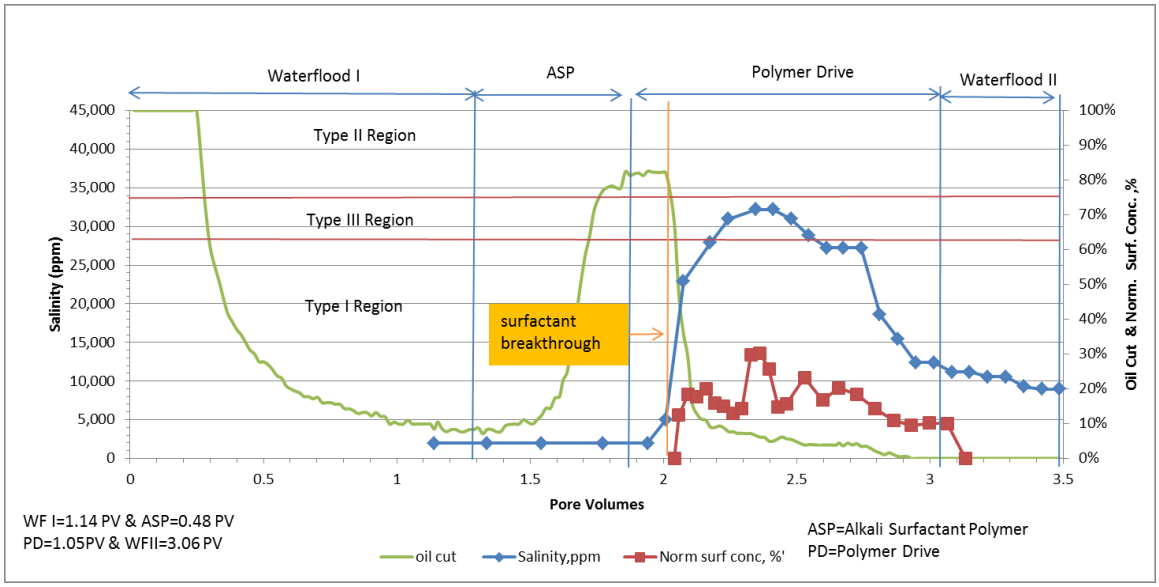

Figure 4.55: Oil cut, effluent surfactant concentration and effluent salinity

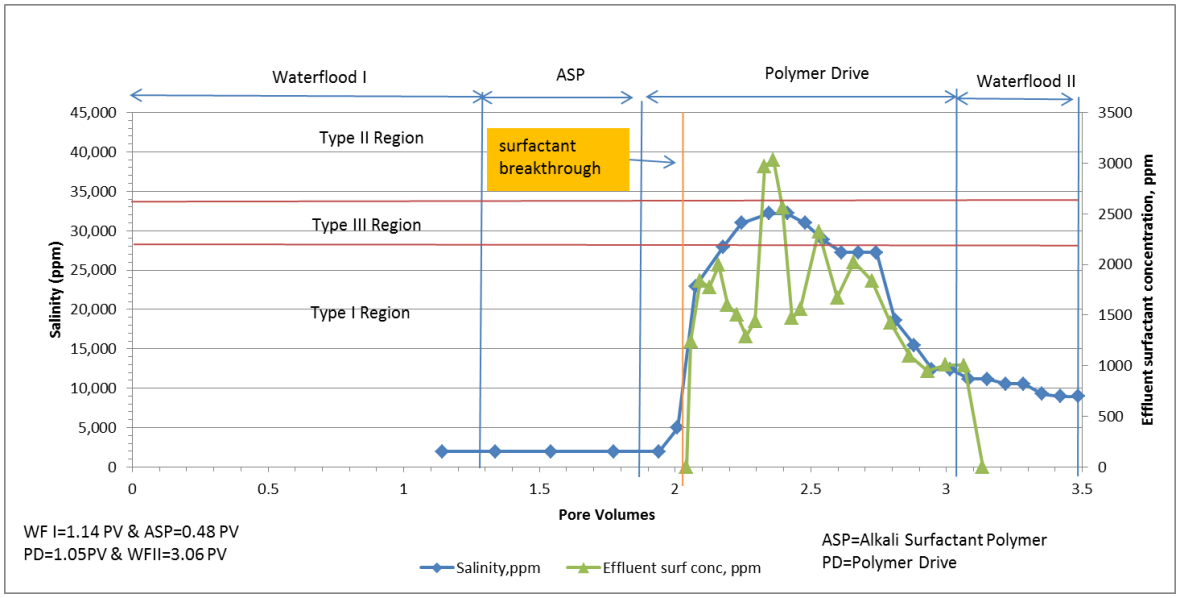

Figure 4.56: Effluent surfactant concentration and salinity

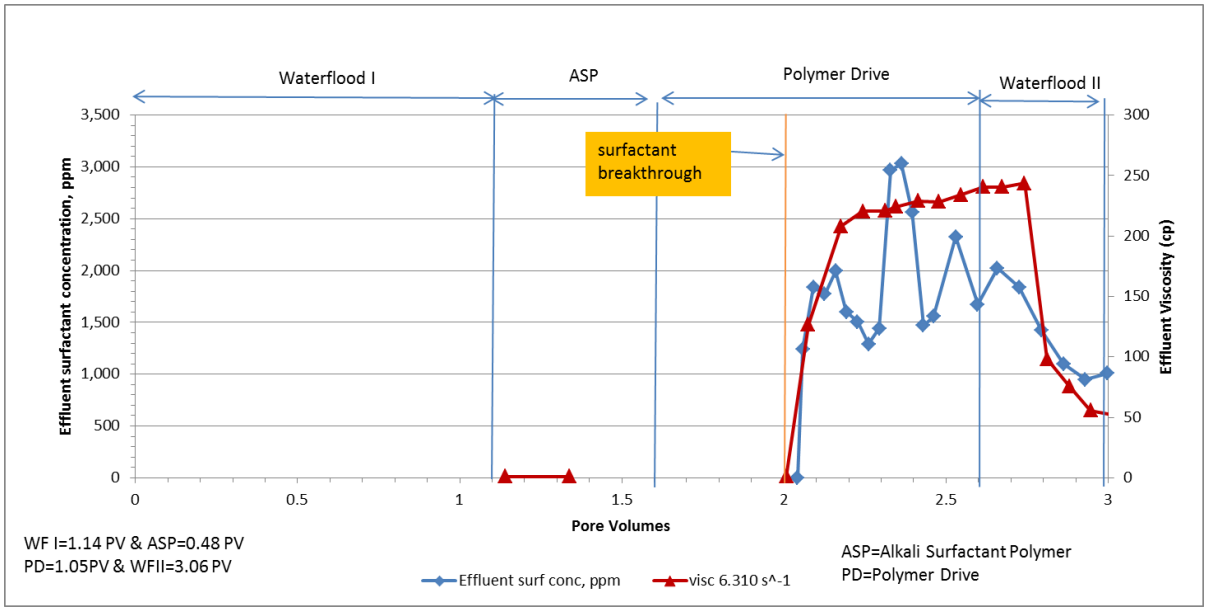

Figure 4.57: Effluent surfactant concentration and viscosity at 6.31 s^{-1} shear rate

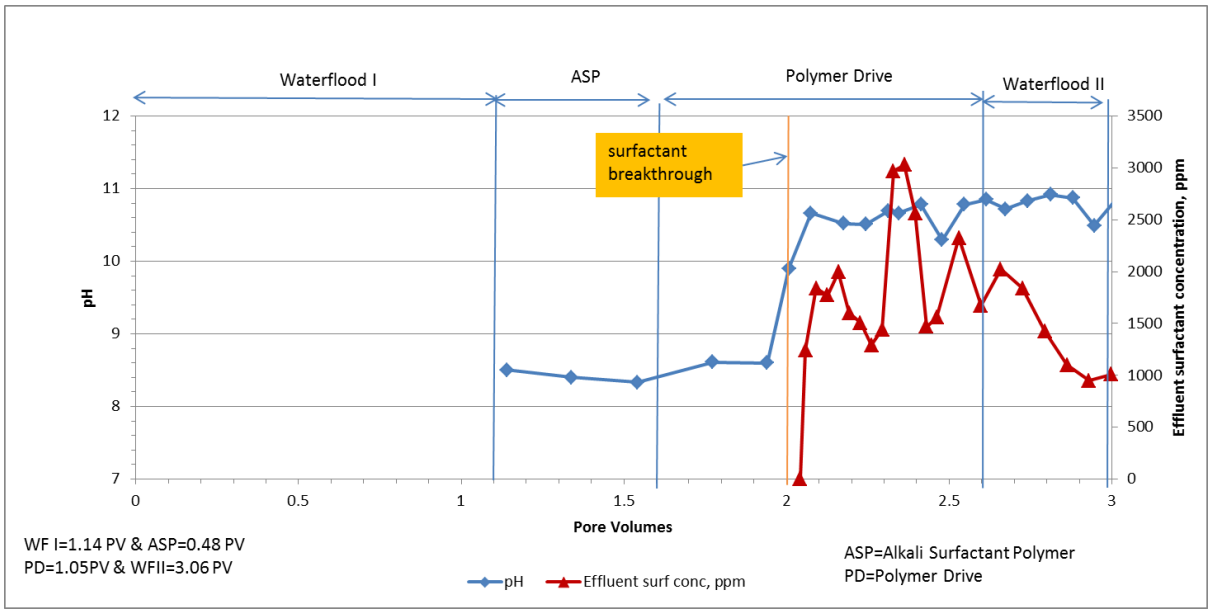

Figure 4.58: Effluent surfactant concentration and pH

Validation of Results

In order to validate that 2D recovery had indeed had very high recovery, the quarter five-spot was opened after the experiment was finished. The sandpack visually was free of oil , no oil sticking on sand was observed. Furthermore, as seen in Figure 4.59 the sandpack was subdivided into 25 zones of 2×2×1 cubic inches volumes and those zones were analyzed for presence of oil. Furthermore, Figure 4.59 shows 3 representative samples of sand taken from three different spots in the sandpack. Sample 1 and 3 were taken from zones that are marked 1 and 3 , and sample 2 was taken from zone 2 as shown in Figure 4.59. Zones 1 and 3 are dead end parts of the quarter five-spot, and zone 2 was the outlet of the sandpack.

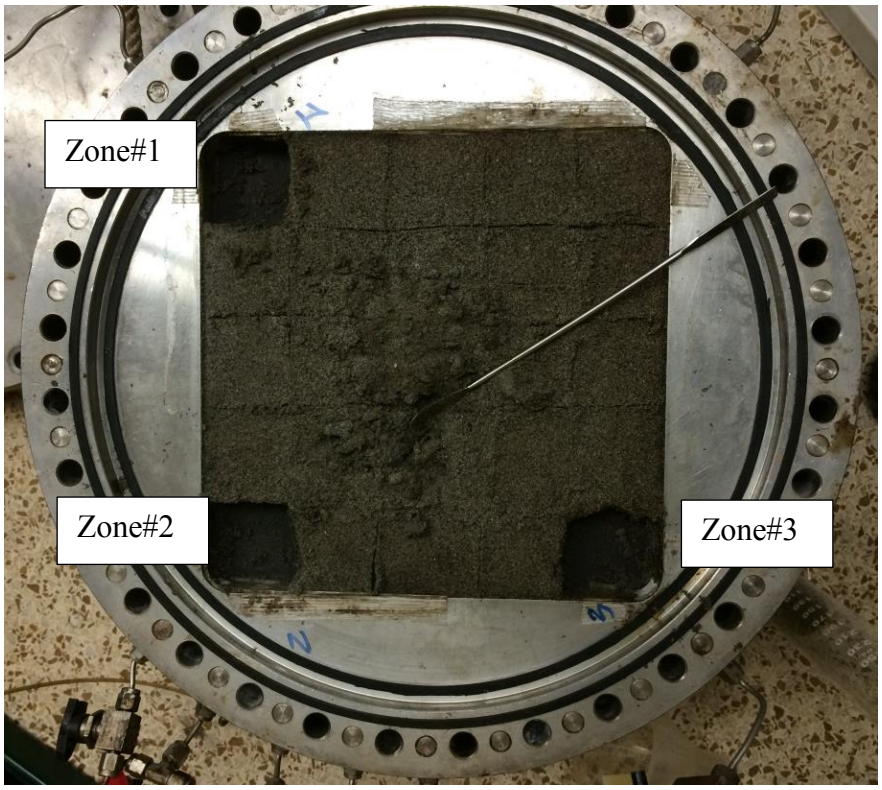

Figure 4.59: Investigated zones of five-spot used for validation

As shown in Figure 4.60, sand samlples were put into 250ml cylinder and were treated with water and significant amount of sodium chloriode (10gm) in order to seprate oil from the sand and water . Futhermore, cyclinder were shaken for several minutes until sodium choloride would completely dissolve in water. Figure 4.60 shows that there was no significant oil present in the sand samples. The sample 2 showed virtually no oil and samples 2 and 3, even though they were taken from dead-end zones of the five spot, produced insignificant amount of oil.

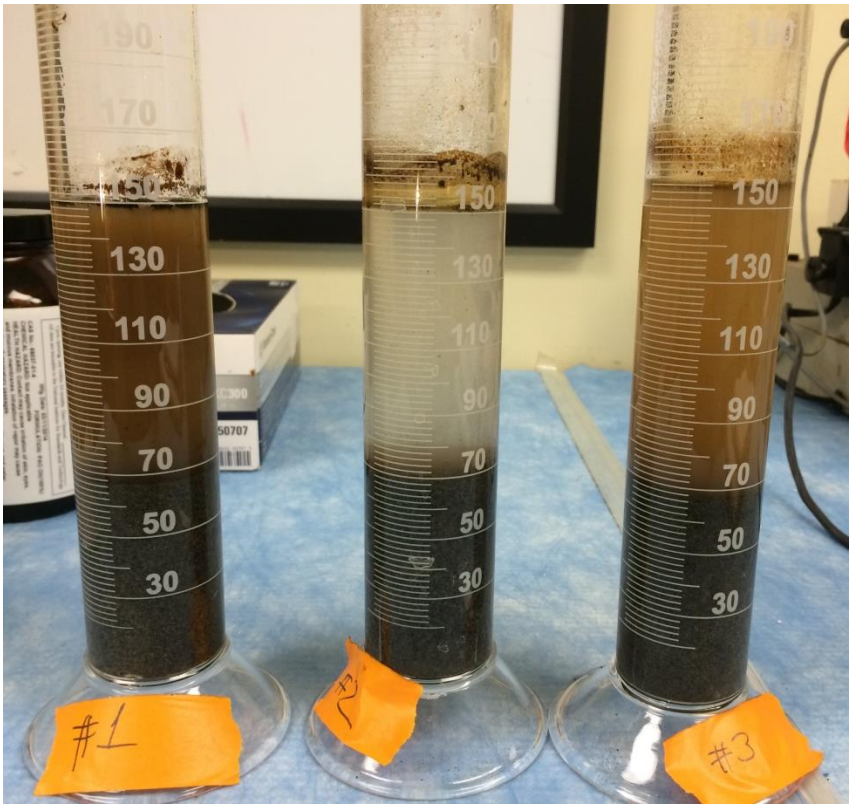

Figure 4.60: Samples from zones 1, 2 and 3 after treatment

4.3.3 ASP5SPOT#2 2D QUARTER FIVE-SPOT SANDPACK FLOOD

The main objective of ASP5spot#2 quarter five-spot flooding was to conduct an unstable flood with less polymer concentration. The ASP5spot#2 experiment flood design was mostly the same as the first ASP5spot#1 flood except for the polymer concentration.

Pore Volume Determination by Brine Tracer Test

Figure 4.61 shows the effluent brine salinity for the 5-spot sandpack when one salinity brine is displaced by another salinity brine in order to determine its pore volume. From Brigham et al.*(*1965) it was found that breakthrough occurs close to 0.72 PV during unit mobility miscible floods. Figure 4.62 shows sweep eficiency plot for this experiment. The breakthrough occurred at around 424 ml injected brine which is supposed to be equal to 0.72 PV accroiding to Brigham et al.(1965) paper. Thus, it was estimated that 5-spot pattern had a pore volume of 588 ml.

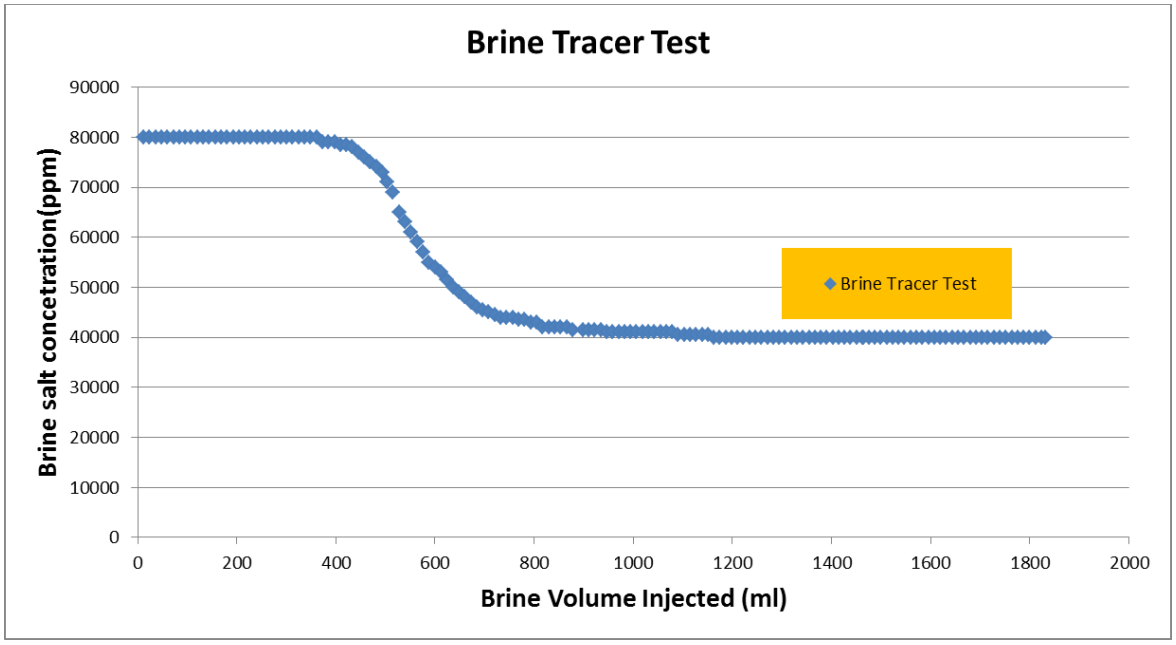

Figure 4.61: Brine tracer test in the ASP5spot#2 quarter five-spot

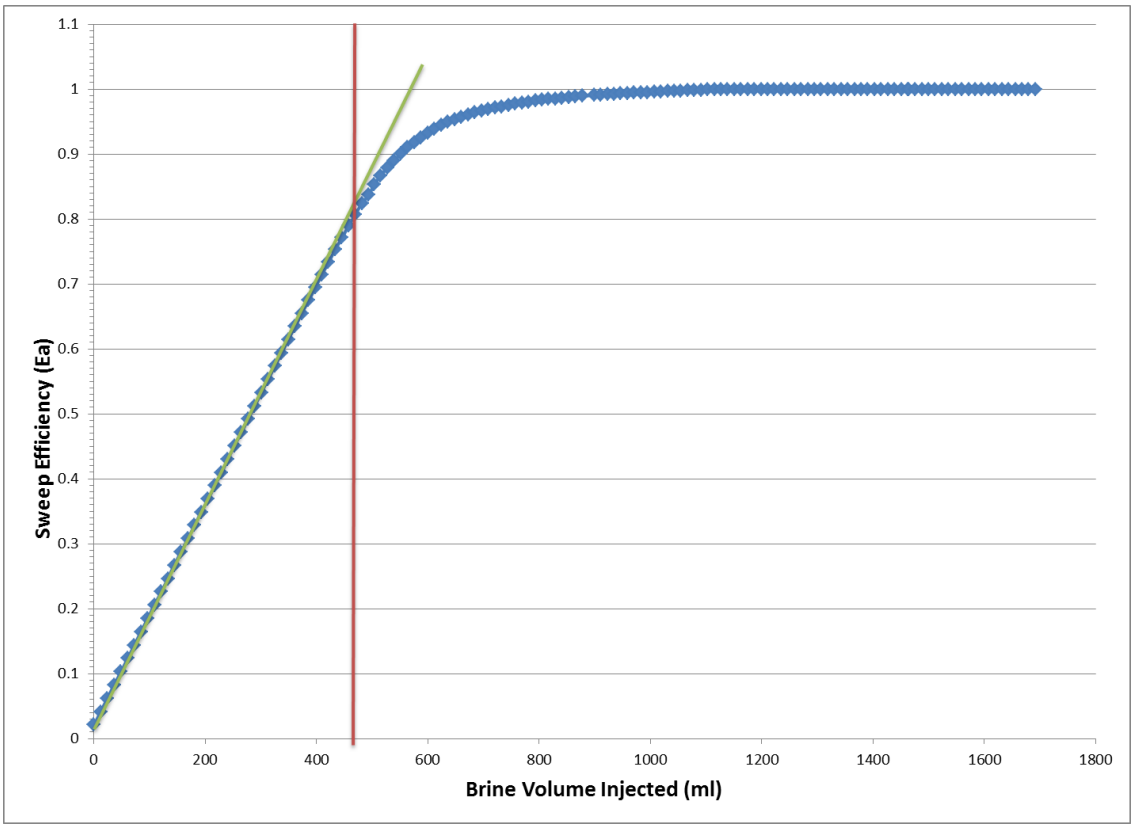

Figure 4.62: Pore volume determination for the ASP5spot#2 quarter five-spot

Properties of ASP5spot#2 Quarter Five-Spot Sandpack

Table 4.13 shows the initial properties of the sandpack before water flooding started. Porosity was determined through tracer test and was equal to 35.9 %. Overburden pressure of 1300 psi was applied to the sandpack. Inititial oil saturation was equal to 84%. The experiment was performed at the room temperature.

Table 4.12: ASP5spot#2 quarter five-spot sandpack properties

ASP5spot#2 Sandpack Properties:	
Outcrop:	reservoir sand
Porosity:	0.359
Dimensions:	10×10×1 $inch^3$
Temperature:	25 ^oC
Overburden Pressure:	1300 psi
Pore Volume:	588.7 ml
OOIP:	497 ml
Soi:	84%

ASP5spot#2 Flood Design

Table 4.14 lists the ASP flood design for the quarter five-spot. There was one big difference between this quarter five-spot flood and the ASP5spot#1 in previous quarter five-spot flood; we decreased polymer concenttration for both ASP and polymer drive from 4750 ppm to 1800 ppm. We chose 1800ppm in order to decrease pressure drop to acceptable values. Other than that, all design parameters remained exactly same as in 1-D ASP flood performed earlier.

Table 4.13: ASP5spot#2 flood design

ASP5spot#2 Flooding Desgin			
Slug Components:	ASP slug:	Polymer Drive I	Softened Reservoir Brine (SRB)
PV injected:	0.57	1.03	3
[HPAM 3630S] ppm	1800	1800	----
[surf#1], wt%	0.75% Alfoterra	----	----
[surf#2], wt%	0.25% Enordet IOS	----	----
[Cosolvent], wt. %	1% IBA		----
ppm Na2CO3	32500	22750	----
TDS ppm	35664.5	25914.5	3164
Frontal velocity, ft/day	0.8	0.8	0.8
Viscosity at 10 s^{-1} & room temp	31.15	31.02	1
Oil Viscosity, s^{-1}	100	100	100
pH	10.84	10.78	8.24

Figure 4.63 shows viscosities of the injected fluids and the oil. The viscosity of both ASP and polymer slugs were equal to ~31 cp at 10 s^{-1} shear rate and 36.6 cp at 6.31 s^{-1} shear rate.

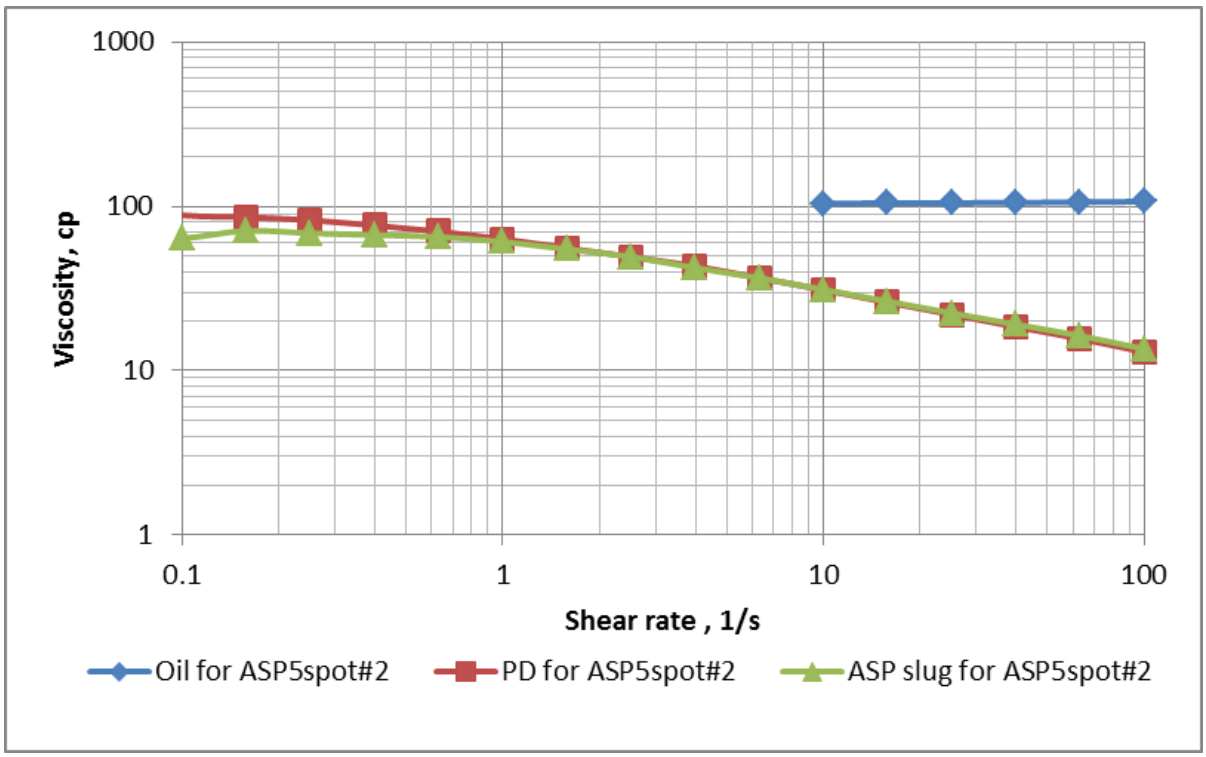

Figure 4.63: Viscosities of ASP, polymer slugs, and the oil

Salinity Gradient Design for ASP5spot#2 Flood

Figure 4.64 shows the phase behavior of surfactant-brine-oil system at different oil saturation and salinity. Salinity Gradient design was employed in the quarter five-spot flood. The quarter five-spot sandpack was waterflooded for 1PV followed by 0.5 PV of ASP and 1 PV of polymer slugs, and finally 2PV of waterflood. The orange dashed line shows the compositional path during the flood where the salinity decreases. Salinity gradient ensures that the surfactant slug crosses Type III region.

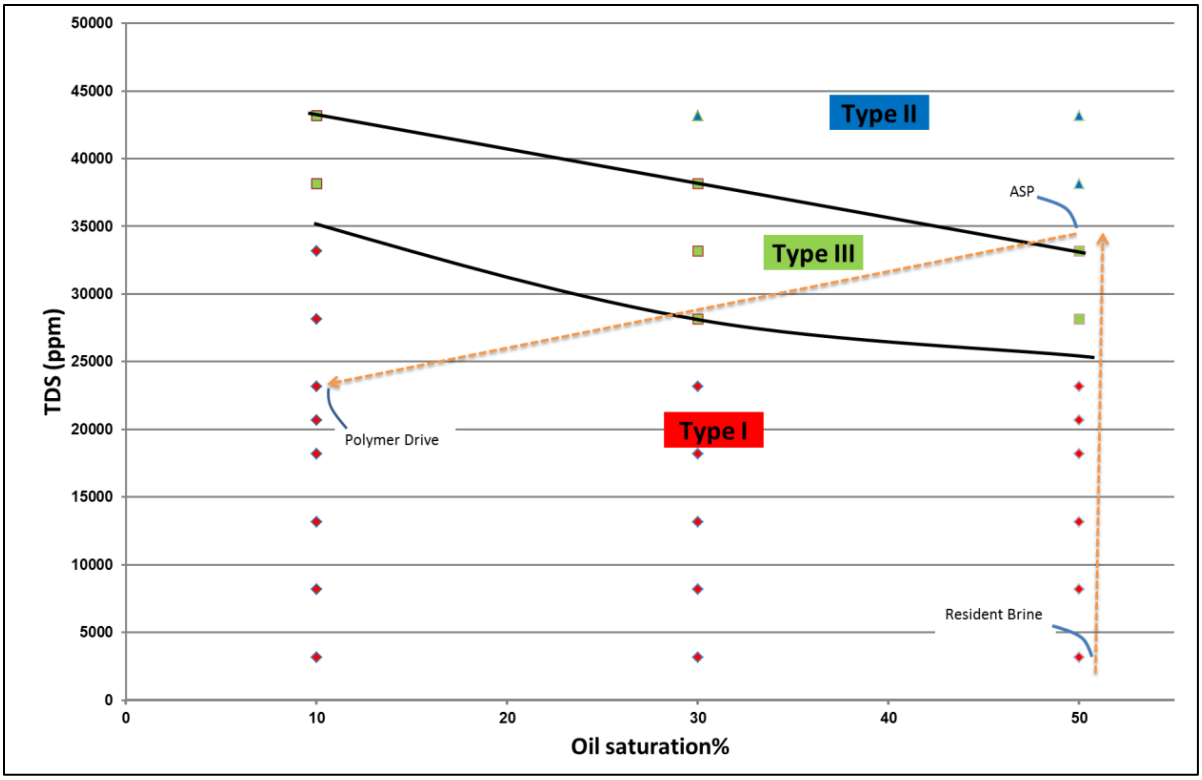

Figure 4.64: Salinity gradient design for ASP5spot#2 flooding

Summary of ASP5spot#2 Flood Results

Table 4.15 shows summary of ASP5spot #2 quarter five-spot sandpack flood. Waterflooding recovered 54% of original oil in place (OOIP) and decreased oil saturation from initial oil saturation of 84% to 38.8%. Chemical flooding including second waterflooding recovered extra 37% of OOIP and increased overall recovery to 90.6% of OOIP. Furthermore, chemical flooding decreased oil saturation from 38.8% to 8.1%. Tertiary recovery was able to recover 80% of remaining oil in place (ROIP). To conclude, unstable ASP5spot#2 sandpack flooding in viscous oil showed recovery good results.

Table 4.14: Summary of ASP5spot#2 flooding results

Soi=84%			
1.07PV	Waterflood I,ml:	Recovery, % OOIP	So
	268.59	54%	38.8%
0.57PV	ASP slug recovery, ml:		
	63.05	13%	28.1%
1.03PV	Polymer Drive , ml:		
	110.73	22%	9.3%
1.93PV	Waterflood II, ml:		
	7.84	2%	8.1%
TOTAL:	TOTAL:	TOTAL:	TOTAL:
4.6 PV	450.22	90.6%	8.1%
1.6PV	ASP+PD:	Tertiary Recovery , % ROIP	
	181.63	80%	8.1%

Figure 4.65 shows cumulative oil recovery, pressure drop, oil cut and saturation for the flood. The maximum pressure was ~ 6.2 psi which is equal to ~5 psi/ft across the pattern. Oil cut reached maximum value of 54% and quickly declined. Furthermore, oil cut shape shows that flood was unstable. Oil cut kept decreasing from it maximum value for about 1PV until no significant amount of oil was coming out; thus, oil cut had long tail. Surfactant breakthrough occurred at ~1.5PV when oil cut reached maximum value. It started to come out after only 0.5 PV injection compared to 0.9PV injection for a stable 2D ASP flood. The ASP flood was unstable. Final oil saturation reached 8.1% at the end of the flood.

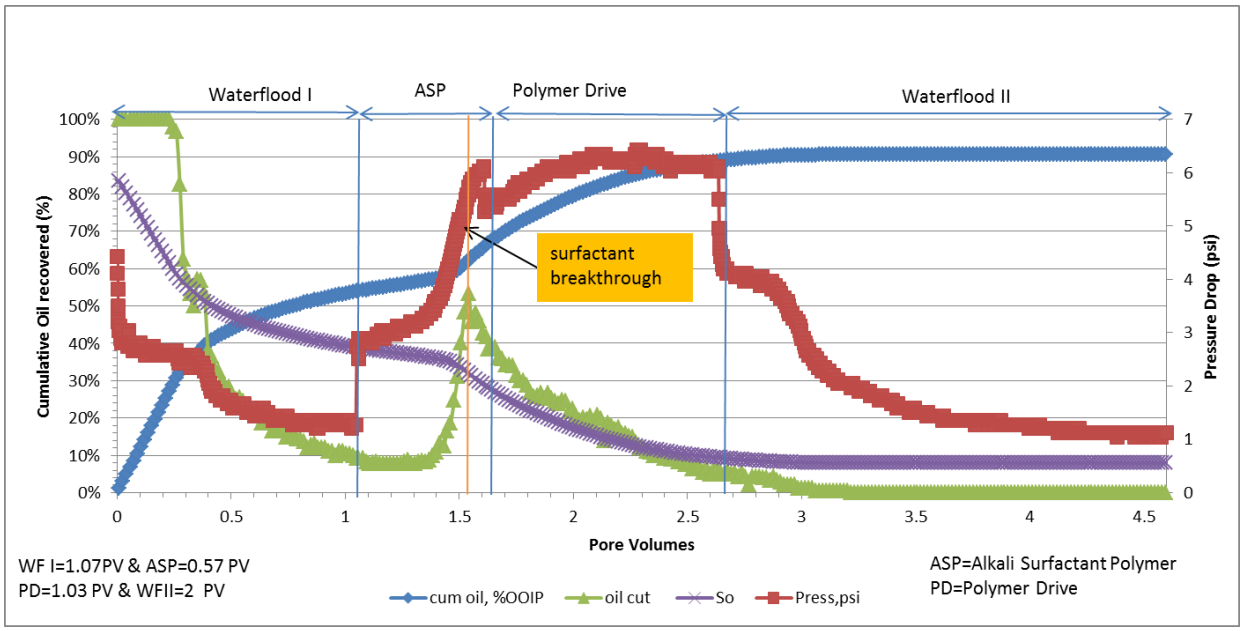

Figure 4.65: Cumulative oil recovery, oil cut, oil saturation and pressure drop

Effluent Analysis

Total salinity, pH and viscosity were measured for each effluent sample. Figures 4.66 to 4.68 show the salinity, pH and viscosity of the effluent samples. Effluent pH increased when surfactant breakthrough occurred at around 1.5 PV and stayed at 10.5 for at least 1.5 PV. Total salinity also increased at the surfactant breakthrough and reached around ~36000 ppm, a higher salinity than the salinity for the type III phase behavior. The effluent samples viscosity also increased after surfactant breakthrough and reached ~35 cp values (at shear rate 6.31 s^{-1}). This shows that the surfactant, alkali and polymer had the same breakthrough. As shown in Figures 4.69-4.71 salinity, pH and viscosity slugs traveled together without separation. Unfortunately, due to HPLC failure it was not possible to measure effluent surfactant concentration.

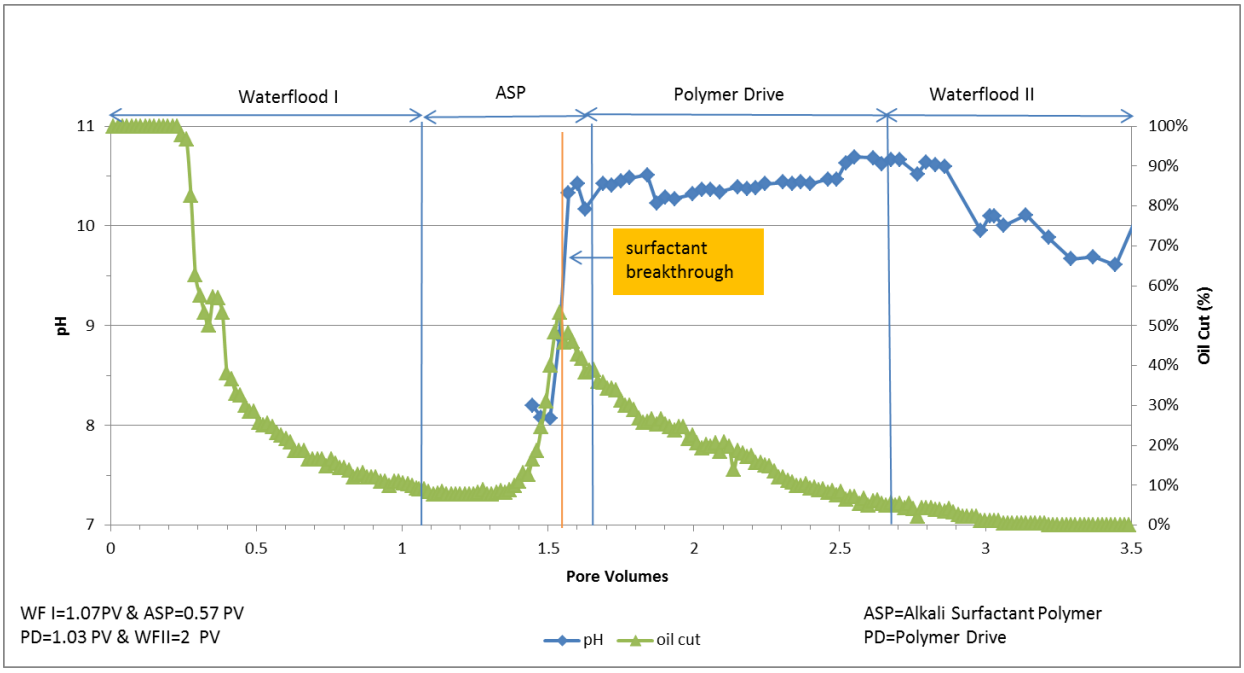

Figure 4.66: Oil cut and effluent pH

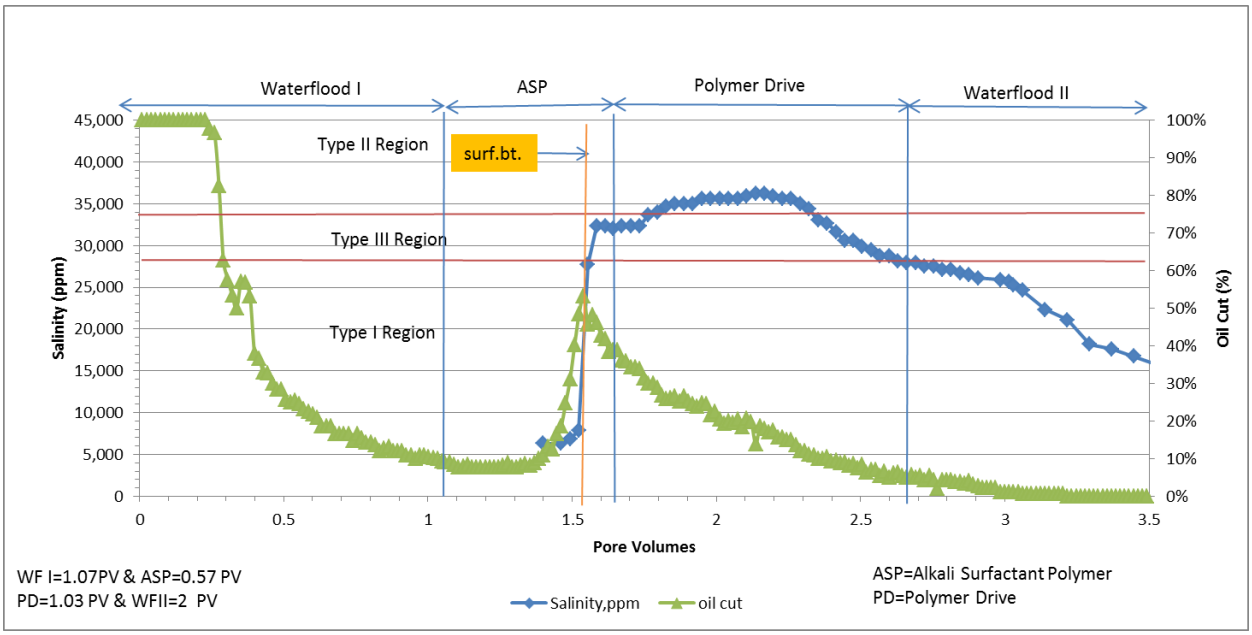

Figure 4.67: Oil Cut and effluent salinity

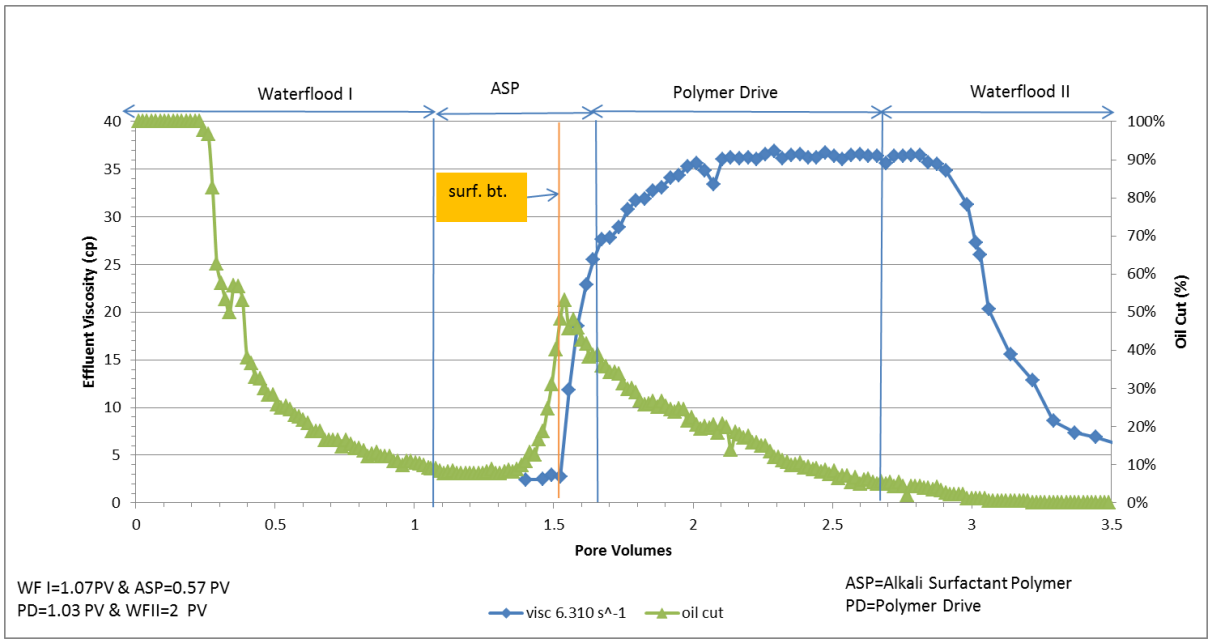

Figure 4.68: Oil cut and effluent viscosity at 6.31 s^{-1} shear rate

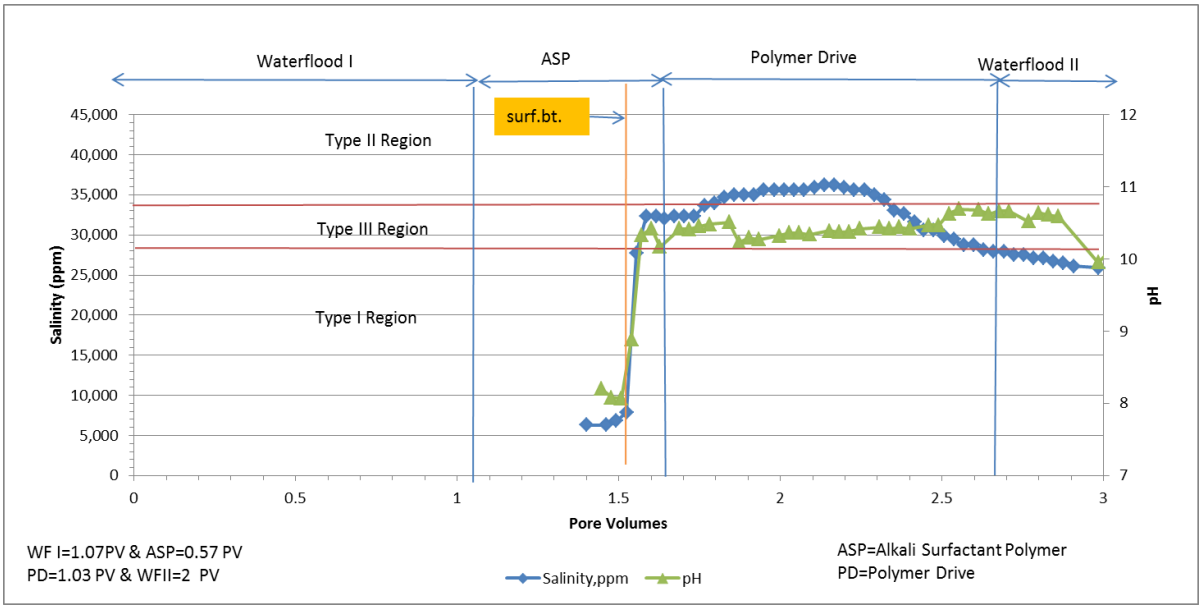

Figure 4.69: Salinity and pH propagation

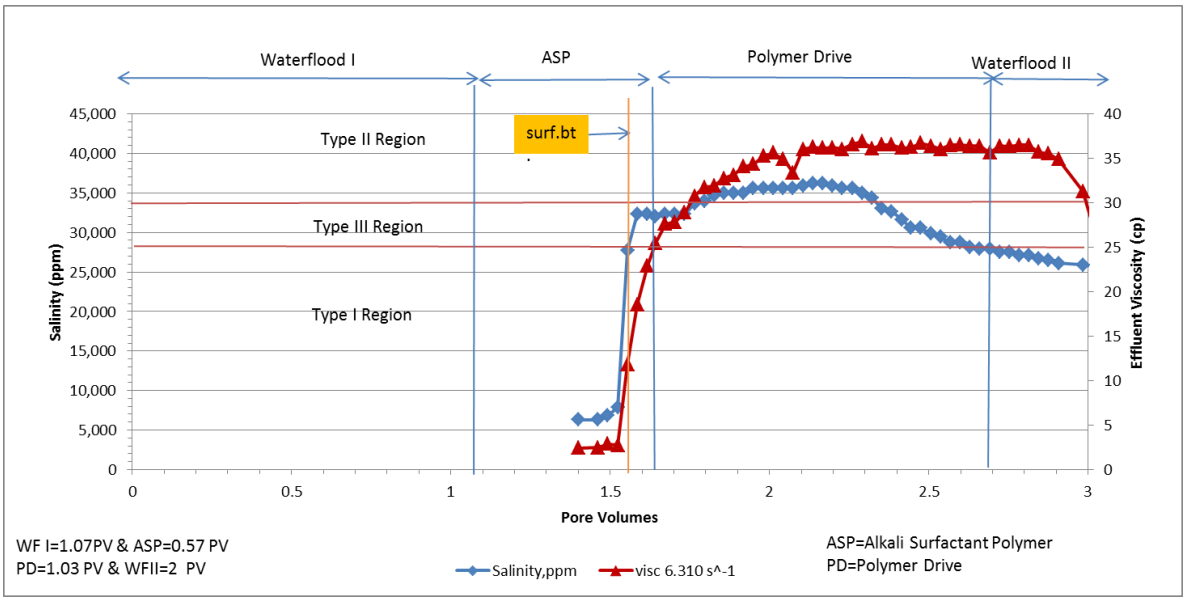

Figure 4.70: Salinity and effluent viscosity at 6.31 s^{-1} shear rate

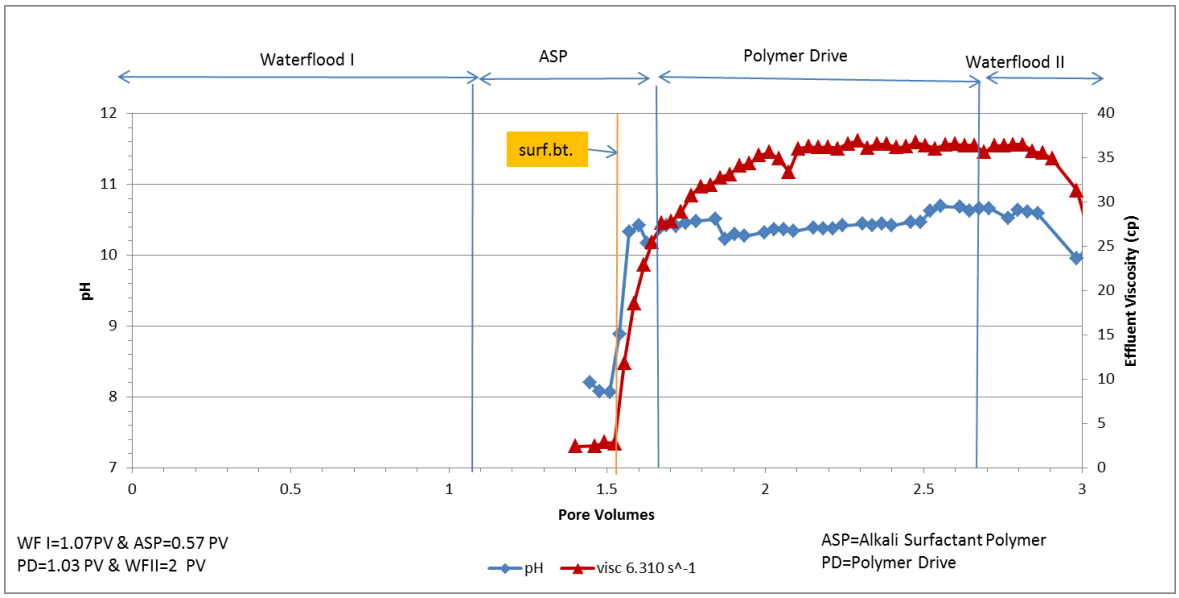

Figure 4.71: pH and effluent viscosity at 6.31 s^{-1} shear rate

CHAPTER 5: CONCLUSIONS AND RECOMMENDATIONS

Waterflood in a viscous oil reservoir is not very efficient because the water fingers through the oil due to adverse viscosity. An alkaline-surfactant-polymer formulation was developed in this research for a 100 cp oil. Since the oil is viscous, it is prudent to test this formulation in a 2D geometry as well as in 1D. The goal of this work was to evaluate the ASP design in both cores and a quarter five-spot pattern.

5.1 Conclusions

Tertiary oil recovery for 1D ASP#1 flood, where the ASP flood design recommended by a company was followed, was 64% of the remaining oil in place after 5 PV of waterflood and the oil saturation at the end of ASP#1 was 14.4 % (from initial oil saturation of 84%). Tertiary oil recovery for 1D ASP#2 flood, where an improved ASP flood design was followed, was 84% of the remaining oil in place after 5 PV of water flooding, and the residual oil saturation at the end of ASP#1 was 5.9 % (from an initial oil saturation of 82%). In ASP#2, I employed a confining pressure of ~1300 psi to emulate field conditions of overburden pressure; the same overburden pressure was also employed during the 5-spot ASP flood.

Tertiary oil recovery for 2D ASP5spot#1 flood was 97% of the remaining oil in place after ~1 PV of water flood, and the final residual oil saturation at the end of 2D ASP5spot#1 flood reached 1.2% from the initial oil saturation of 88%. Tertiary oil recovery for 2D ASP5spot#2, where polymer concentration was reduced from around 5000ppm to 1800ppm, was 80% of remaining oil place after 1 PV of water flood, and the residual oil saturation at the end of to 2D ASP5spot#1 decreased to 8.1% from the initial oil saturation of 84%.

The most important factor in ASP floods was the polymer drive viscosity. Comparison of 1D unstable ASP#1 flood and 1D stable ASP#2 flood clearly shows the importance of polymer

drive viscosity. Overall ASP performance suffers greatly if mobility ratio between ASP slug and polymer drive is adverse. Thus, it is recommended to use enough polymer to keep mobility ratio between ASP slug and polymer drive favorable.

From a stable 1D experiment the importance of salinity gradient was clearly shown. Even though there was enough surfactant and polymer used during the flood, having the salinity in the over optimum region caused high surfactant retention. If less surfactant would have been used, the overall oil recovery would have suffered greatly since surfactant does not propagate properly due to retention.

Stable 2D flood showed behavior similar to stable 1D flood behavior in a homogenous sandpack. Interestingly, unstable 2D flood performed well even with adverse mobility ratio between oil/water bank and ASP slug.

Even though oil recovery in stable 2D ASP5spot#1 flood was excellent, the pressure drop of 25 psi/ft was high, not attainable for field applications. Compared to stable 2D ASP5spot#1, unstable 2D ASP5spot#2 recovered less oil, but still oil recovery was high, 80%. Furthermore, decreasing the viscosity of the chemical slug from ~180 cp (at 10 s^{-1} in stable 2D ASP5spot#1 flood) to ~30 cp (at 10 s^{-1} in unstable 2D ASP5spot#2 flood) decreased the pressure drop from 25 psi/ft (in stable 2D ASP5spot#1 flood) to 5 psi/ft (in unstable 2D ASP5spot#2 flood). Thus, pressure drop falls with the polymer viscosity. Further decrease in polymer concentration could lead to even lower pressure drop across the 2D pattern while still recovering significant amount of oil.

5.2 Recommendations and Future Work

- Conduct both 1D and 2D experiments at lower polymer concentrations in the ASP formulation.

- Simulate these floods and develop a method to scale up these results to field scale.

REFERENCES

Adkins S., Pinnawala Arachchilage G. W. P., Solairaj, S., Lu, J., Weerasooriya U., and Pope G.. 2012. Development of Thermally and Chemically Stable Large-Hydrophobe Alkoxy Carboxylate Surfactatns. Proceedings of SPE Improved Oil Recovery Symposium.Tulsa, Oklahoma, 14-18 April.

Adkins S., Liyanage P., Pinnawala Arachchilage G. W. P., Mudiyanselage T., Weerasooriya U., and Pope G.. 2010. A New Process for Manufacturing and Stabilizing High-Performance EOR Surfactants at Low Cost for High-Temperature, High-Salinity Oil Reservoirs. Proceedings of SPE Improved Oil Recovery Symposium. Tulsa, Oklahoma, 25-28 April.

Bansal, V. K., & Shah, D. O. 1977. Microemulsions: Theory and Practice. New York, New York: Academic Press.

Bourrel, M., Schechter, R.S., 1988. Microemulsions and related system, formulation, solvency, and physical properties. Marcel Dekker, Inc.

Brigham, W. E., & Smith, D. H. (1965, January 1). Prediction Of Tracer Behavior In Five-Spot Flow. Society of Petroleum Engineers. doi:10.2118/1130-MS.

Delshad, M., Bhuyan, D., Pope, G.A., Lake, L.W., 1986. Effect of capillary number on the residual saturation of a three-phase micellar solution. Paper SPE 14911 presented at the SPE/DOE fifth Symposium on Enhanced Oil Recovery, Tulsa, 20-23 April.

Dombrowsky, H. S., Brownell, L.E., 1954. Residual equilibrium saturation of porous media. Industrial and Engineering Chemistry (Ind. Eng. Chem.) 46, 1207.

Dyes, A. B., Caudle, B. H. and Erickson, R. A. 1954. Oil production after breakthrough as influenced by mobility ratio, *Trans.*, AIME, **201**, 81-86.

Flaaten, A.K.2007. Experimental Study of Microemuslion Characterization and Optimization in Enhanced Oil Recovery: A Design Approach for Resrvoirs with High Salinity and Hardness. MS Thesis, The University of Texas at Austin, Austin, Texas.

Fortenberry P. R. Experimental Demonstration and Improvement of Chemical EOR Techniques in Heavy Oils. M.S Thesis, University of Texas at Austin, Austin, Texas, 2013.

Gao, B., and Shaarma, M.M. 2013. A New Family of Anionic Surfactants for Enhanced-Oil-Recovery Applications. SPEJ 18(5): 829-840.

Green, D. W. and Willhite, G. P. 1998. Enhanced oil recovery, SPE Textbook Series, Volume 6, Society of Petroleum Engineers, Richardson, TX, USA.

Gogarty, W. B., 1967. Mobility control with polymer solutions, *Soc. Pet. Eng. J.*, 161-170.

Gogarty,W. B., Meabon, H.P., Milton, H.W., 1970. Mobility control design for miscible—type waterfloods using micellar solutions. JPT(February), 141-147.

Habermann, B. 1960. The Efficiency of Miscible Displacement as a Function of Mobility Ratio. **219.** 264-72. Trans., AIME

Healy, R.N., Reed, R.L., Stenmark, D.G., 1976. Multiphase microemulsion systems. SPEJ (June), 147-160; Trans, AIME, 261.

Hsieh W. C., and Shah D. O. 1976. The Effect of Chain Length of Oil and Alcohol As Well as Surfactant to Alcohol Ratio on the Solubllization, Phase Behavior and Interracial Tension of Oil / Brine / Surfactant / Alcohol Systems. *SPEJ* 6594.

Huh, C., 1979. Interfacial tension and solubilizing ability of a microemulsion phase that coexists with oil and brine. J. Coll. Int. Sci. 71, 408-428.

Kumar, R.2013. Enhanced Oil Recovery of Heavy Oils by Non-Thermal Chemical Methods. PhD dissertation, University of Texas, Austin, TX USA.

Levitt, D.B., Jackson, A.C., Heinson, C., Britton, L.N., Malik, T., Dwarakanath, V., Pope, G.A. 2006. Identification and Evaluation of High-Performance EOR Surfactants. *SPE Re.s Eng.*, **12**(2): 243-253. SPE 100089-PA. doi: 10.2118/100089-PA

Lake, L. 1989. *Enhanced Oil Recovery.* Englewood Cliffs, New Jersey: Prentice Hall

Li, Y., Zhang. W., Kong, B., Puerto, M., Bao, X., Sha, O., Shen, Z., Yang, Y., Liu , Y., Gu, S., Miller , C., and Hirasaki, G.J. 2014. Mixtures of Anionic-Cationic Surfactants: Anew Approach for Enhanced Oil Recovery in Low-Salinity, High Temperature Sandstone Reservoir. Paper SPE 169051 presented at SPE IOR Symposium, Tulsa, Oklahoma, 12-16 April.

Maerker, J. M., & Gale, W. W. 1992. Surfactant Flood Process Design for Loudon. Society of Petroleum Engineers. doi:10.2118/20218-PA

Mohanty, K.K., Salter, S.J., 1983. Multiphase flow in porous media: III. Oil mobilization, transverse dispersion and wettability. Paper SPE 12127 presented at the 58th Annual Conference of the SPE, San Francisco, 5-8 October.

Moore, T.F., Slobod, R.C., 1955. Displacement of oil by water-effect of wettability, rate, and viscosity on recovery. Paper SPE 503-G presented at the SPE Annual Fall Meeting, New Orleans, 2-5 October.

Nelson, R.C., Lawson, J.B., Thigpen, D.R., Stegemeier, G.L. 1984. Cosurfactant-Enhanced Alkaline Flooding. Paper SPE 12672 presented at the SPE Enhanced Oil Recovery Symposium, Tulsa, Oklahoma, 15-18 April. doi: 10.2118/12672-MS.

Pope, G.A., Tsaur, K., Schechter, R.S., Wang, B., 1982. The effect of several polymers on the phase behavior of micellar fluids. SPEJ(December), 816-830.

Puerto, M.C., Hirosaki, G.J., Miller, C.A., Reznik, C., Dubey, S., Barnes, J.R., and van Kuijk, S.2014. Effects of Hardness and Cosurfactant on Phase Behavior of Alcohol-free Alkyl Propoxylated Sulfate Systems. Paper SPE 169096 presented at SPE IOR Symposium, Tulsa, Oklahoma, 12-16 April.

Puig, J. E., Franses, E. I., Davis, H. T., Miller, W. G., & Scriven, L. E.1979.On Interfacial Tensions Measured With Alkyl Aryl Sulfonate Surfactants. Society of Petroleum Engineers. doi:10.2118/7055-PA

Rosen, M.J. 1989. Surfactants and Interfacial Phenomena. Second edition. New York. John Wiley and Sons.

Sahni V., Dean R. M., Britton C., Kim D. H., Weerasooriya U., and Pope A., 2010. The Role of Co-Solvents and Co-Surfactants in Making Chemical Floods Robust. Paper SPE 130007 presented at the SPE Improved Oil Recovery Symposium, Tulsa, Oklahoma 24-28th April 2010.

Salter, S.1977. The Influence of Type and Amount of Alcohol on Surfactant-Oil-Brine Phase Behavior and Properties. Society of Petroleum Engineers. doi:10.2118/6843-MS

Sanz, C. A., & Pope, G. A. 1995. Alcohol-Free Chemical Flooding: From Surfactant Screening to Coreflood Design. Society of Petroleum Engineers. doi:10.2118/28956-MS

Sharma, H., Weerasooriya, U., Pope, G. A., & Mohanty, K. K. 2014. Ammonia-Based ASP Processes for Gypsum-Containing Reservoirs. Society of Petroleum Engineers. doi:10.2118/170825-MS

Sheng, J.J. Modern Chemical Enhanced Oil Recovery: Theory and Practice. Elsevier, Burlington, MA, 2011.

Solairaj S. 2011. New Method of Predicting Optimum Surfactant Structure for EOR. M.S Thesis, University of Texas at Austin, Austin, Texas.

Stegemeier, G.L. 1977. Mechanism of Entrapment and Mobilization of Oil in Porous Media. New York City: Academic Press.

Wade, W. H., Morgan, J. C., Jacobson, J. K., & Schechter, R. S. 1977. Low Interfacial Tensions Involving Mixtures of Surfactants. Society of Petroleum Engineers. doi:10.2118/6002-PA

Walker, D.L. Experimental Investigation of the Effect of Increasing the Temperature of ASP Flooding, M.S. Thesis, The University of Texas at Austin, Austin, Texas, 2011.

Wang, D., Liu., Wu, W., Wang, G., Novel Surfactants that Attain Ultra-Low Interfacial Tension between Oil and High Salinity Formation Water without adding Alkali, Salts, Co-surfactants, Alcohols, and Solvents. Paper SPE 127452 presented at SPE EOR Conference at Oil & Gas West Asia, 11-13 April, Muscat, Oman, 2010.

Winsor, P., 1954. Solvent Properties of Amphilic Compounds. Butterworths, London.

Yang, H., Britton, C., Liyanage, P.M., Solairaj, S., Kim, D.H., Nguyen, Q., Weerasooriya, U., Pope, G.A. 2010. Low-Cost, High-Performance Chemicals for Enhanced Oil Recovery. Paper presented at the SPE Improved Oil Recovery Symposium, Tulsa, Oklahoma, 24-28 April. doi: 10.2118/129978-MS

Zhao P., Jackson A. C., Britton C., Kim D. H., Britton L. N., Levitt D. B., and Pope G., 2008. Development of High-Performance Surfactants for Difficult Oils. SPE 13432 Paper presented at the SPE IOR Symposium, Tulsa, Oklahoma.

VITA

Almas Aitkulov was born in Taraz, Kazakhstan. After completing his work at Physics-Mathematics School for Gifted Children, Almaty, Kazakhstan, in 2006, he entered Texas A&M University. In 2010, he transferred to the University of Texas at Austin, Austin, Texas. He received the degree of Bachelor of Science in Petroleum Engineering from the University of Texas at Austin, Austin in May 2012. In September, 2012, he entered the Graduate School at the University of Texas at Austin.

Address: almas.aitkulovs@yahoo.com

This manuscript was typed by the author.